NASA Contractor Report 175031

Low Reynolds Number Boundary Layers in a Disturbed Environment

(NASA-CR-175031) LOW REYNOLD'S NUMBER BOUNDARY LAYERS IN A DISTURBED ENVIRONMENT Ph.D. Thesis - August, 1985 - Final Report (Case Western Reserve Univ.) 98 p HC A05/MF A01 CSCL 20D G3/34

N86-17665

Unclas 05342

Dong-Kee Paik and Eli Reshotko

Case Western Reserve University
Cleveland, Ohio

January 1986

Prepared for the
Lewis Research Center
Under Grant NAG 3-230

NASA

TABLE OF CONTENTS

CHAPTER I

INTRODUCTION

An understanding of the transition process and development of the turbulent boundary layer under highly disturbed conditions would have numerous engineering applications. Many significant flows develop in environments which are not quiescent. The behavior of boundary layers in disturbed environments presents a new and perhaps more complex problem than in quiescent environments, yet the solutions to the problem under disturbed conditions have many potential applications. One particular area which would benefit greatly from an ability to locate the transition region is the design of turbomachinery blading.

The gas side heat transfer to cooled turbine blades is greatly dependent on how much of the blade is laminar and how much is turbulent. Graham (ref. 1) has pointed out that it is important to be able to predict the transition location for the boundary layer on turbine blades in order to properly assess the cooling requirements for turbine blades. However, difficult transition prediction is for flight in a quiescent environment, it is much more so for the highly disturbed flow that exists in a combustion chamber. The resulting low Reynolds number turbulent boundary layer is also not well understood.

For a flow environment that is not quiescent, if initial disturbance levels are large enough to be considered non-linear, then the important linear regime of the quiescent environment is bypassed and the traditional views of the transition process that are based on an initially quiescent environment are inapplicable. The term 'bypass transition' has been introduced by Morkovin to describe transition in disturbed environments that initially have finite non-linear amplitudes.

Although it is hardly understood, bypass transition is a common phenomenon. Transition in fully developed Poiseuille pipe flow is a bypass phenomenon since the parabolic laminar velocity profile in a pipe is stable to all infinitesimal disturbances that have been considered to date. This transition must therefore come about as a result of large disturbances in the entrance region. This statement is substantiated by the results of Wygnanski and Champagne (ref. 2) and of Wygnanski, Sokolov and Friedman (ref. 3) who have also mapped out the properties of the resultant turbulent puffs.

There have been prior attempts at explaining instability for finite disturbances through a form of non-linear stability theory. Based on the Stuart-Watson formalism which considers the fundamental disturbance together with its harmonics (refs. 4 and 5), Herbert (ref. 6) has found that for finite amplitude disturbances, the minimum critical Reynolds number is reduced to about 2900 from its value for infinitesimal disturbances of about 5770. Herbert shows

further that for finite disturbances, the wave number band that is amplified is significantly increased over that for infinitesimal disturbances. He also indicates that plane Poiseuille flow may display a metastable non-linear equilibrium state for some finite amplitude level. Attempts to do the same analysis for flat plate boundary layers are complicated by the necessity of doing the analysis in a non-parallel manner because of the closeness of the region of interest to the leading edge of the plate. The existence of subcritical instability or metastable equilibria for boundary layers has not been established.

Another possible influence on transition is the response of the disturbance vorticity field to its being convected past the rounded leading edge of a plate. Morkovin (ref. 7) has addressed the many phenomena ascribed to this flow. He indicates that the boundary layer tends to remain laminar around the leading edge even in the presence of a disturbance vorticity field but that it might contribute to earlier that expected transition.

It is the intent of the present program to study experimentally the character of the transition process for boundary layers in a highly disturbed environment as might be experienced on turbine blades, and to delineate the character of the resulting low Reynolds number turbulent boundary layer. The results of this experiment will help guide later analytic and experimental work.

Although the original objective of this experiment was to study the transition process in a disturbed environment, this has

proved somewhat elusive. The bulk of the presented data concern the properties of very low Reynolds number turbulent boundary layers with $280 < Re_\theta < 700$. In this Reynolds number region, Reynolds number effects are important due to the increased influence of the viscous superlayer and its turbulent counterpart. These effects manifest themselves as a rapidly diminishing wake strength in this Reynolds number range.

This range of Reynolds number is of particular interest for it harbors many controversies and disputes regarding the applicability of the most important similarity rule in turbulent flow, namely the 'law of the wall.' Purtell et al. (ref. 8) investigated low Reynolds number boundary layers to help settle the debate. By tripping the boundary layer in the absence of free stream turbulence, they concluded that the log-linear region is an inherent characteristic of the turbulent boundary layer even at low Reynolds numbers.

The effect of free stream turbulence on the turbulent boundary layer growth rate and on the increases in skin friction has been reported in many previous studies (refs. 9-16). Most of these authors, though, had much higher Reynolds numbers in their flows than in the current investigation which concentrates on the lower range.

Based on the Taylor (ref. 17) and Dryden et al. (ref. 18) recommendations that the study of free stream turbulence effects be considered by analyzing both the free stream turbulence intensity

and dissipation length scale, Hancock (ref. 13) introduced a so called 'free stream turbulence parameter.' He correlated many features of the turbulent boundary layer with this parameter. Later contributions were made by Blair (refs. 14 & 15) and Castro (ref. 16) to better the correlation.

Meier (ref. 12) reported, based on a study he made at low turbulence levels, that the dissipation length scale and its spectra depend largely on the geometry of the settling chamber and shape of grids even if the turbulence intensity remains unchanged. But he suggested that the skin friction is not very sensitive to the length scale since the length scale is normally much larger than the boundary layer thickness.

The aforementioned correlations obtained by Hancock and others involves the values of data in a quiescent environment (no grid) as a reference quantity. In fact, no complete agreement on this value has been settled on yet. For instance, the results of Coles (ref. 19) and Purtell et al. (ref. 8) reveal significant differences in friction coefficient at the same Reynolds numbers. So also between Hancock and Castro. Indeed, there is no agreement between any of these authors.

Thus, if the reference quantity is not reliably determined, the universality or even the applicability of the correlations of refs. 13-16 has to be limited in some sense.

In the present study, most of the results are presented on the basis of turbulence intensities alone rather than with respect to

any turbulence parameter. The dissipation length scales are in the range of 5 to 20 boundary layer thicknesses.

CHAPTER II

EQUIPMENT AND PROCEDURE

2.1 Equipment

The experiments were performed in a low speed wind tunnel located in the Department of Mechanical and Aerospace Engineering at Case Western Reserve University. The tunnel is a small, open-circuit system shown in Figure 1. A flat plate is situated in the middle of the tunnel bisecting the flow. The leading edge of the plate has an elliptical shape rather than the original rounded edge. The shape was altered in order to avoid possible separation at the leading edge which would trip the flow and thereby preclude the study of transition and of the resulting low Reynolds number turbulent flow under disturbed free-stream conditions alone. At the end of plate downstream of the working surface, a deflector exists to ensure that the stagnation point remains on the upper side of the plate where data are taken. Further downstream from the deflector is an adaptor which connects the centrifugal blower to the tunnel. The blower can pull air through the system at about 6 m/sec (u_e/ν = 393,600/m).

The tunnel has a relatively high residual test section turbulence level of about 1.5%. Higher turbulence levels required for this study were generated by three different biplane grids constructed from rectangular bars inserted at the entrance to the

settling chamber. The blockage and turbulence levels were respectively 67% and 5-6% for grid 1, 76% and 6-7% for grid 2, and 50% and 4-5% for grid 3.

The location of the grids at the entrance to the settling chamber rather than downstream of the contraction is to secure a more uniform free stream turbulence level in the test section. The shapes of the grids and their dimensions are shown in Fig. 2.

The sensor for collecting velocity data is a TSI 1218 boundary layer type hot wire probe. The wire diameter is 0.00015 in. The probe is mounted in a slotted guide and can traverse longitudinally and vertically in the spanwise midplane of the tunnel. The vertical position of the probe can be adjusted to an accuracy of better than 30 microinches via a boundary layer type vertical control rack from United Sensor and Control Corp. Longitudinal position has an accuracy of only one millimeter which is sufficient.

Mean and fluctuating longitudinal velocities were respectively monitored using a T.S.I. model 1054-A2 Constant Temperature Hotwire Anemometer and a DISA 55D35 RMS Unit. The anemometer was designed by the manufacturer to have its best performance in the operating speed range of the present tunnel.

The on-line hotwire signals were collected into an IMSAI 8080 Microprocessor which was used as an analogue-to-digital converter at a sampling rate of one reading per millisecond over a period of 66 seconds for a single data point.

The digitized values were then stored on the department's PDP 11/40, thus allowing for further signal processing such as averaging as well as Fast Fourier Transform extraction of the spectrum up to about 1000 Hz. Greater flexibility in obtaining spectra was achieved by use of an HP 3582A spectrum Analyzer since the analyzer had various filters and averaging modes.

2.2 Procedure

Since this investigation is focused on both the transitional behavior of disturbed flows and the resulting low Reynolds number turbulent bounday layer, therefore, flows with length Reynolds numbers below 200,000 were of primary concern. Data were taken at longitudinal stations up to 30 cm from the leading edge with a more detailed concentration on the first 18 cm.

Great care was taken in order to insure accuracy in the probe position while traversing in the vertical direction. A magnifying glass was used to minimize the possible positioning error when the probe supporter touched the wall, and a level indicator was used to set the verticality of the track for the rod which carries the probe.

The sampling points in the vertical direction were at 20 to 30 locations spaced at intervals ranging from 3 mils at the wall to 0.1 inch near the edge of the boundary layer. Finer divisions would yield better profiles, but taking a larger number of sampling points might require a long enough time for environmental changes

to alter the flow profiles. Thus, the sampling scheme above was selected to optimize the accuracy of the measurements of flow profiles while minimizing the effect of the very slowly varying environment.

Precision in the value of the distance of the probe location from the wall when the supporter of the probe touched the wall was obtained by the use of a cathetometer to measure the actual distance. This equipment also made it possible to get an additional digit of accuracy.

Every test was accompanied by a calibration of the system for consistant data acquisition. Signals from the hot-wire anemometers and the rms indicator were monitored by oscilloscopes to verify the readings on the meters. There was good agreement between the instruments.

The hot-wire probe was calibrated by using a wall-mounted pitot-tube and a Cox Instrument micromanometer to yield a calibration relation corresponding to the linear output of the anemometer. By blocking the centrifugal blower, several different speeds could be obtained. With data taken at the various speeds, a linear relationship was acquired for the anemometer output. The calibrations were done before proceeding to each successive axial station, since probes are sensitive to changing environmental conditions such as room temperature and relative humidity.

2.3 Data Reduction

At each probe location, longitudinal mean and rms velocities were obtained. Spectra obtained by the spectrum analyzer were plotted using a Honeywell Model 55 X-Y Pen Recorder. Various data reductions were performed on the VAX system of the Dept. of Electrical Engineering of CWRU.

Curve fitting by 'cubic spline interpolation' of the raw mean profiles enabled the calculation of the displacement thickness δ^*, momentum thickness Θ, and shape factor H, by performing Simpson's rule integrations. One of the fitted profiles and the corresponding measured profile are shown in fig. 3 for an illustration of the results of the spline fit.

The elimination of positioning error by physical means was not possible, no matter how carefully the probe was placed and its position measured. Instead, to reduce probe positioning error, a numerical technique was developed which adjusted both the innermost probe position value and the friction velocity until the resulting profile fit a law-of-the-wall curve with a minimal error. Thus the optimal value for the probe position at closest approach to the wall, y_o, and the frictional velocity u_τ could be obtained. Finding the best fit using two degrees of freedom did prove successful and the results are presented in Chapter 3.

CHAPTER III

RESULTS AND DISCUSSION

3.1 Mean Flow

Figure 4 shows how the Reynolds number, Re_θ, and the shape factor, H, vary with distance from the leading edge in the longitudinal direction. Fig. 4a shows the effect of the free stream turbulence level on momentum thickness Reynolds number, Re_θ. (Hereafter, the term Reynolds number, Re, will refer to Re_θ unless otherwise stated.) Note that all the points plotted here have length Reynolds numbers under 100,000. Yet they all have Re's much higher than those expected from a low turbulence environment. Even without a grid, where the turbulence level in the free stream is about 1.5%, the boundary layer is transitional and its thickness is nearly twice the Blasius value.

In Fig. 4b, for the no grid case, the shape factor declines from 2.4 to 1.8 indicating transitional behavior while with the grids (higher free stream turbulence levels), the transition to turbulent flow occurs rapidly. In fact, by the 9 cm position for grid 2 (Re below 400) the profile has a shape factor of less than 1.6, and beyond the 12 cm location (Re = 400), the curve has nearly leveled out.

Fig. 5 shows the variation of shape factor H, with Reynolds number. Present data and other recent data are compared. The

present points lie below the others, possibly because the data in most of the other experiments were obtained in the absence of significant free stream turbulence.

Despite the scatter in the data caused by the high sensitivity of H to the positional accuracy of the probe, a trend can still be detected. Namely, that increase in free-stream disturbance level will result in decrease in the shape factor with respect to Reynolds number. This trend is in qualitative agreement with the results of other investigators such as Hancock (ref. 13), Castro (ref. 16) and Blair (ref. 15). They considered the effects of both turbulence intensity and dissipation length scale in deducing some correlation between their parameter (free stream turbulence parameter) and the variation of shape factor. Also plotted on the Fig. 5 is a solid line which is calculated from the law of the wall formula to present a reference in explaining the sizable departure of the current data from the others, when the wake strength in the mean profiles has vanished. More explanation on the calculation will be presented later in sec.3.2.3.2.

3.2 Wall Skin Friction

3.2.1 Determination of u_τ

Friction velocities were obtained by fitting the profiles to the Musker (ref. 20) law-of-the-wall formula.

$$u^+ = 5.424\arctan[(2y^+ - 8.15)/16.7] - 3.52 + \log_{10}\{(y^+ + 10.6)^{9.6}/(y^{+2} - 8.15y^+ + 86)^2\} \qquad (1)$$

This explicit expression for the turbulent mean velocity distribution over a smooth wall has validity over the law-of-the-wall region and in the log-linear region matches the constants suggested by Coles (ref. 19).

Figs. 6.b and 6.d show the procedure of selecting the value of friction velocity. By plotting the data points for different assumed values of u_τ, a best fit can be made. The best one can be chosen visually and compared with the one that the computer calculated by a least squares procedure. The difference between the two tends to be under 3%. However, visual selection of the quantity will be more reliable, since the computer evaluation did not exclude points in the sublayer which apparently depart from the basic curve due to the close proximity of the probe to the wall.

The presence of the wall affects the probe reading in two ways. Coles (ref.19) found that putting a tube or a probe near enough to a wall will cause a 'chute' to form between the probe and the wall. The velocities around the probe will be higher than without the presence of the wall. The probe alters the local flow field and measures a velocity which would differ from the velocity of the fluid in the absence of the probe. Also the wall can transfer heat from the probe more effectively than air, and by moving the probe closer to the wall, the heat transfer increases. Since both of these factors contribute to a larger heat transfer rate from the probe to its surroundings, the false velocity reading

which results will be higher than the true velocity in the very near proximity of the wall.

3.2.2 Similarity Features of the Experimental Profiles

Figures 6.a through 6.g contain the plots of the mean velocity distributions on the Musker curve for different streamwise locations. Figures 6.a to 6.c are for grid 1 while figures 6.d through 6.g are for grid 2. The characteristics of the profiles are summarized in Table 1. Reynolds numbers for all of these profiles are less than 532, and no significant wake strengths are observed in any of these profiles. Coles (ref. 19) upon examining a number of different sets of experimental results, concluded that the wake strength disappears entirely below a Reynolds number just below 500, but this conclusion was disputed by some later authors such as Purtell et al. (ref. 8), Castro (ref. 16) and others. These latter authors found that the wake strength did not decrease as rapidly in the lower region of Reynolds number as Coles suggested. Indeed, they found the wake function remained finite for all Reynolds numbers at which they obtained profiles.

While there is that difference of opinion in the absence of free stream turbulence, no dispute exists over the role of free stream turbulence in diminishing wake strength. Coles also noted the effect in 1962 and Blair (ref. 15) provided further confirmation of this behavior. Blair's results show that even for the much higher Reynolds number of 3,000, a free stream turbulence level of

5.3% made the wake strength almost vanish. Similiar effects are reported by Hancock (ref. 13) at Re = 1800 and by Castro (ref. 16) at Re = 600.

Also observable from the fig. 6's is that as the Reynolds number increases, more points fall in the linear region. The extent of the logarithmic region which decreases with decreasing Reynolds number is now a well known phenomenon of the turbulent boundary layer. However, some controversy still remains over the existence of the log-linear region at very low Reynolds numbers. Preston (ref. 23), Granville (ref. 22) and Landweber (ref. 21) have argued that the log-linear region disappears below some Reynolds number. These authors believe that the overlap region which overlaps the inner and outer region in the turulent boundary ceases to exist when Reynolds number becomes small enough, namely in the vicinity of Re = 800. On the other hand, Purtell et al. (ref. 8) established from their data that while the absolute thickness of the linear region becomes small, the proportion of the region to the overall boundary layer thickness tends to remain between 15 and 25 percent. One should observe that if even a few of the data points were shifted by less than the error bar of 3%, the linear region would be clearly visible. Smits et al. (ref. 25) were even able to show the log-linear region at Reynolds number as low as 261. Moreover, if the assertion of Simpson (ref. 24), who argued that the Von Karman constant is Reynolds number dependent, i.e.,

$$k(\mathrm{Re}) = k(6000)\,(6000/\mathrm{Re})^{1/8}$$

$$\text{where,} \quad k(6000) = 1/5.62 \qquad (2)$$

is correct, the variation of the constant itself should exceed 30% for the current Reynolds numbers. And thus the proposed profile should depart some 12% from the curve suggested by Coles, which is not supported by the present data.

Thus the log-linear region seems to be an inherent characteristic of the turbulent boundary layer, as Purtell et al. stated, even in the very low range of Reynolds number down to about 300. And recalling that this state of turbulence was generated in the present experiment by disturbing the free stream rather than by tripping the boundary layer flow, this feature seems to be independent of the method of turbulence generation.

3.2.3 Reynolds Number Dependency of Skin Friction

Figure 7 shows the variation of skin friction through the parameter u_e/u_τ with respect to Reynolds number and a comparison with other recent data.

3.2.3.1: Minimum Re for Turbulent Flow

Preston (ref. 23), from the similarity and close agreement of the Reynolds number for the circular pipe and flat plate, suggested the lower limit for which fully developed turbulent flow occurs as Re = 320 with a rather limited data confirmation, while the aforementioned (sec 3.2) Smits et al. (ref. 25), by applying a pin-type

turbulent stimulator, obtained a turbulent profile at Re = 285, and even at Re = 261 in the presence of a strong favorable pressure gradient.

In the present experiments, post-transitional turbulent boundary layers are obtained at Re = 280.

3.2.3.2 Influence of Free Stream Turbulence on u_e/u_τ

Those points of Purtell et al., which are in the same Reynolds number range as the present data (Fig. 7), were obtained in the absence of free stream turbulence and have skin friction coefficients that are about 5% lower. The difference in the skin friction coefficient seems to be coming from the residual wake strength at their Reynolds numbers (i.e., from their data, $\Delta u / u_\tau = 1.0$ at Re = 465) (ref. 8). Again, the present profiles showed no discernable wake strength. Coles' suggested zero wake strength point is at Re = 425 and at a value of u_e/u_τ slightly above the present data spread.

An important issue to be discussed here is how much the free stream turbulence in this low range of Reynolds number can influence the skin friction. For flows at higher Reynolds numbers, many researchers have reported a turbulence effect which significantly elevates the skin friction, for instance, 7% turbulence in the free stream causes an increase in skin friction of some 20% over that in a quiet environment (ref. 15).

A most plausible hypothesis has been advanced by Huffman and

Bradshaw (ref. 28) through their comparison of turbulent boundary layers developing under a quiescent irrotational free stream and the turbulent flow in pipes where the 'turbulent core' is not quiescent and irrotational. In the latter flow, there is no observable wake, while in the former there is very definitely a wake component to the velocity profiles. For the turbulent boundary layer at low Reynolds numbers in quiescent environments, Huffman and Bradshaw attribute the erosion of the wake component to the increased importance of the 'viscous superlayer' - the interface between the boundary layer and the irrotational external flow - in eroding the wake component. For external flows at elevated free stream turbulence - by analogy to the situation in pipes - the wake component is eroded more severly if not entirely as in the present results.

These effects can be assessed quantitatively as well. Musker (ref. 20) states an expression for the turbulent boundary layer profile as follows:

$$\begin{aligned} u^+ = {} & 5.424 \arctan\{(2y^+ - 8.15)/16.7\} \\ & + \log_{10}\{(y^+ + 10.6)^{9.6}/(y^{+2} - 8.15y^+ + 86)^2\} \\ & - 3.52 + \pi/k\ \{6(y/\delta)^2 - 4(y/\delta)^3\} \\ & + 1/k\ (y/\delta)^2(1 - y/\delta) \end{aligned} \qquad (3)$$

The first three terms on the right side are an analytic expression for the law of the wall that is consistent in the log-linear region with Cole's constants. The term having the coefficient π is an

algebraic form of the Coles wake function, and the last term on the right side is an additional wake term due to Granville (ref. 22) providing for a zero derivative at the edge of the boundary layer.

Plotted on figure 7 is a line representing the results of integrating the Musker profile without the Coles and Granville wake terms. This seems to be a good representation of the present data over the limited range of Reynolds number investigated herein. The details of obtaining integrated boundary layer information from various forms of equation 3 are developed in Appendix A.

The variation of skin friction coefficient itself is plotted in figure 8 with respect to Reynolds number. Here the present data are compared with additional sets of reference data, emphasizing the effect of free stream turbulence in increasing the skin friction. Blair's data (ref. 14) represented by hexagons, were obtained under levels of turbulence similar to those of the present experiment. Note the increase in skin friction. The roughly 20% increase in skin friction due to the presence of turbulence in Blair's data agrees with the trend of increasing skin friction in the present data obtained for a somewhat lower range of Reynolds number.

3.3 Disturbance Profiles and Spectra for the Turbulent Flow

Figures 9 and 10 show the longitudinal turbulence intensity distribution at various values of Reynolds number for the Grid 1 data and Grid 2 data respectively. The peak value of the u'/u_τ is

about 2.3 at y+ = 13. The approximate similarity in wall units, u'/u_τ against y+ seems to be in good agreement with the data of Castro (ref. 16) and of Purtell et al. (ref. 8).

Recalling that the mean velocity profiles have shown law-of-the-wall similarity even at these low Reynolds numbers, a Reynolds number effect seems to persist in the turbulence intensity beyond the peak locations (y+ > 13) in Figs. 9 and 10. The lower the value of Re, the lower the values of u' in the outer portion of the boundary layer. This decrease in u' might be caused by the suppression of all but the largest scales of turbulence as the Reynolds number decreases (refs. 26 and 27). The variation is much less pronounced in the present experiment because of the very limited range of Reynolds number. Figs. 11 and 12 show the disturbance spectra measured along the line of maximum amplitude with increasing distance from the leading edge for grids 1 and 2 respectively. The averaging time for these spectra is 2 minutes and the Tollmien-Schlichting band is out to about 150 Hz. As mentioned earlier, the turbulence levels of these grids are 5-6% and 6-7% respectively, and the mean profiles exhibited the behavior of fully-developed turbulent flow. Although a plot of the amplitude ratio versus downstream distance is not presented here, one can easily see from figures 11 and 12 that there is no evidence of significant growth or decay of disturbances anywhere in the frequency range of 0 to 250 Hz.

This behavior is very interesting. However, this result cannot be conclusive until one examines all of the causes which could affect the growth or decay of the disturbances, and analyze the individual effects separately. Nevertheless, it is peculiar. The behavior will appear even more anomalous after we look at the fashion of growing turbulence without the presence of a grid in the next section. As a matter of fact, for this short region of the analysis the amount of decay of the disturbances generated by grid 1 and 2 was not significant.

3.4 Transitional behavior (No-grid data analysis)

Figure 13 shows the development of the boundary layer for the no grid data with increasing distance from the leading edge. The reference parameter δ here is calculated from the integral quantities H and δ^* using the relation, $\delta/\delta^* = (H+1)/(H-1)$ rather than attempting to select it from the scattered points of the measured profiles.

Length Reynolds numbers for these profiles are in the range between 20,000 to 70,000. None of these profiles shows the standard laminar flow behavior and the flow is believed to be undergoing transition.

The u' spectral data of these profiles are shown in Fig.14. These spectra are again taken at the height in the boundary layer where disturbance amplitude is maximum.

A typical disturbance spectrum outside the boundary layer is

shown in Fig. 15 along with those for Grids 1 and 2. The turbulent intensities in the boundary layer are of the order of 10 times the free stream level (Fig. 16). The relative amplitudes of some selected frequencies are shown in Fig. 17. Due to the technical difficulties experienced, the accuracy of these data is doubtful, however, it is possible to extract some limited information from this test. General behavior of the disturbances shows more or less a resemblance to what is obtained in linear stability studies although with an enormous difference in the magnitudes. Amplitudes of large eddies having low frequencies are dominant, and show less variance in proceeding downstream, while those of the small eddies grow faster. But once when all the disturbances underwent some transition - at 15 cm where the shape factor is 1.9 - neither noticable growth nor decay are observed. This trend is very much consistent with the one which was examined from Grids 1 and 2 data earlier.

CHAPTER 4

SUMMARY AND CONCLUSIONS

1. No standard laminar flow was observed in any of the measured profiles. Turbulent profiles are identified for Re_θ as low as 280.
2. At turbulence levels of about 1-1/2% (no grid) the boundary layer is transitional over the measurement domain. Transition occured progressively sooner as the turbulence level was increased using grids.
3. No wake strengths are observed for the turbulent mean flow profiles at turbulence levels of 5% - 7% (grids 1 and 2).
4. The existence of the log-linear region even at Re_θ as low as 280 makes it possible to deduce the wall skin friction by fitting the mean profile to the law of the wall formula. The skin friction distribution thus obtained closely follows that calculated from the law of the wall with Coles constants and with zero wake strength.
5. The sharp decrease in shape factor with Reynolds number at turbulence levels of 5% - 7% is consistent with the expectation for zero wake strength.

REFERENCES

1. Graham, R.W.: Fundamental mechanisms that influence the Estimate of Heat Transfer to Gas Turbine Blades. NASA Tech. Memo 79128, August, 1979.

2. Wygnanski, I.J. and Champagne, F.H.: On transition in a pipe. Part I. The origin of puffs and slugs and the flow in a turbulent slug, JFM 59 Part 2, 1973, pp. 281-335.

3. Wygnanski, I.J., Sokolov, M. and Friedman, D.: On transition in a pipe, Part 2, The equilibrium puff, JFM 69 Part 2, May 1975, pp. 283-304.

4. Stuart, J.T.: On the non-linear mechanics of wave disturbances in stable and unstable parallel flows, Part 1. The basic behavior in plane Poiseuille flow. JFM Vol. 9, pt. 3, 1960, pp. 353-370.

5. Watson, J.: On the non-linear mechanics of wave disturbances in stable and unstable parallel flows, Part 1. The basic behavior in plane Poiseuille flow. JFM Vol. 9, pt. 3, 1960, pp. 353-370.

6. Herbert, T.: Finite Amplitude Stability of Plane Parallel Flows. AGARD-CP-224, 1977, pp. 3-1 to 3-10.

7. Morkovin, M.V.: On the Question of Instabilities Upstream of Cylindrical Bodies. NASA Contractor Report 3231, December 1979.

8. Purtell, L.P., Klebanoff, P.S., Buckley, F.T.: Turbulent Boundary Layer at Low Reynolds Number, Phys. Fluids 24(5), May 1981, pp. 802-811

9. Charnay, G., Compte-Bellot, G., and Mathieu, J.: Development of a Turbulent Boundary Layer on a Flat Plate in an External Turbulent Flow, AGARD CP93 Paper No. 27, 1971.

10. McDonald, H., Kreskovsky, J.P.: Effect of free stream turbulence on the turbulent boundary layer, Int. J. Heat Mass Transfer, Vol. 17. pp. 705-716.

11. Robertson, J.M., and Holt, C.F.: Stream Turbulence Effects on Turbulent Boundary Layers, J. Hydraulics Division, Proc. ASCE, Vol. 93, HY6, 1972, pp. 1095-1099.

12. Meier, H.U. and Kreplin, H.P.: Influence of Freestream Turbulence on Boundary Layer Development, AIAA Journal, Vol. 18, No. 1, 1980, pp. 11-15.

13. Hancock, P.E.: Effect of Freestream Turbulence on Turbulent Boundary Layers, Ph.D. thesis, Imperial College, University of London, 1980.

14. Blair, M.F.: Influence of Freestream Turbulence on Turbulent Boundary Layer Heat Transfer and Mean Profile Development, Part I - Experimental Data, Journal of Heat Transfer Feb. 1983, Vol. 105, pp. 33-40.

15. Blair, M.F.: Influence of Freestream Turbulence in Turbulent Boundary Layer Heat Transfer and Mean Profile Development, Part II - Analysis of Results, Journal of Heat Transfer Feb. 1983, Vol. 105, pp. 41-47.

16. Castro, I.P.: Effects of Free Stream Turbulence on Low Reynolds Number Boundary Layers, ASME Jour. Fluids Engineering, vol. 106, Sept. 1984, pp. 298-306.

17. Taylor, G.I.: The Statistical Theory of Isotropic Turbulence, Journal of the Aerospace Sciences, Vol. 4, 1937, pp. 311-315.

18. Dryden, H.L., Schubauer, G.B., Mook, W.C, Jr. and Skramstad, H.K.: Measurements of Intensity and Scale of Wind Tunnel Turbulence Levels in the External Free Stream, Paper 76-05, Proceedings of the Tenth Congress of the International Council of Aerospace Sciences (ICAS), Ottawa/Canada, 1976, pp. 89-99.

19. Coles, D.E.: The Turbulent Boundary Layer in a Compressible Fluid, RAND Corporation Report R-403-PR, 1962.

20. Musker, A.J.: Explicit Expression for the Smooth Wall Velocity Distribution in a Turbulent Boundary Layer, AIAA Journal Vol. 17, No. 6, June, 1979, pp. 655-657.

21. Landweber, L.: The Frictional Resistance of Flat Plates in Zero Pressure Gradient, Trans. SNAME, Vol. 61, 1953, pp. 5-32.

22. Granville, P.S.: Drag and Turbulent Boundary Layer of Flat plates at Low Reynolds Numbers, J. Ship Res. 21, 1, 30 (1977).

23. Preston, J.H.: The minimum Reynolds number for a turbulent boundary layer and the selection of a transition device, J. Fluid Mechanics 3, 373 (1958).

24. Simpson, R.L.: Characteristics of turbulent boundary layers at low Reynolds numbers with and without transpiration, Journal of Fluid Mechanics, Vol. 42, Part 4, July 1970, pp. 769-802.

25. Smits, A.J., Matheson, N., Joubert, P.N.: Low-Reynolds-Number Turbulent Boundary Layers in Zero and Favorable Pressure Gradients, Journal of Ship Research, Vol.27, No. 3, September 1983, pp. 147-157.

26. Klebanoff, P.S., Tidstrom, K.D., and Sargent, L.M.: The three-dimensional nature of boundary-layer instability, J. Fluid Mechanics, 12, 1 (1962).

27. Head, M.R., Bandyopadhyay, P.: New Aspects of turbulent boundary-layer structure, J. Fluid Mechanics, (1981), Vol. 107, pp. 297-338.

28. Huffman, G.D., and Bradshaw, P.: A Note on von Karman's Constant in low Reynolds number turbulent flows, Journal of Fluid Mechanics, Vol. 53, 1972, pp. 54-60.

29. Murlis, J., Tsai, H.M., and Bradshaw, P.: The structure of turbulent boundary layers at low Reynolds numbers, J. Fluid Mechanics, (1982), Vol. 122, pp. 13-56.

TABLE I

BOUNDARY LAYER PROFILE CHARACTERISTICS

No-Grid; Rounded L.E shape

Location	δ^* mm	θ mm	H	Re_θ	u_e m/sec	C_p	U_τ m/sec	$C_f \times 10^3$
3	1.400	.440	3.18	187	6.69	-.145		
6	1.575	.641	2.46	264	6.45	-.066		
9	1.616	.718	2.25	286	6.24	.002		
12	1.451	.684	2.12	276	6.33	-.025		
15	1.747	.919	1.90	366	6.25	.000		
18	1.663	.893	1.86	360	6.32	-.023		

No-Grid; Modified L.E shape

Location	δ^* mm	θ mm	H	Re_θ	u_e m/sec	C_p	U_τ m/sec	$C_f \times 10^3$
5	1.274	.514	2.48	209	6.39	-.045		
10	1.402	.653	2.15	260	6.26	-.005		
15	1.652	.810	2.04	322	6.25	.000		
20	1.939	1.051	1.84	419	6.27	-.007		
25	2.022	1.125	1.79	451	6.27	-.009		
30	2.087	1.214	1.72	488	6.31	-.022		

Grid 1

Location	δ^* mm	θ mm	H	Re_θ	u_e m/sec	C_p	U_τ m/sec	$C_f \times 10^3$
3	.956	.409	2.34	170	6.55	-.147		
6	1.272	.668	1.90	253	5.94	.056		
9	1.268	.747	1.70	279	5.87	.078	.341	6.76
12	1.619	1.045	1.55	400	6.00	.037	.335	6.24
15	1.825	1.213	1.50	473	6.12	.000	.332	5.91
18	1.976	1.371	1.44	532	6.09	.009	.329	5.85

ORIGINAL PAGE IS
OF POOR QUALITY

TABLE I (Concluded)

Grid 2

Location	δ^* mm	θ mm	H	Re_θ	u_e m/sec	C_p	U_τ m/sec	$C_f \times 10^3$
3	1.039	.434	2.40	173	6.23	-.039		
6	1.228	.719	1.71	280	6.09	.005	.351	6.63
9	1.516	.959	1.58	375	6.11	-.002	.341	6.24
12	1.619	1.105	1.47	432	6.11	-.002	.335	6.02
15	1.745	1.213	1.44	475	6.11	.000	.332	5.92
18	1.827	1.288	1.42	505	6.12	-.005	.329	5.79

Grid 3

Location	δ^* mm	θ mm	H	Re_θ	u_e m/sec	C_p	U_τ m/sec	$C_f \times 10^3$
5	1.129	.529	2.13	212	6.24	-.069		
10	1.460	.827	1.77	326	6.16	-.042		
15	1.797	1.134	1.58	439	6.03	.000		
20	2.242	1.591	1.41	619	6.07	-.011	.317	5.45
25	2.407	1.709	1.41	667	6.09	-.018	.311	5.22
30	2.598	1.841	1.41	743	6.29	-.087		

TABLE II

EVALUATION OF u_τ BY LEAST SQUARES SCANNING

Location	Grid-type	u_τ (m/sec)	Y_o (cm)	Error (m^2/sec^2)	Remark
6 cm	G2	.338	.013	.890	W.final pts.
		.341	"	.797	W.0 "
9 cm	"	.332	"	.668	W. "
		.335	.010	.593	W.0 "
12 cm	"	.329	.018	.468	W. "
		.332	"	.287	W.0 "
15 cm	"	.326	.020	.320	W. "
		.329	"	.246	W.0 "
18 cm	"	.323	.023	.304	W. "
		.326	.020	.194	W.0 "
9 cm	G1	.326	.013	1.261	W. "
12 cm	"	.323	.015	.823	W. "
15 cm	"	.323	.015	.812	W. "
18 cm	"	.317	.018	.838	W. "
20 cm	G3	.317	.018	.961	W. "
25 cm	"	.311	.018	1.135	W. "

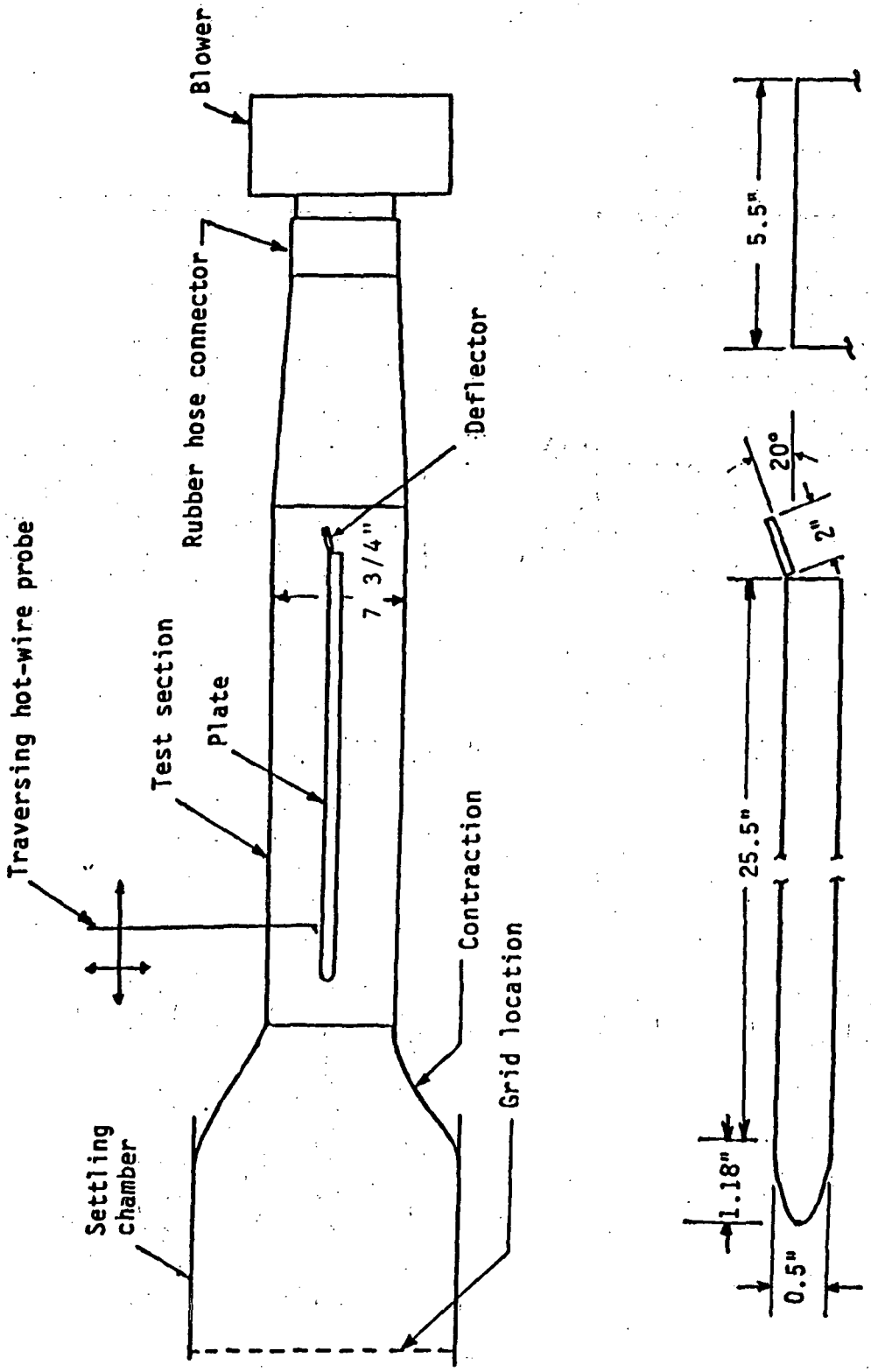

Fig. 1 Schematic diagrams of wind tunnel and test plate.

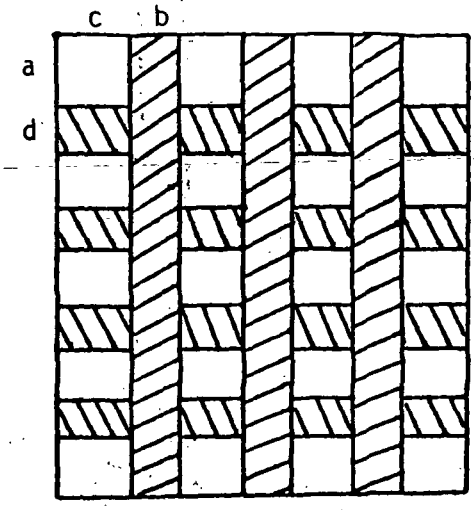

Grid 1

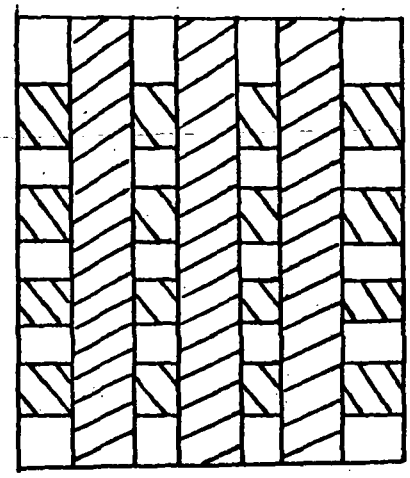

Grid 2

Grid	a	b	c	d
1	4.4	3.8	5.7	4.4
2	3.5	4.4	3.2	5.1
3	2.5	1.2	2.5	1.0

(cm)

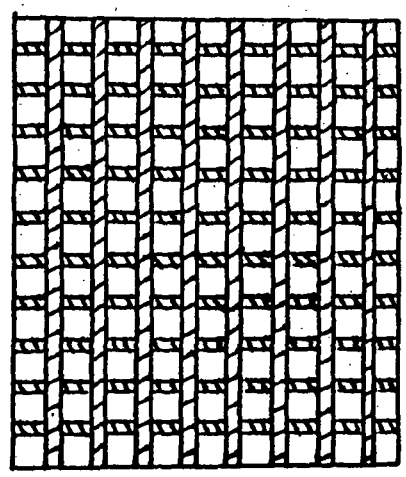

Grid 3

Fig. 2 Shapes and Dimensions of Grids

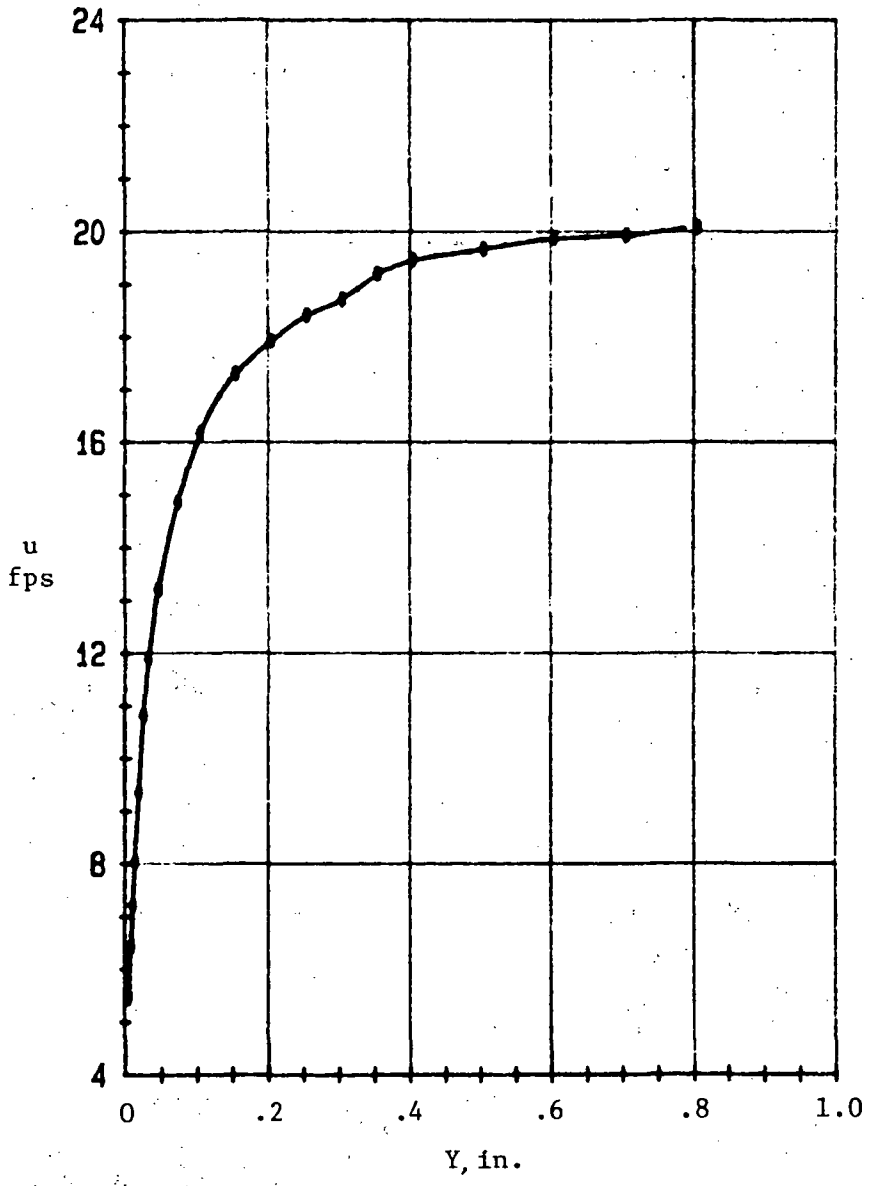

Fig. 3 One of the fitted profiles by Cubic Spline Interpolation and the corresponding measured profile.

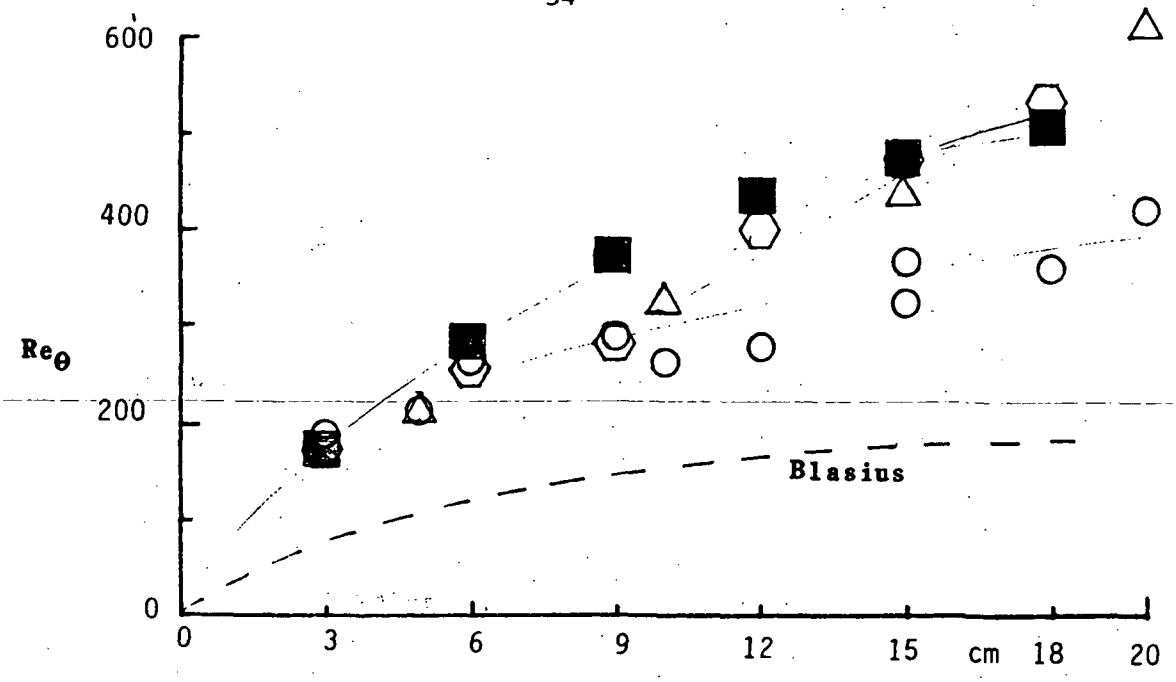

Fig.4a Effect of the Free Stream Level on Reynolds number

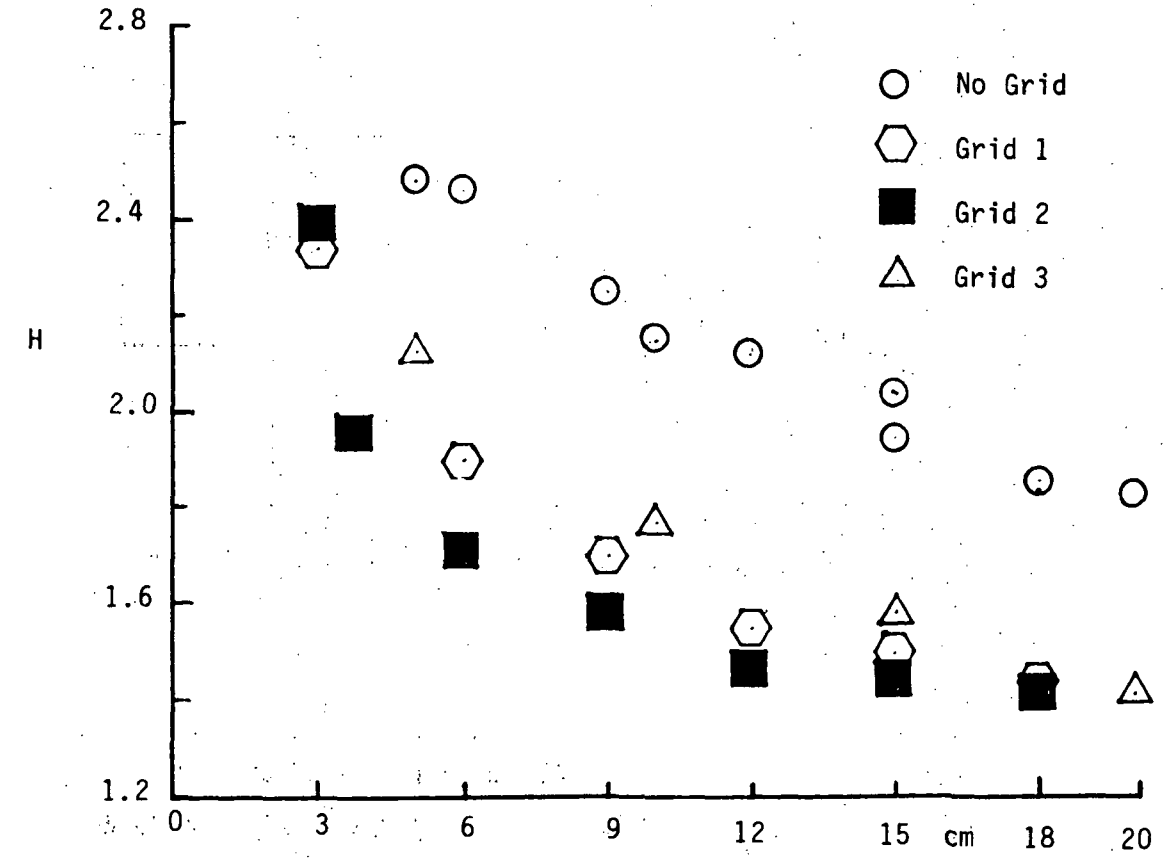

Fig.4b Variation of shape factor,H along the streamwise distance from leading edge

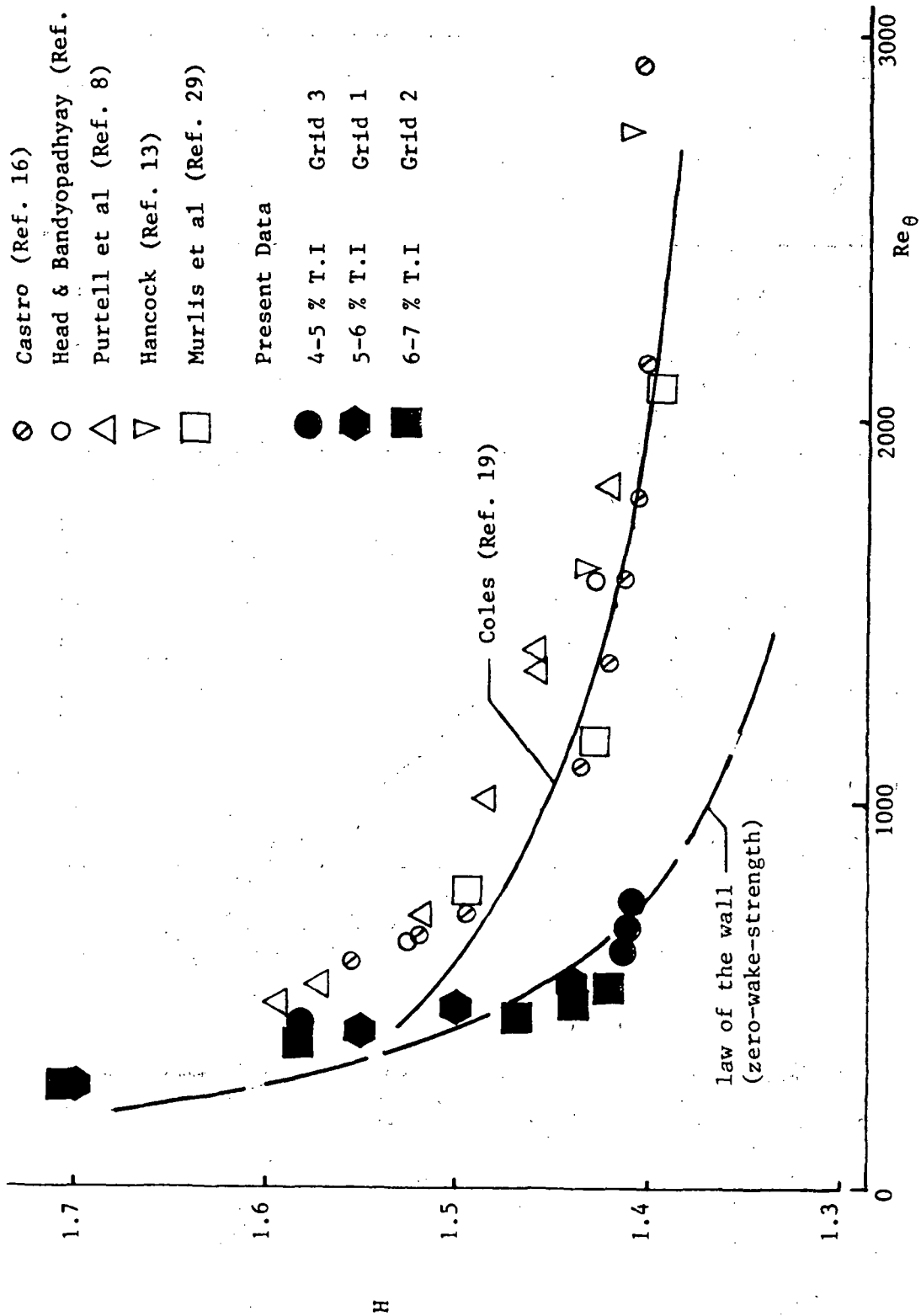

Fig.5. Variation of shape factor H, with Reynolds number

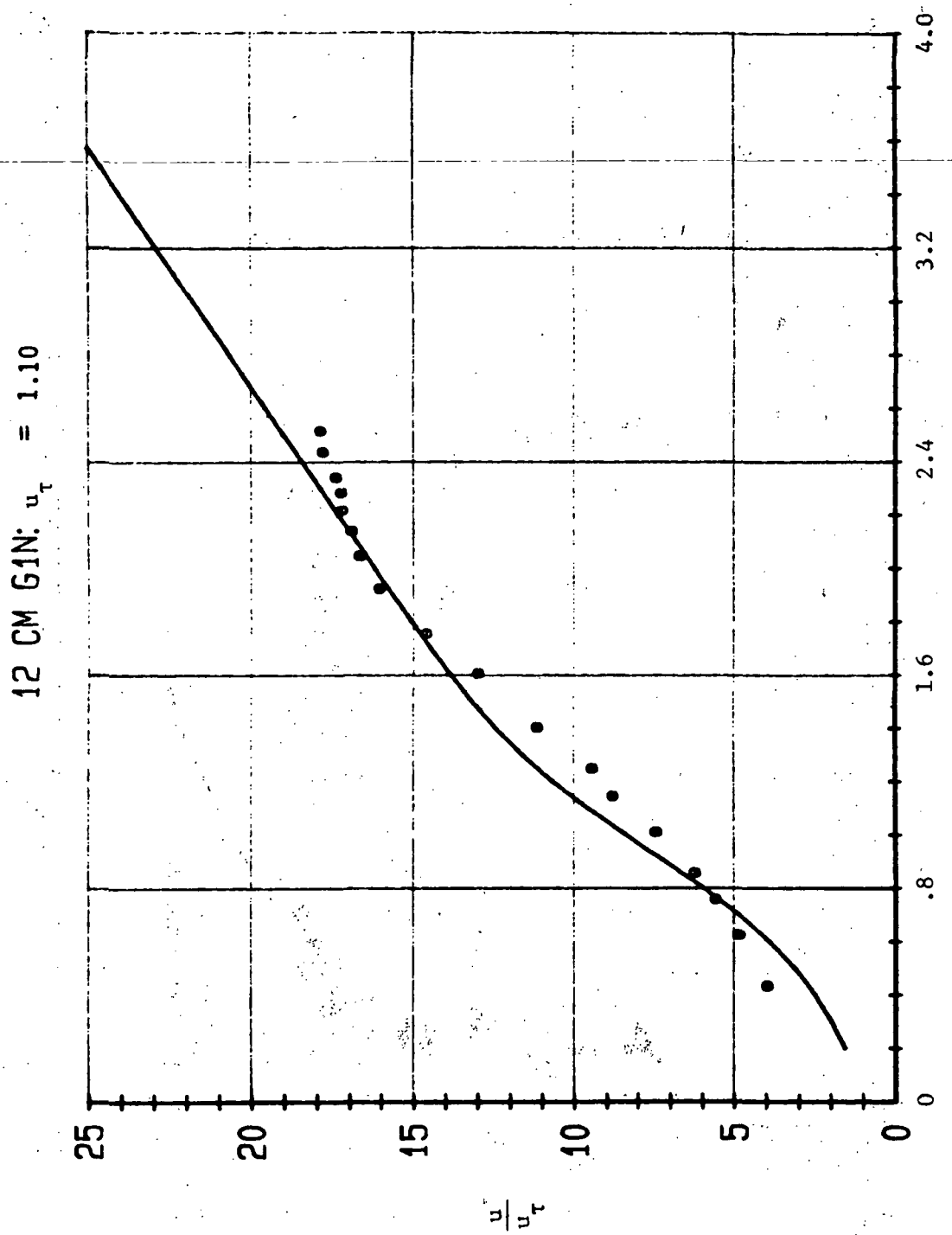

Fig.6a Mean Velocity Profile at 12 cm with Grid 1.

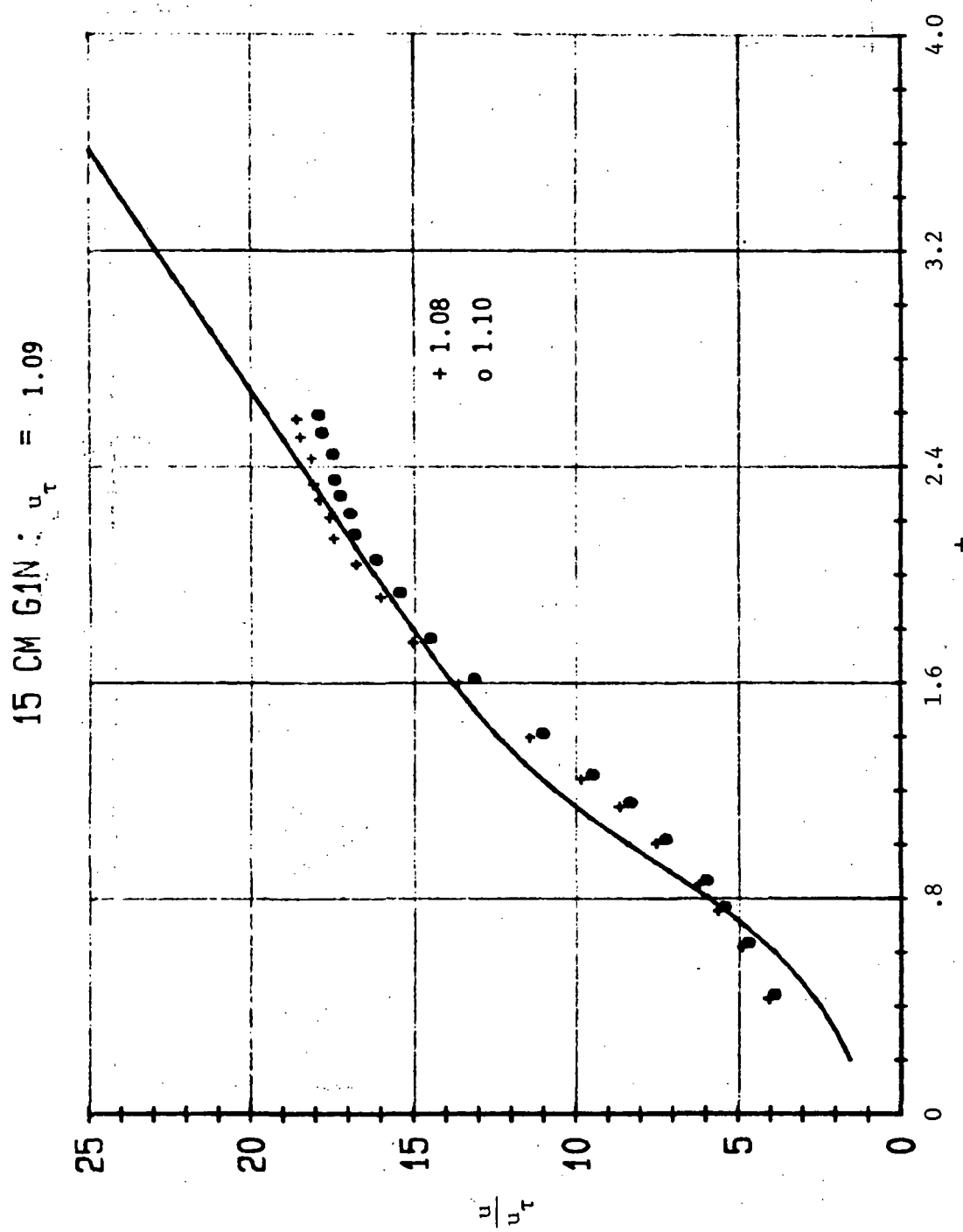

Fig.6b Mean Velocity Profile at 15 cm with Grid 1
showing a selection of friction velocity u_τ

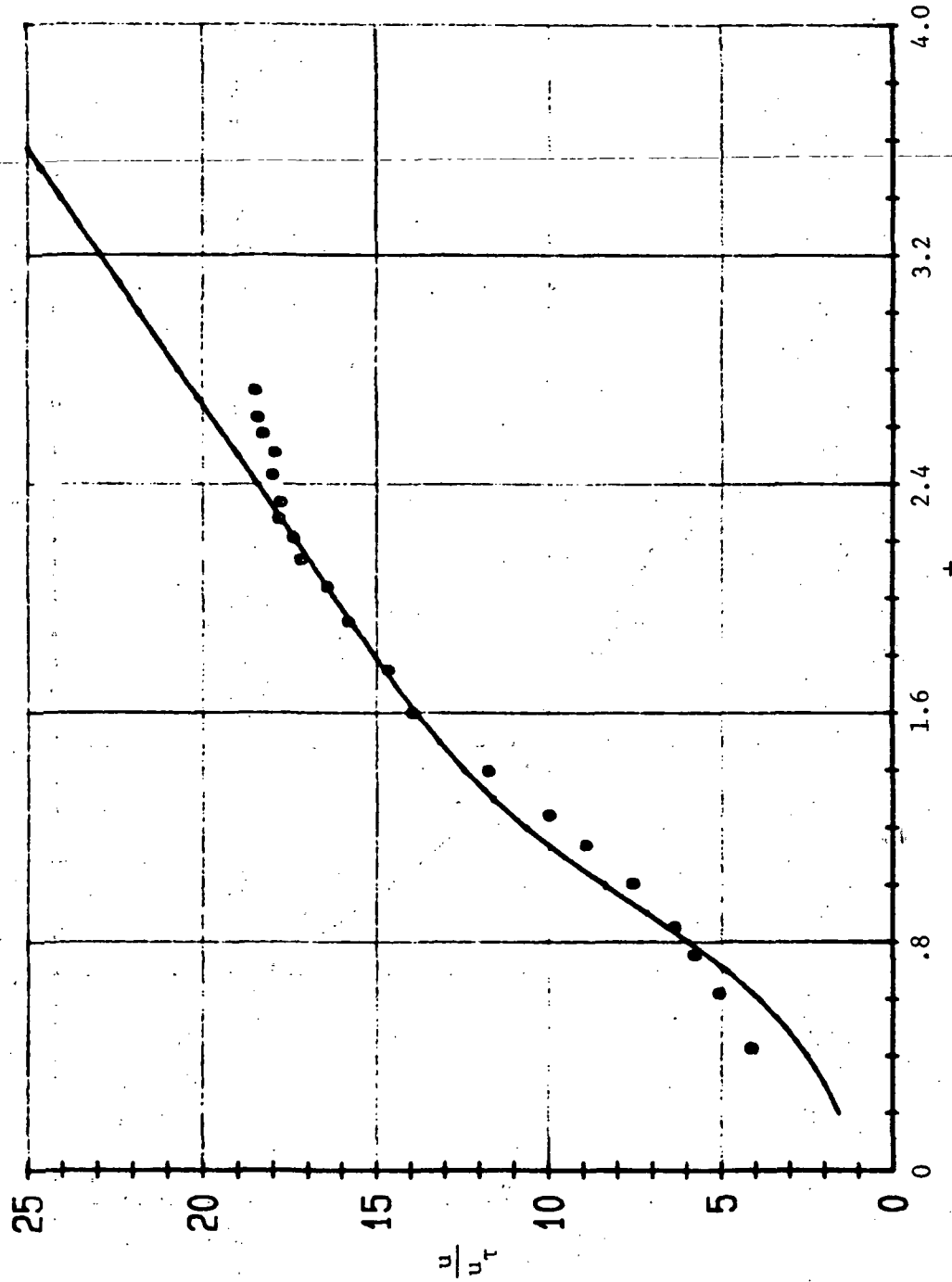

Fig.6c Mean Velocity Profile at 18 cm with Grid 1.

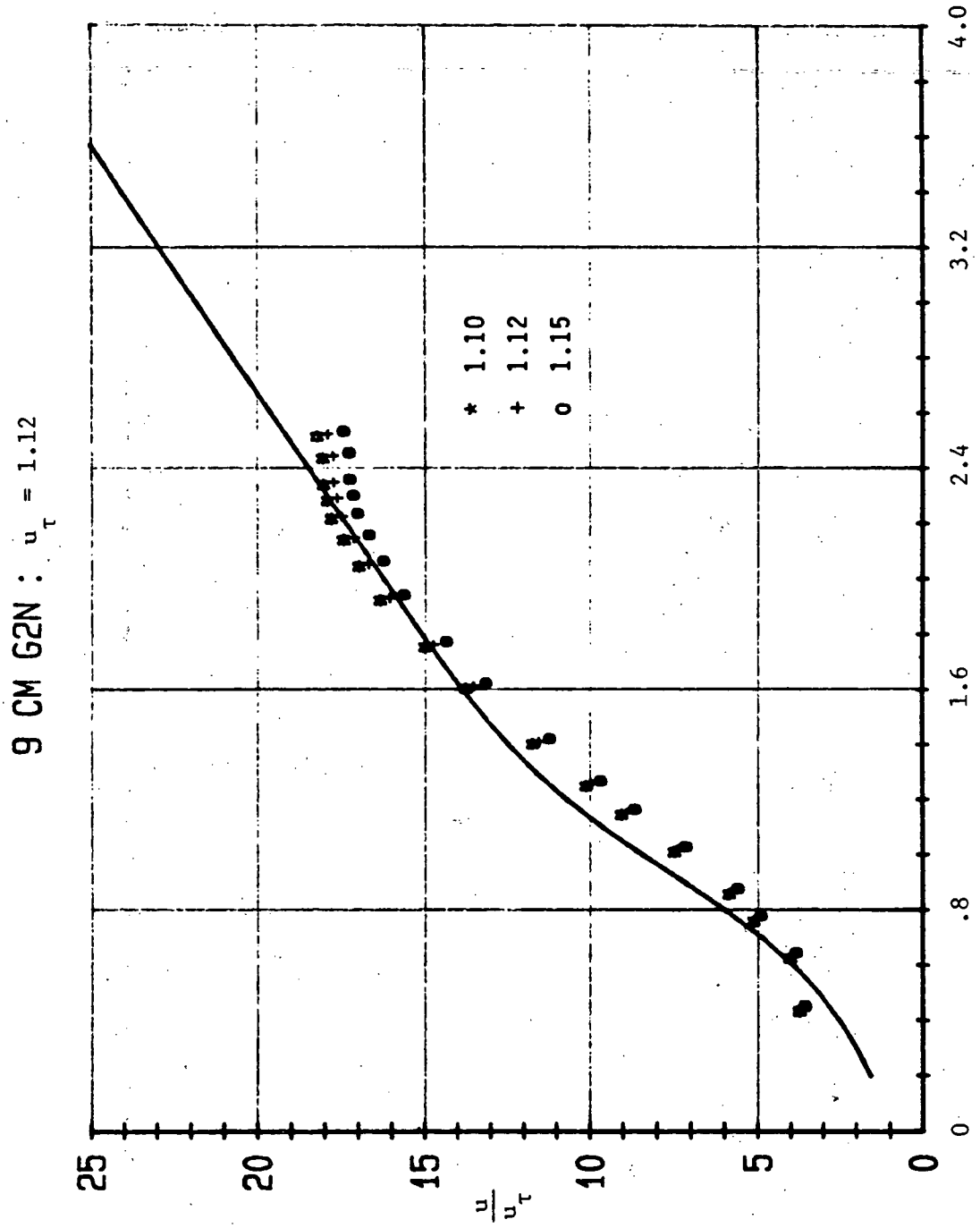

Fig.6d Mean Velocity Profile at 9 cm with Grid 2
showing a selection of friction velocity u_τ

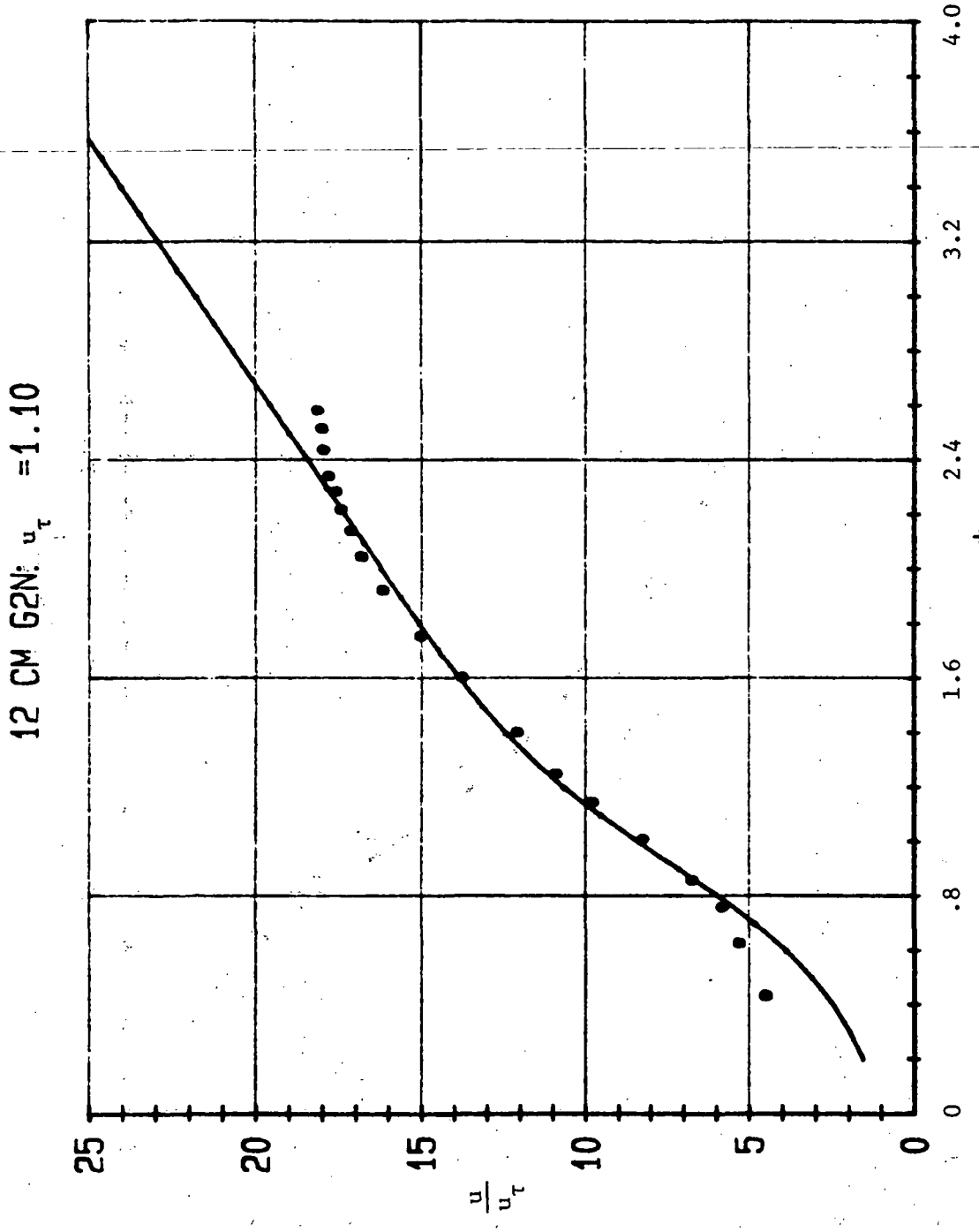

Fig. 6e Mean Velocity Profile at 12 cm with Grid 2.

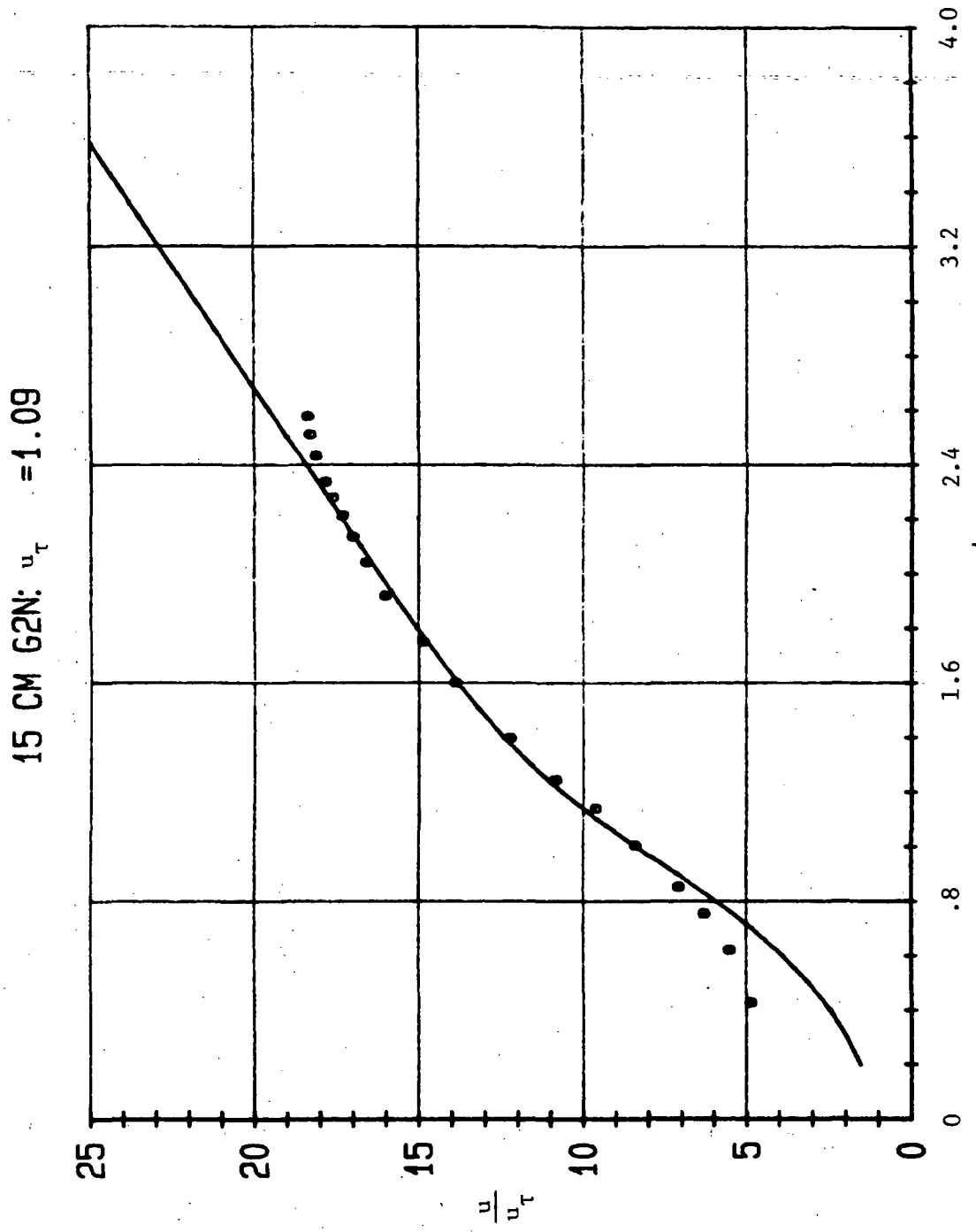

Fig.6f Mean Velocity Profile at 15 cm with Grid 2.

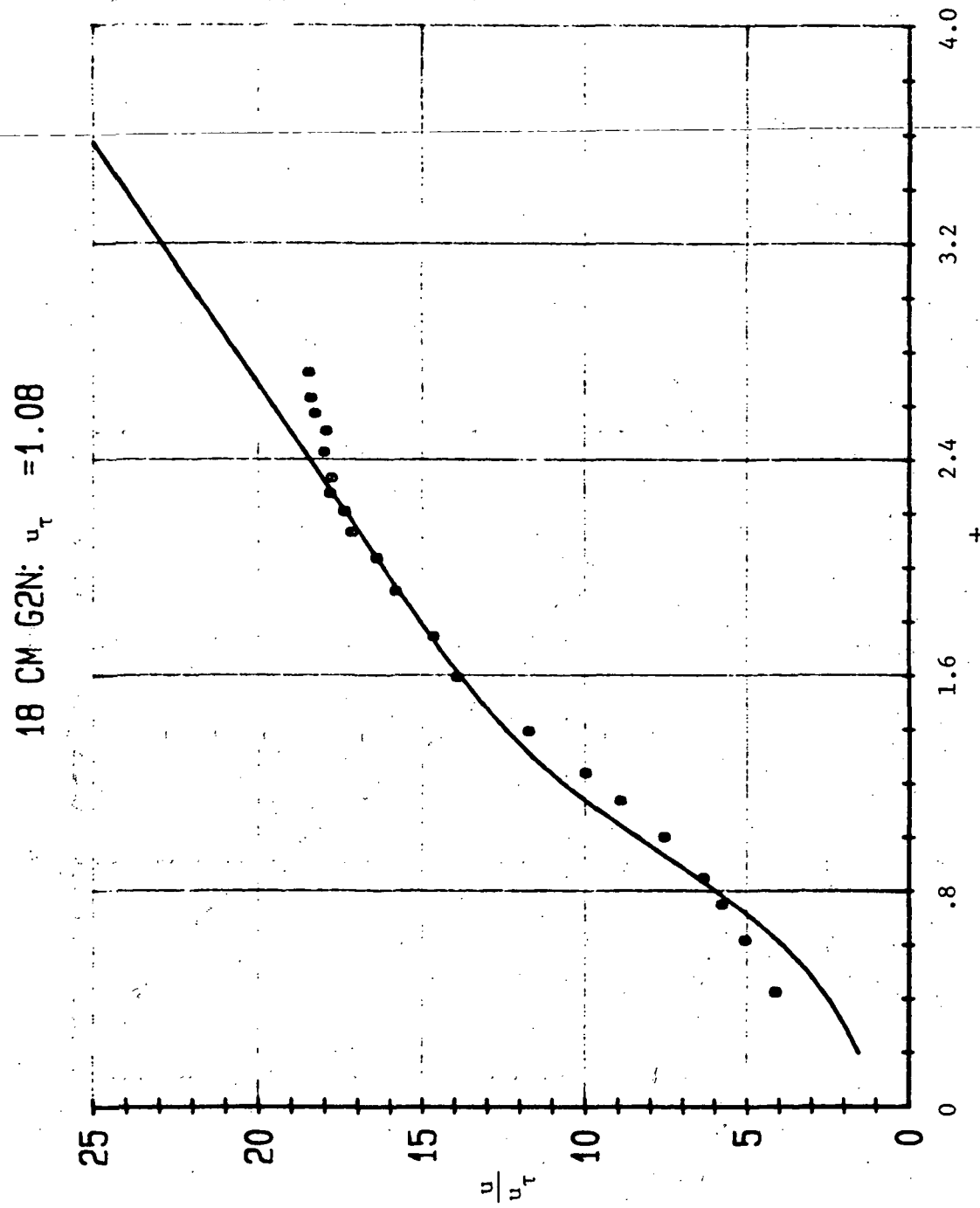

Fig.6g Mean Velocity Profile at 18 cm with Grid 2.

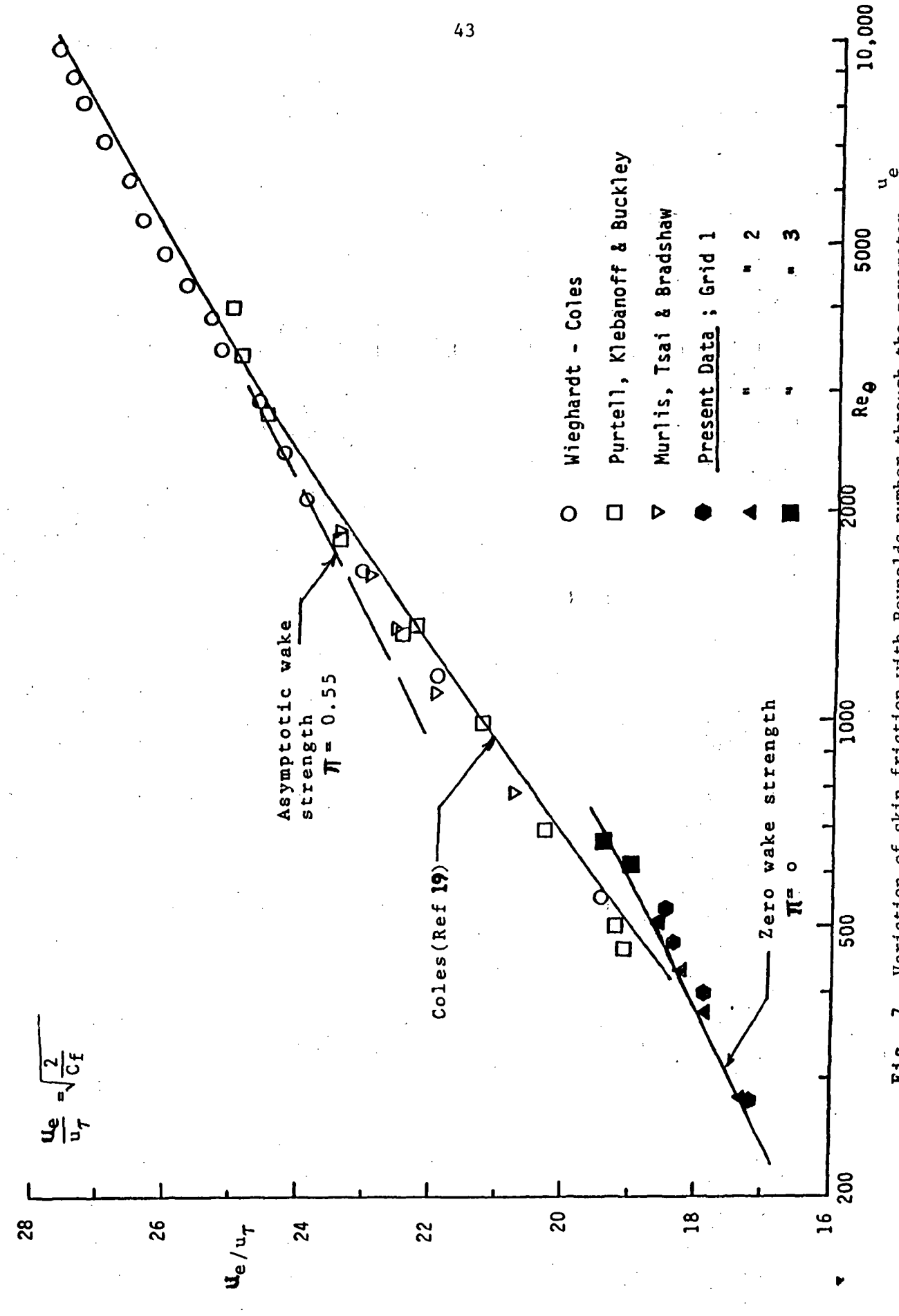

Fig. 7. Variation of skin friction with Reynolds number through the parameter $\frac{u_e}{u_\tau}$, comparison with other data.

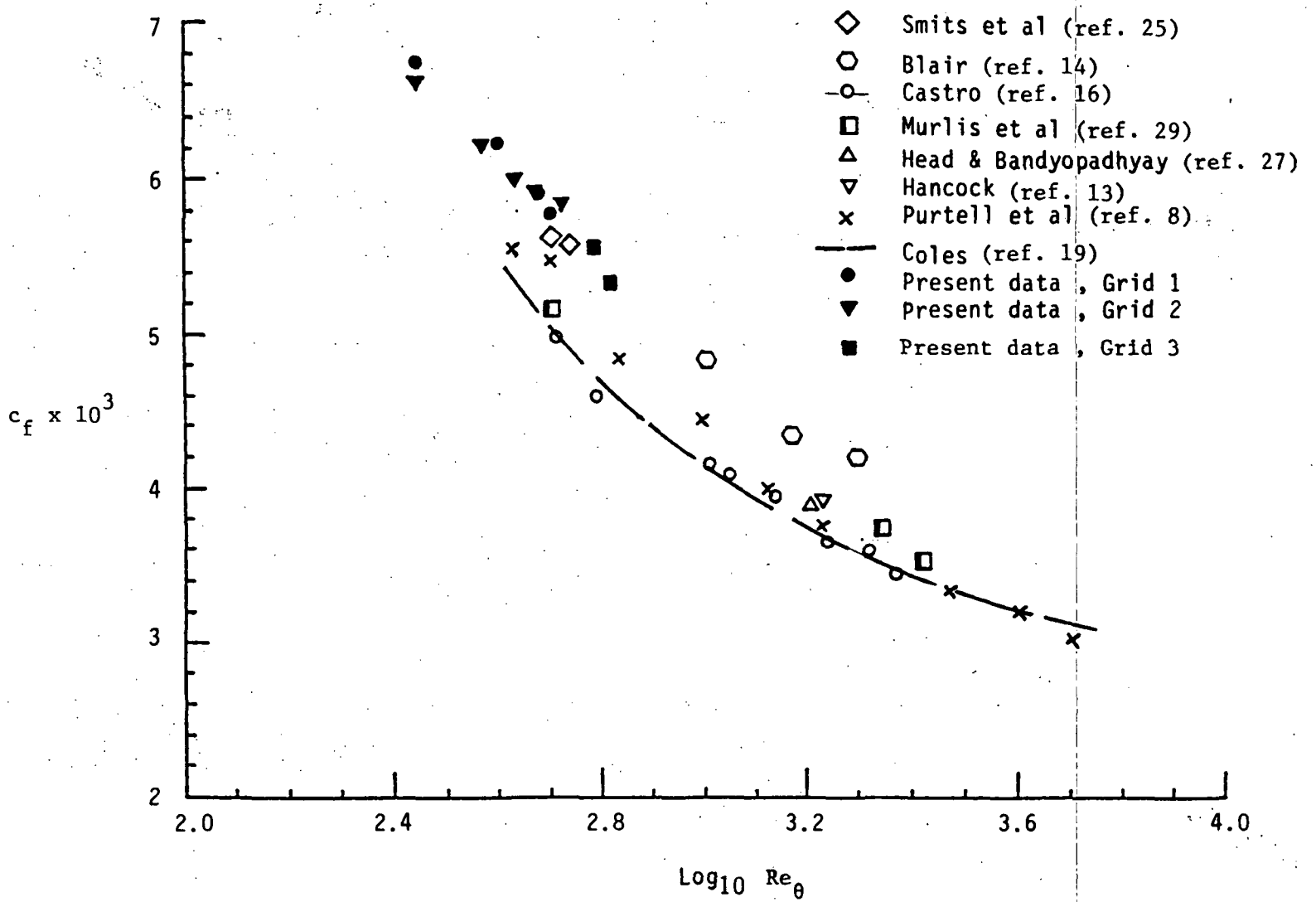

Fig.8. Variation of skin friction with Reynolds number, Re_θ comparison with additional set of data

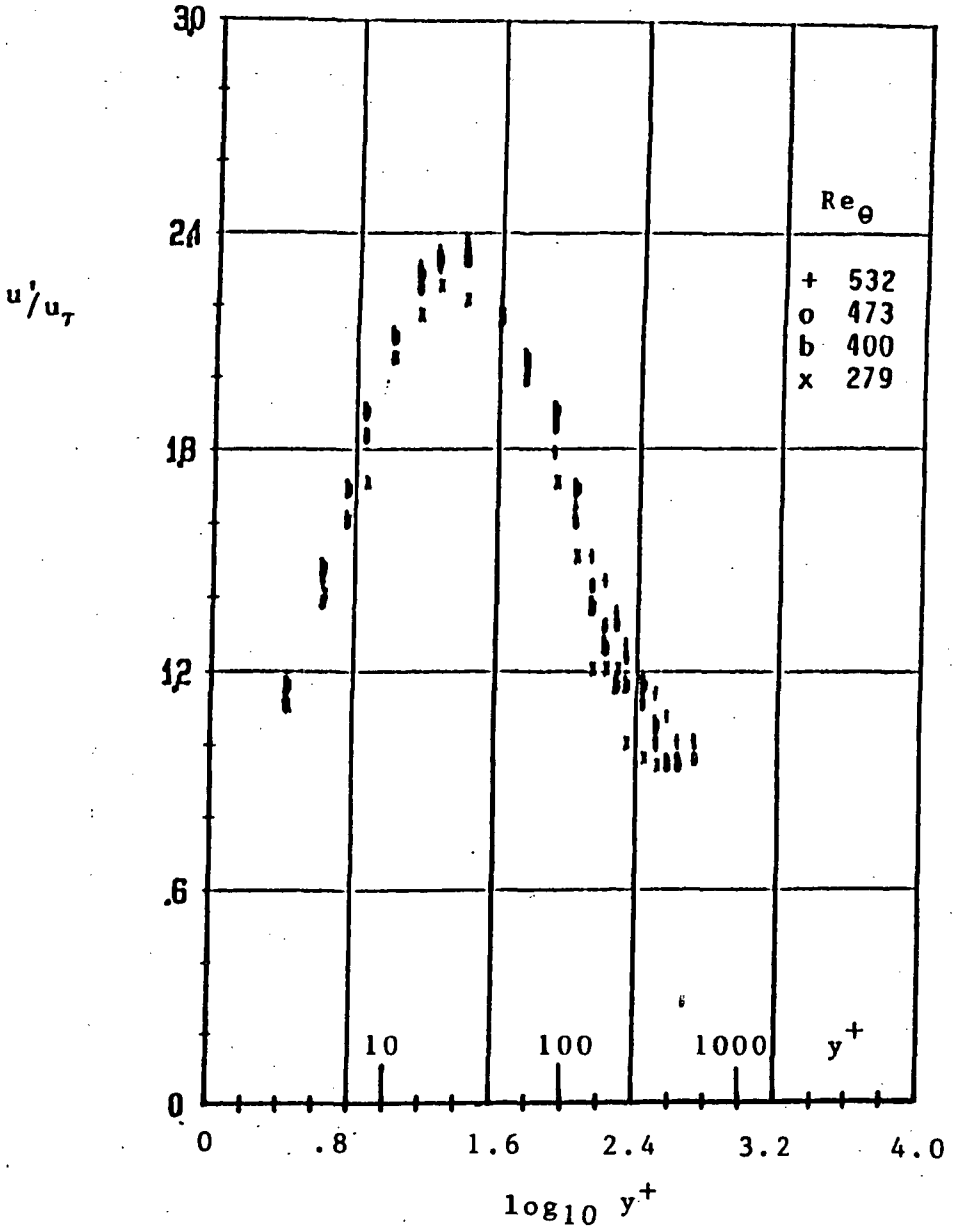

Fig. 9. Distribution of longitudinal fluctuating velocity, Grid 1.

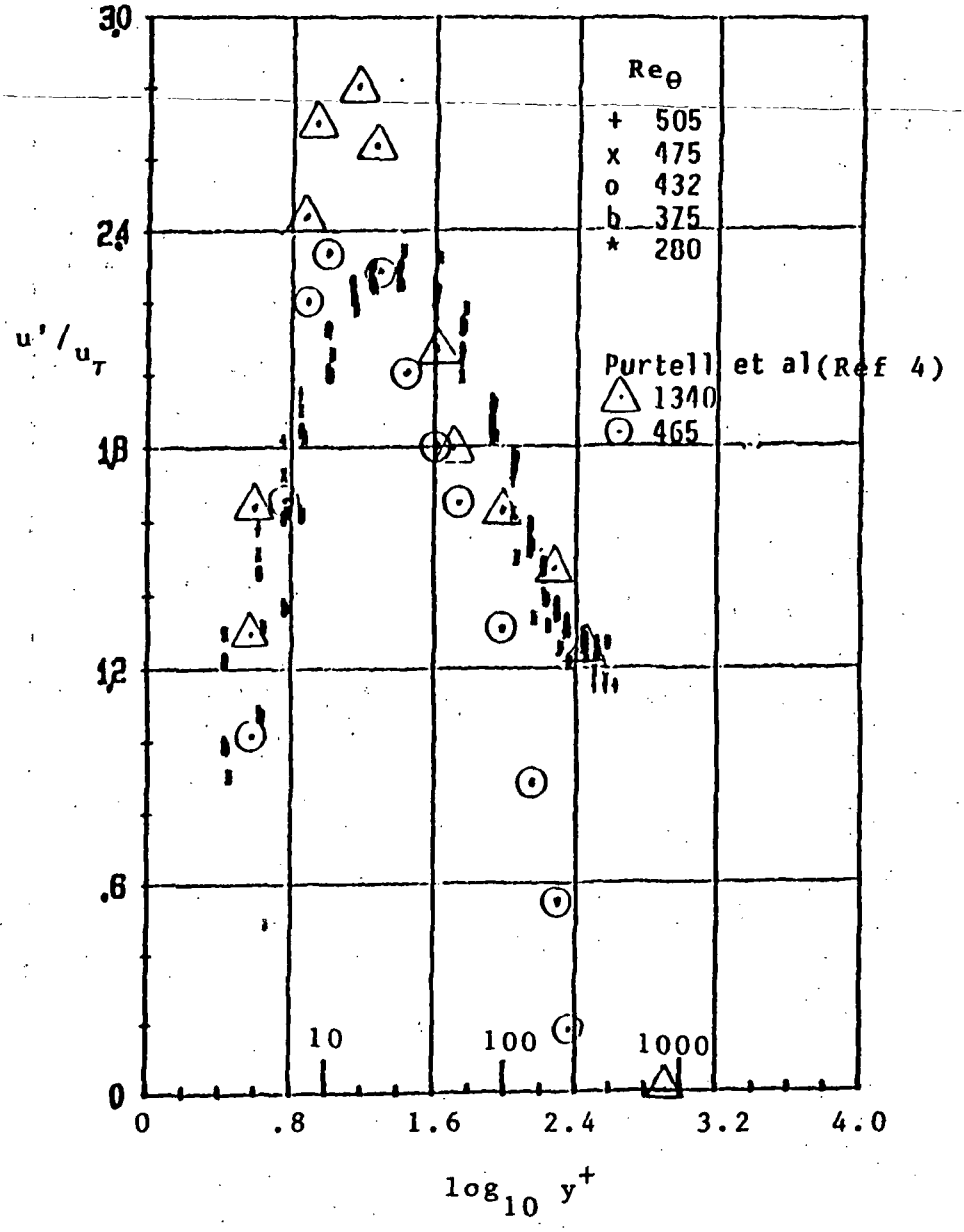

Fig. 10. Distribution of longitudinal fluctuating velocity, Grid 2

ORIGINAL PAGE IS
OF POOR QUALITY

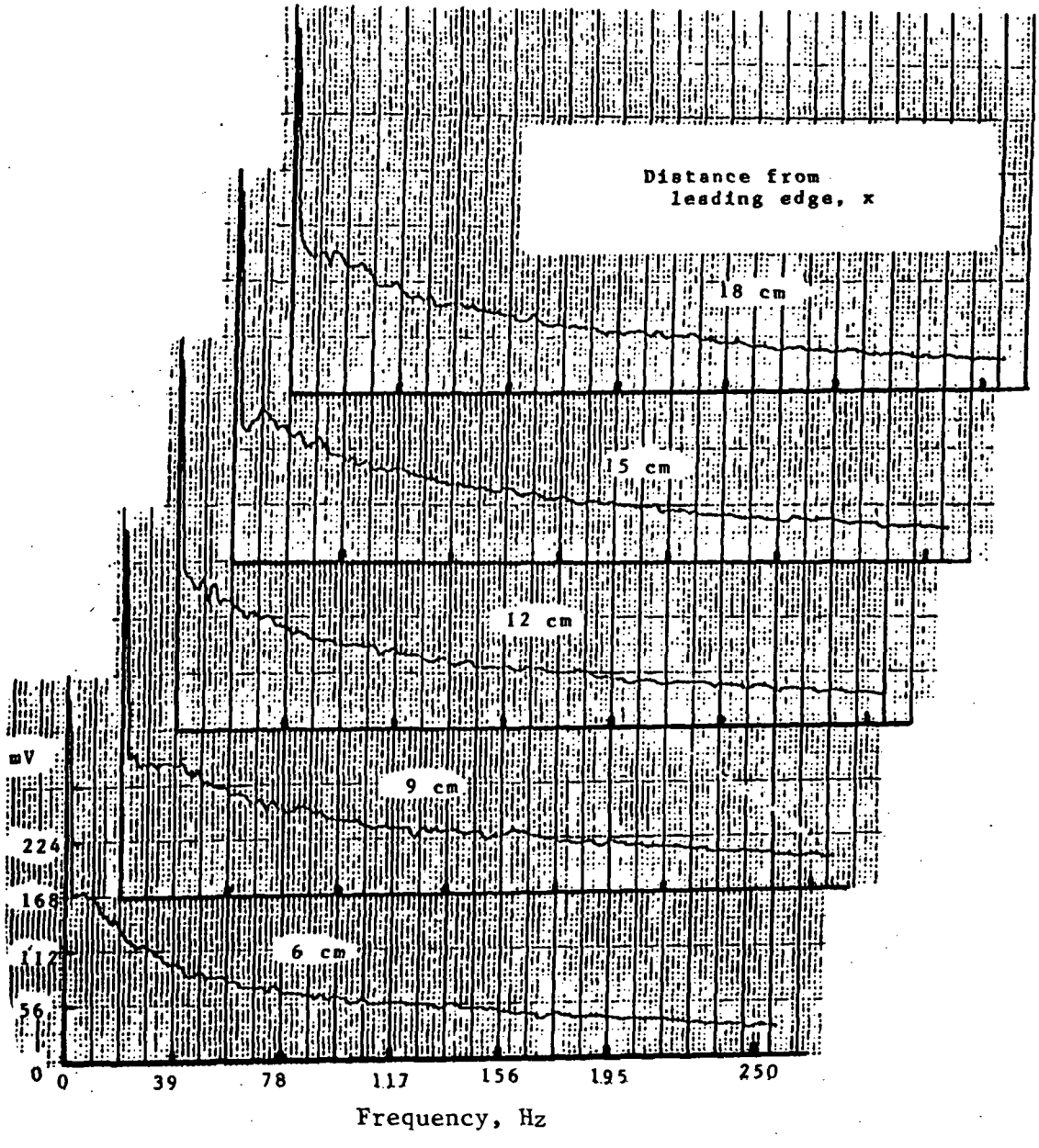

Fig. 11. Disturbance spectra measured along the line of maximum amplitude, Grid 1

ORIGINAL PAGE IS
OF POOR QUALITY

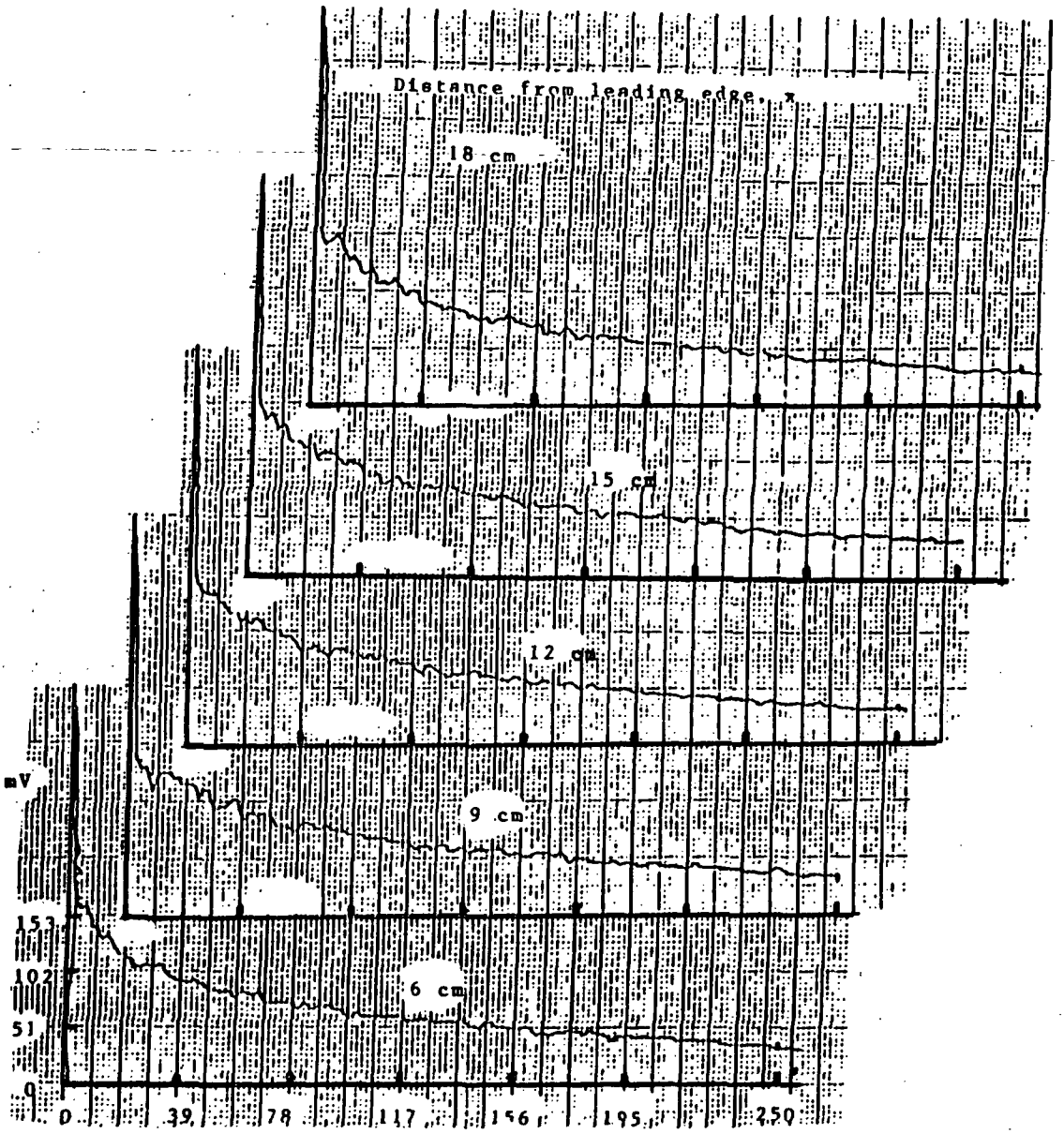

Fig. 12. Disturbance spectra measured along the line of maximum amplitude, Grid 2

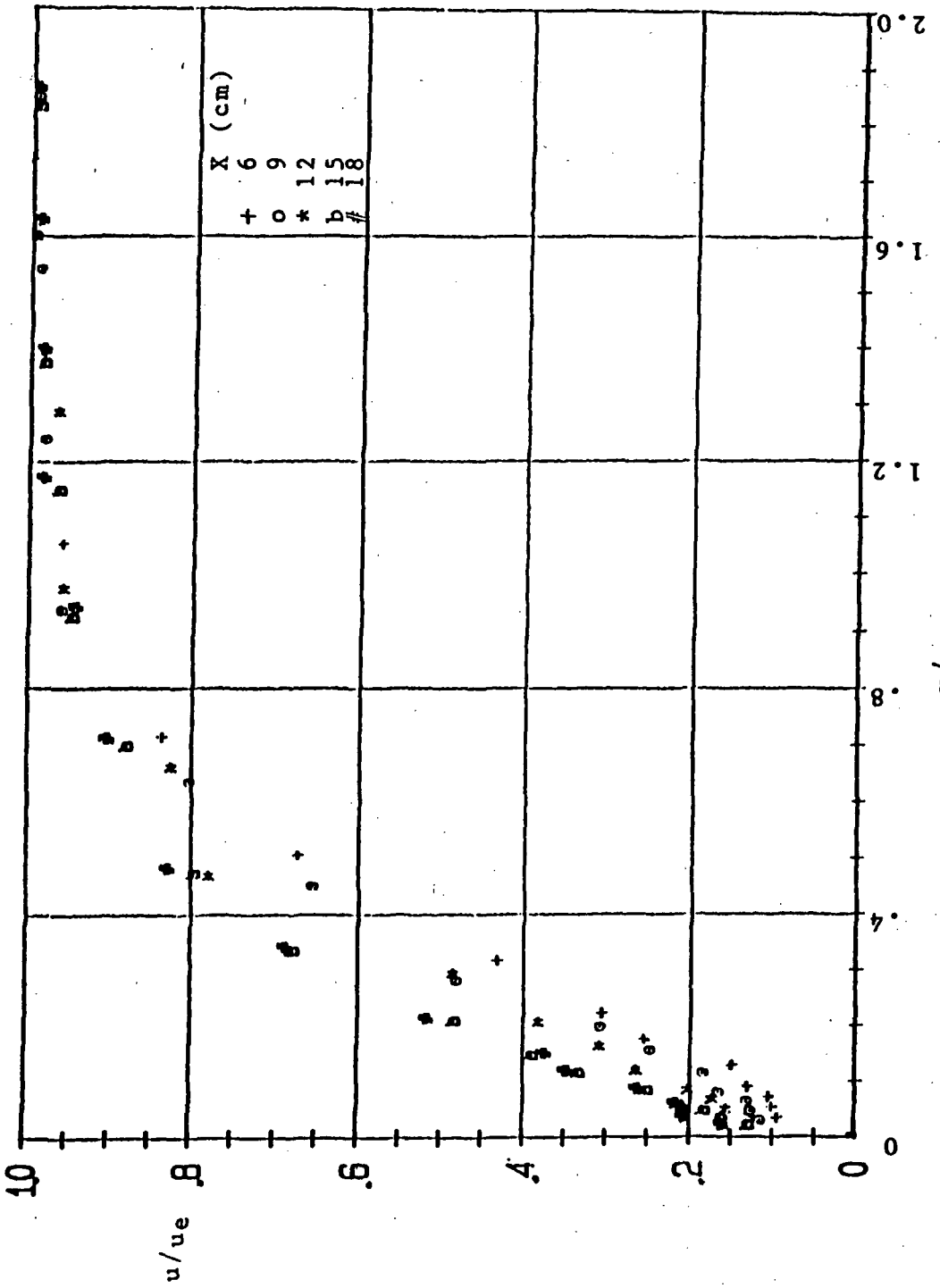

Fig. 13. Development of the boundary layer, No Grid

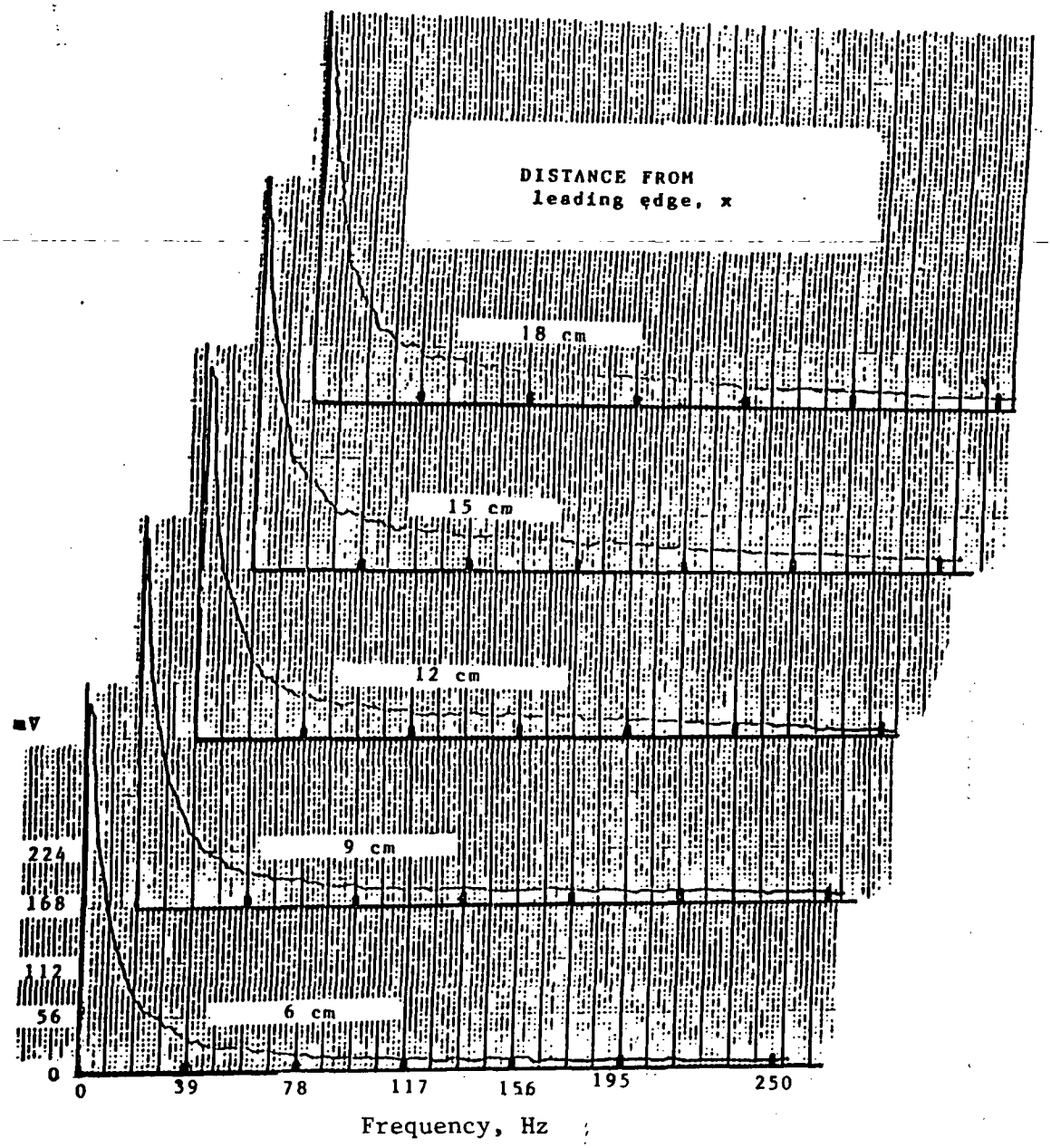

Fig. 14. Disturbance spectral data inside the boundary layer, no-grid

ORIGINAL PAGE IS
OF POOR QUALITY

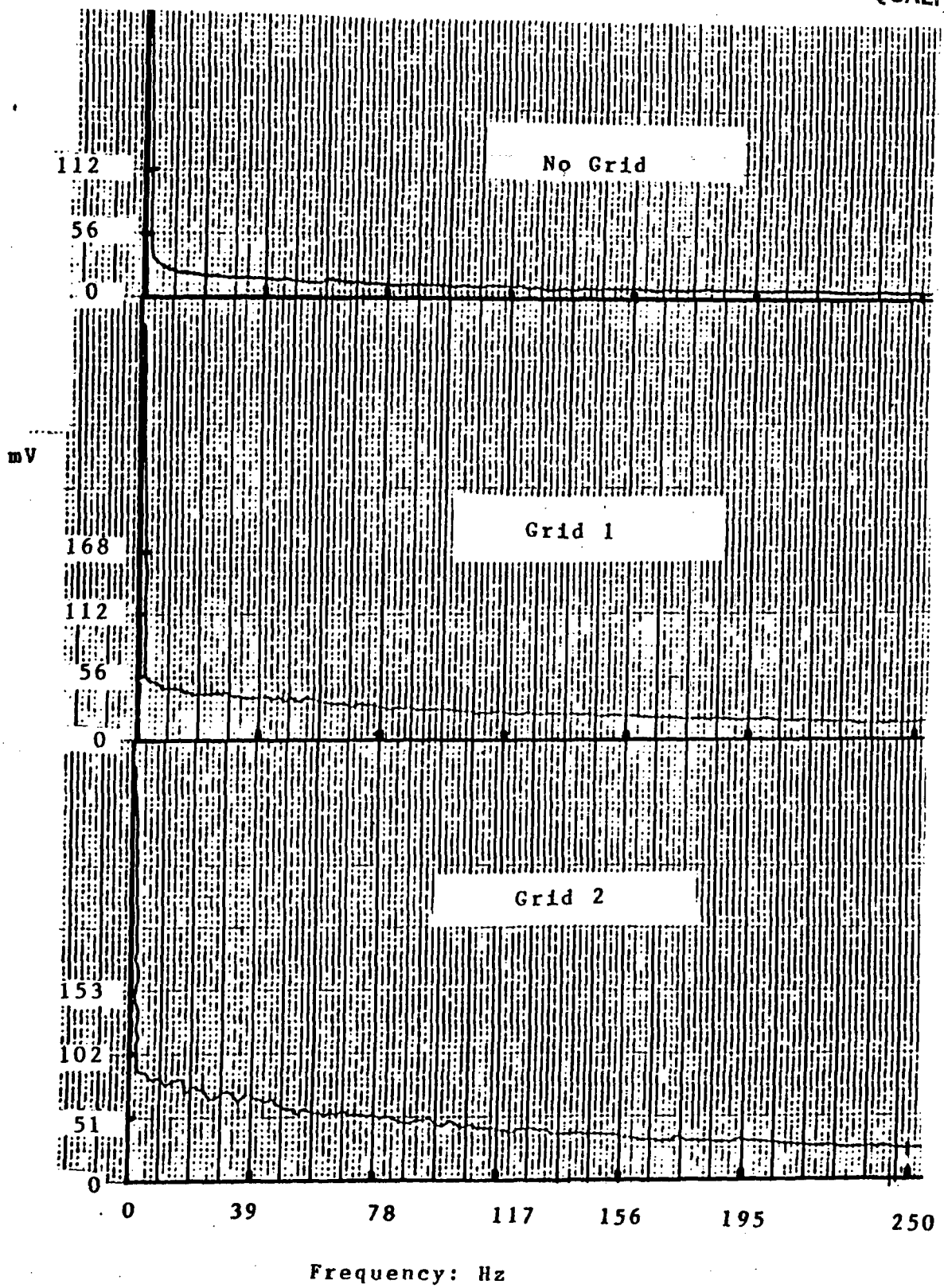

Fig. 15. Free stream disturbance spectra, 0-250 Hz.

ORIGINAL PAGE IS
OF POOR QUALITY

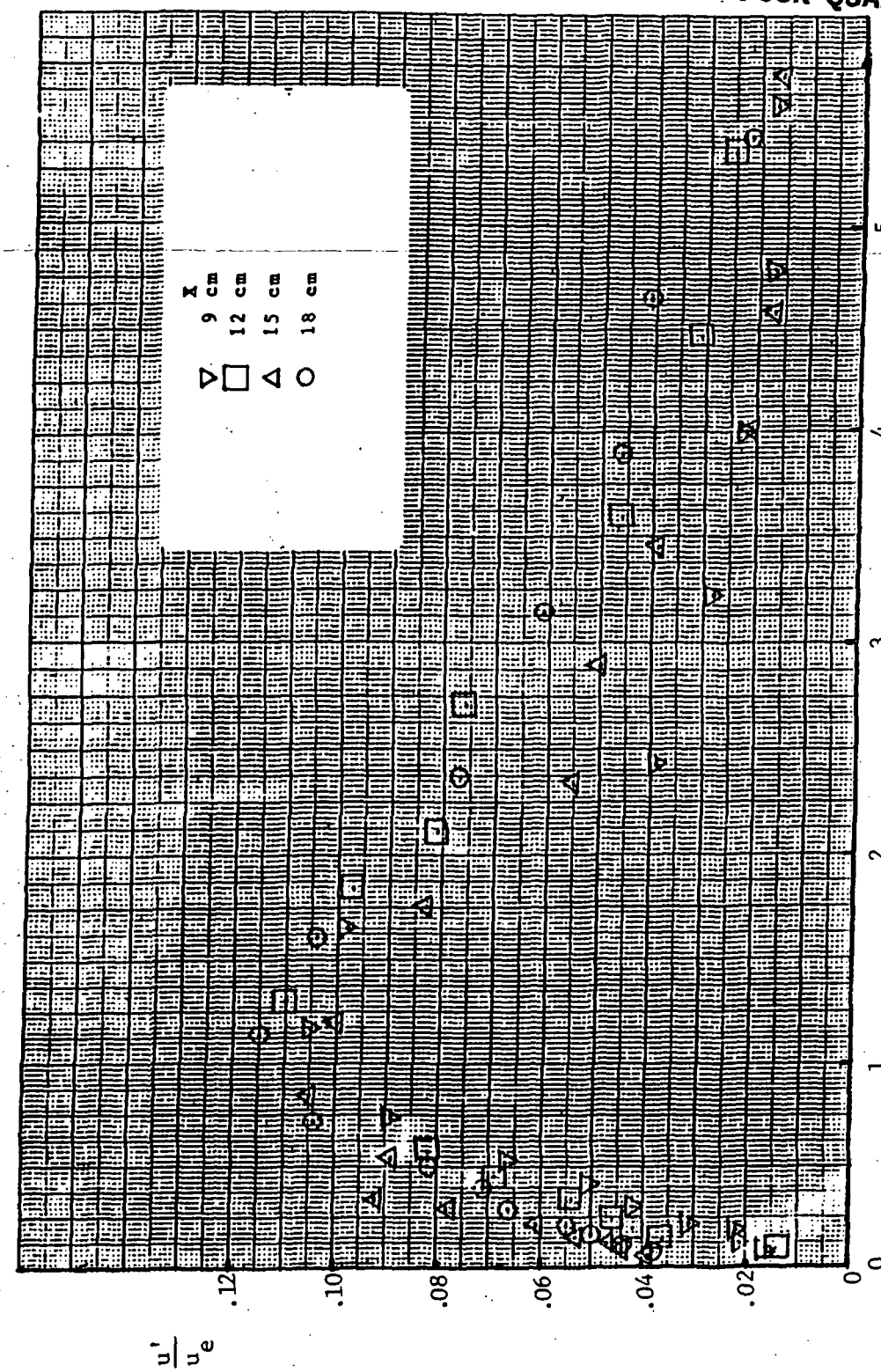

Fig. 16. Disturbance amplitude profiles for the no grid case

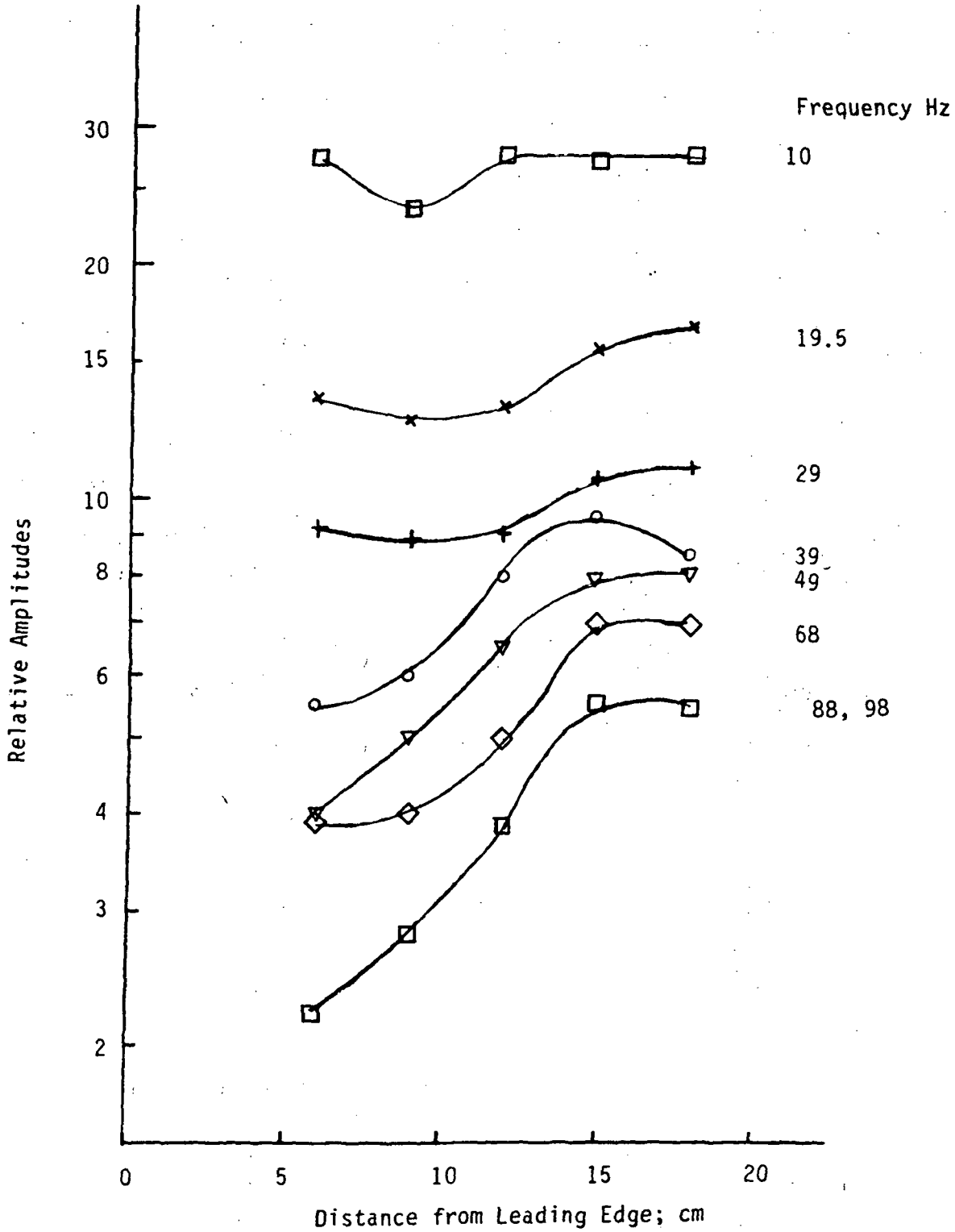

Fig.17. Relative amplitudes of selected frequences; No Grid

APPENDIX A

PROPERTIES OF VARIOUS PROFILE MODELS OF THE FLAT PLATE TURBULENT BOUNDARY LAYER

It is known from long experience with boundary layer integral methods that for any profile function, one can integrate the profile to obtain expressions and values for the various integral thicknesses and shape factors. It is helpful for the present purposes to do so for the profile function of Musker (ref. 20) presented in the text as equation (3).

Because that function is presented in wall units, the integrations will also provide a skin friction relationship as a function of say Re_θ for each assumed value of the wake strength π. This should be helpful in obtaining a better assessment of the variation of wake strength with free-stream turbulence level at low Reynolds numbers.

Musker's expression for the turbulent boundary layer velocity profile is:

$$\begin{aligned} u^+ = \; & 5.424 \tan^{-1}\{(2y^+ - 8.15)/16.7\} \\ & + \log_{10}\{(y^+ + 10.6)^{9.6}/(y^{+2} - 8.15y^+ + 86)^2\} - 3.52 \\ & + \pi/k \; \{6(y/\delta)^2 - 4(y/\delta)^3\} \\ & + 1/k \; (y/\delta)^2(1 - y/\delta) \end{aligned} \qquad (3)$$

The first two lines on the right side are an analytic expression

for the law-of-the-wall that is consistent in the log-linear region with Coles' constants. The term having the coefficient π is an algebraic form of the Coles wake function, and the last term on the right side is an additional wake term due to Granville (ref. 22) providing for a zero derivative at the edge of the boundary layer. Results will be calculated and tabulated herein without the Granville wake term (Musker-Coles) as well as with inclusion of that term (Musker-Coles-Granville).

The quantities that are calculated and presented are as follows:

$$u_e^+ = u_e/u_\tau = u^+(\delta^+)$$

$$Re_\theta = \int_0^{\delta^+} u^+ dy^+ - \frac{1}{u_e^+} \int_0^{\delta^+} u^{+2} dy^+$$

$$Re_{\delta^*} = u_e^+ \delta^+ - \int_0^{\delta^+} u^+ dy^+$$

$$H = \delta^*/\theta = Re_{\delta^*}/Re_\theta$$

The results for the Musker-Coles profile are tabulated in Table A-1 while the results including the Granville wake term are tabulated in Table A-2.

Wake Strength

Experimentally, the wake strength, $\Delta u/u_\tau$, is identified as the maximum departure of the velocity profile in wall units from the log-linear relation as shown in the following sketch:

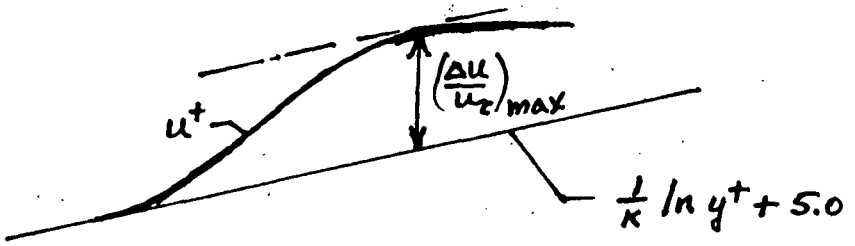

For the Coles wake function, the maximum value of the wake strength is

$$\left(\frac{\Delta u}{u_\tau}\right)_{max} = \frac{2\pi}{\kappa} \qquad \text{(A-1)}$$

and occurs at $y/\delta = 1$. The wake strength is zero for $\pi = 0$.

For the Coles-Granville wake function, the maximum wake strength is

$$\left(\frac{\Delta u}{u_\tau}\right)_{max} = \frac{4}{27\kappa} \frac{(6\pi+1)^3}{(4\pi+1)^2} \qquad \text{(A-2)}$$

and occurs at

$$\left(\frac{y}{\delta}\right)_{max} = \frac{2}{3}\left(\frac{6\pi+1}{4\pi+1}\right) \qquad \text{(A-3)}$$

For the Coles-Granville wake function, the wake strength becomes zero for $\pi = -1/6$. The wake strength at $y/\delta = 1$ is still $2\pi/k$

which is less than the maximum. Nevertheless, the velocity u_e^+ at $y/\delta = 1$ is larger than the value of u^+ at the location of maximum wake strength. These relations for the Coles-Granville wake function are given in Table A-3 for $-1/6 < \pi < 0.7$.

Comparison with Experimental Data

Skin friction data in the form of u_e/u_τ vs. Re_θ are compared to the results for the Musker-Coles profile in figure A-1, and to those for the Musker-Coles-Granville profile in figure A-2. The present data which display no visible wake are slightly better represented by the $\pi = -1/6$ curve of figure A-2 than by the $\pi = 0$ curve of figure A-1. With respect to shape factor (figure A-3), there is very little difference between the results for the two different wake representations for zero wake strength.

TABLE A1

INTEGRAL PROPERTIES OF THE MUSKER-COLES PROFILE

Π	δ^+	u_e/u_τ	$\int_0^{\delta^+} u^+ dy^+$	Re_θ	Re_{δ^*}	H
0.0	30.	13.01	273.0	52.	117.	2.27
0.0	45.	14.18	477.7	77.	160.	2.07
0.0	60.	14.94	696.3	103.	200.	1.94
0.0	75.	15.50	924.8	129.	238.	1.85
0.0	90.	15.95	1160.8	154.	275.	1.78
0.0	105.	16.33	1403.1	181.	312.	1.73
0.0	120.	16.66	1650.6	207.	349.	1.68
0.0	135.	16.95	1902.7	234.	385.	1.65
0.0	150.	17.21	2158.9	260.	422.	1.62
0.0	165.	17.44	2418.8	287.	458.	1.60
0.0	180.	17.65	2681.9	314.	495.	1.57
0.0	195.	17.84	2948.1	341.	531.	1.56
0.0	210.	18.02	3217.1	369.	568.	1.54
0.0	225.	18.19	3488.8	396.	604.	1.52
0.0	240.	18.35	3763.5	417.	640.	1.53
0.0	255.	18.49	4039.1	451.	677.	1.50
0.0	270.	18.63	4317.5	479.	713.	1.49
0.0	285.	18.76	4599.5	508.	748.	1.47
0.0	300.	18.89	4880.4	535.	786.	1.47
0.0	315.	19.00	5164.6	562.	822.	1.46
0.0	330.	19.12	5450.5	590.	858.	1.45
0.0	345.	19.23	5738.1	618.	895.	1.45
0.0	360.	19.33	6027.2	647.	931.	1.44
0.0	375.	19.43	6317.9	675.	967.	1.43
0.0	390.	19.52	6610.0	703.	1004.	1.43
0.0	405.	19.61	6903.5	731.	1040.	1.42
0.0	420.	19.70	7198.4	759.	1076.	1.42
0.0	435.	19.79	7494.5	788.	1113.	1.41
0.0	450.	19.87	7792.5	816.	1149.	1.41
0.0	465.	19.95	8091.2	845.	1185.	1.40
0.0	480.	20.03	8391.2	866.	1221.	1.41
0.0	495.	20.10	8692.2	902.	1257.	1.39
0.0	510.	20.17	8993.4	930.	1294.	1.39
0.0	525.	20.24	9296.6	950.	1331.	1.40
0.0	540.	20.31	9602.0	980.	1366.	1.39
0.0	555.	20.38	9907.3	1017.	1402.	1.38
0.0	570.	20.44	10213.5	1045.	1438.	1.38
0.0	600.	20.57	10827.2	1101.	1513.	1.37
0.0	630.	20.68	11445.9	1159.	1585.	1.37
0.0	660.	20.80	12068.2	1216.	1658.	1.36
0.0	690.	20.91	12693.7	1274.	1731.	1.36
0.0	720.	21.01	13322.4	1331.	1804.	1.35
0.0	750.	21.11	13954.2	1389.	1876.	1.35
0.0	780.	21.20	14589.0	1447.	1949.	1.35
0.0	810.	21.29	15226.5	1505.	2022.	1.34
0.0	840.	21.38	15866.8	1563.	2094.	1.34
0.0	870.	21.47	16509.6	1621.	2167.	1.34
0.0	900.	21.55	17155.0	1679.	2240.	1.33
0.0	930.	21.63	17802.8	1731.	2313.	1.34
0.0	960.	21.71	18453.0	1789.	2385.	1.33
0.0	990.	21.78	19105.4	1847.	2458.	1.33
0.0	1020.	21.85	19760.1	1905.	2531.	1.33
0.0	1050.	21.92	20416.9	1963.	2603.	1.33

TABLE A1 (continued)

Π	δ^+	u_e/u_τ	$\int_0^{\delta^+} u^+ dy^+$	Re_θ	Re_{δ^*}	H
0.0	1080.	21.99	21075.8	2022.	2676.	1.32
0.0	1110.	22.06	21736.7	2080.	2749.	1.32
0.0	1140.	22.12	22399.5	2147.	2821.	1.31
0.0	1170.	22.19	23064.3	2205.	2894.	1.31
0.0	1200.	22.25	23731.0	2264.	2967.	1.31
0.0	1230.	22.31	24399.5	2323.	3039.	1.31
0.0	1260.	22.37	25067.6	2379.	3114.	1.31
0.0	1290.	22.42	25739.5	2438.	3187.	1.31
0.0	1320.	22.48	26413.0	2497.	3260.	1.31
0.0	1350.	22.53	27088.2	2556.	3333.	1.30
0.0	1380.	22.59	27765.1	2614.	3406.	1.30
0.0	1410.	22.64	28443.5	2673.	3478.	1.30
0.0	1440.	22.69	29123.5	2732.	3551.	1.30
0.0	1470.	22.74	29805.0	2791.	3624.	1.30
0.0	1500.	22.79	30488.0	2849.	3697.	1.30
0.0	1530.	22.84	31172.4	2908.	3770.	1.30
0.0	1560.	22.89	31858.3	2967.	3843.	1.29
0.0	1590.	22.93	32545.6	3026.	3915.	1.29
0.0	1620.	22.98	33234.3	3086.	3988.	1.29
0.0	1650.	23.02	33924.3	3145.	4061.	1.29
0.0	1680.	23.07	34615.6	3199.	4134.	1.29
0.0	1710.	23.11	35308.3	3258.	4207.	1.29
0.0	1740.	23.15	36002.2	3317.	4279.	1.29
0.0	1770.	23.19	36697.4	3376.	4352.	1.29
0.0	1800.	23.23	37393.8	3435.	4425.	1.29
0.0	1830.	23.27	38091.4	3494.	4498.	1.29
0.0	1860.	23.31	38790.3	3553.	4571.	1.29
0.0	1890.	23.35	39490.3	3612.	4644.	1.29
0.0	1920.	23.39	40191.5	3671.	4716.	1.28
0.0	1950.	23.43	40893.8	3731.	4789.	1.28
0.0	2040.	23.54	43007.4	3908.	5008.	1.28
0.0	2130.	23.64	45130.7	4086.	5226.	1.28
0.0	2220.	23.74	47263.2	4264.	5444.	1.28
0.0	2310.	23.84	49404.5	4442.	5663.	1.27
0.0	2400.	23.93	51554.4	4621.	5881.	1.27
0.0	2490.	24.02	53712.6	4808.	6100.	1.27
0.0	2580.	24.11	55878.5	4987.	6318.	1.27
0.0	2670.	24.19	58052.1	5166.	6537.	1.27
0.0	2760.	24.27	60233.1	5343.	6755.	1.26
0.0	2850.	24.35	62418.4	5520.	6977.	1.26
0.0	2940.	24.42	64613.4	5699.	7195.	1.26
0.0	3030.	24.50	66814.9	5878.	7414.	1.26
0.0	3120.	24.57	69023.0	6058.	7633.	1.26
0.0	3210.	24.64	71237.4	6237.	7851.	1.26
0.0	3300.	24.71	73458.0	6417.	8070.	1.26
0.0	3390.	24.77	75684.5	6596.	8289.	1.26
0.0	3480.	24.83	77916.9	6776.	8507.	1.26
0.0	3570.	24.90	80154.8	6956.	8726.	1.25
0.0	3660.	24.96	82398.3	7136.	8945.	1.25
0.0	3750.	25.02	84647.3	7316.	9163.	1.25
0.0	3840.	25.07	86901.4	7496.	9382.	1.25
0.0	3930.	25.13	89160.6	7676.	9601.	1.25
0.0	4020.	25.19	91425.0	7857.	9819.	1.25
0.0	4110.	25.24	93694.2	8037.	10038.	1.25
0.0	4200.	25.29	95968.1	8218.	10257.	1.25
0.0	4290.	25.34	98246.8	8398.	10475.	1.25
0.0	4380.	25.39	100530.0	8579.	10694.	1.25
0.0	4470.	25.44	102817.9	8760.	10913.	1.25
0.0	4560.	25.49	105109.9	8941.	11131.	1.25

TABLE A1 (continued)

Π	δ^+	u_e/u_τ	$\int_0^{\delta^+} u^+ dy^+$	Re_θ	Re_{δ^*}	H
0.1	30.	13.50	280.3	54.	125.	2.29
0.1	45.	14.67	488.6	82.	171.	2.08
0.1	60.	15.42	711.0	110.	214.	1.95
0.1	75.	15.99	943.1	138.	256.	1.86
0.1	90.	16.44	1182.8	166.	297.	1.79
0.1	105.	16.82	1428.7	195.	338.	1.74
0.1	120.	17.15	1679.9	223.	378.	1.69
0.1	135.	17.44	1935.7	252.	418.	1.66
0.1	150.	17.69	2195.5	282.	459.	1.63
0.1	165.	17.93	2459.0	311.	499.	1.60
0.1	180.	18.14	2725.8	340.	539.	1.58
0.1	195.	18.33	2995.7	370.	579.	1.56
0.1	210.	18.51	3268.4	400.	619.	1.55
0.1	225.	18.68	3543.7	430.	659.	1.53
0.1	240.	18.83	3822.1	453.	698.	1.54
0.1	255.	18.98	4101.3	490.	739.	1.51
0.1	270.	19.12	4383.4	520.	779.	1.50
0.1	285.	19.25	4669.1	552.	817.	1.48
0.1	300.	19.37	4953.6	581.	859.	1.48
0.1	315.	19.49	5241.4	611.	899.	1.47
0.1	330.	19.61	5531.0	642.	939.	1.46
0.1	345.	19.71	5822.2	672.	979.	1.46
0.1	360.	19.82	6115.1	703.	1019.	1.45
0.1	375.	19.92	6409.4	734.	1059.	1.44
0.1	390.	20.01	6705.2	764.	1099.	1.44
0.1	405.	20.10	7002.3	795.	1139.	1.43
0.1	420.	20.19	7300.9	826.	1179.	1.43
0.1	435.	20.27	7600.7	857.	1219.	1.42
0.1	450.	20.36	7902.3	888.	1258.	1.42
0.1	465.	20.44	8204.7	919.	1298.	1.41
0.1	480.	20.51	8508.3	943.	1338.	1.42
0.1	495.	20.59	8813.0	981.	1378.	1.40
0.1	510.	20.66	9117.8	1012.	1419.	1.40
0.1	525.	20.73	9424.7	1035.	1459.	1.41
0.1	540.	20.80	9733.7	1067.	1498.	1.40
0.1	555.	20.87	10042.7	1106.	1538.	1.39
0.1	570.	20.93	10352.6	1138.	1577.	1.39
0.1	600.	21.05	10973.6	1199.	1659.	1.38
0.1	630.	21.17	11599.7	1261.	1739.	1.38
0.1	660.	21.29	12229.2	1324.	1819.	1.37
0.1	690.	21.39	12862.1	1386.	1899.	1.37
0.1	720.	21.50	13498.1	1449.	1979.	1.37
0.1	750.	21.60	14137.2	1512.	2059.	1.36
0.1	780.	21.69	14779.3	1575.	2139.	1.36
0.1	810.	21.78	15424.2	1639.	2219.	1.35
0.1	840.	21.87	16071.7	1702.	2299.	1.35
0.1	870.	21.96	16721.9	1765.	2379.	1.35
0.1	900.	22.04	17374.6	1828.	2459.	1.35
0.1	930.	22.12	18029.7	1886.	2539.	1.35
0.1	960.	22.19	18687.2	1949.	2619.	1.34
0.1	990.	22.27	19347.0	2012.	2699.	1.34
0.1	1020.	22.34	20009.0	2076.	2779.	1.34
0.1	1050.	22.41	20673.1	2139.	2859.	1.34
0.1	1080.	22.48	21339.3	2203.	2939.	1.33
0.1	1110.	22.55	22007.5	2266.	3019.	1.33

TABLE A1 (continued)

Π	δ^+	u_e/u_τ	$\int_0^{\delta^+} u^+ dy^+$	Re_θ	Re_{δ^*}	H
0.1	1140.	22.61	22677.7	2338.	3099.	1.33
0.1	1170.	22.67	23349.8	2402.	3179.	1.32
0.1	1200.	22.74	24023.8	2466.	3259.	1.32
0.1	1230.	22.80	24699.6	2530.	3340.	1.32
0.1	1260.	22.85	25375.0	2592.	3422.	1.32
0.1	1290.	22.91	26054.2	2656.	3502.	1.32
0.1	1320.	22.97	26735.1	2720.	3582.	1.32
0.1	1350.	23.02	27417.6	2784.	3662.	1.32
0.1	1380.	23.08	28101.8	2848.	3742.	1.31
0.1	1410.	23.13	28787.5	2912.	3822.	1.31
0.1	1440.	23.18	29474.9	2976.	3903.	1.31
0.1	1470.	23.23	30163.6	3040.	3983.	1.31
0.1	1500.	23.28	30854.0	3104.	4063.	1.31
0.1	1530.	23.33	31545.7	3169.	4143.	1.31
0.1	1560.	23.37	32239.0	3233.	4223.	1.31
0.1	1590.	23.42	32933.6	3297.	4303.	1.31
0.1	1620.	23.46	33629.5	3362.	4383.	1.30
0.1	1650.	23.51	34326.9	3426.	4464.	1.30
0.1	1680.	23.55	35025.5	3486.	4544.	1.30
0.1	1710.	23.60	35725.5	3550.	4624.	1.30
0.1	1740.	23.64	36426.8	3615.	4704.	1.30
0.1	1770.	23.68	37129.3	3679.	4784.	1.30
0.1	1800.	23.72	37833.0	3743.	4864.	1.30
0.1	1830.	23.76	38538.0	3808.	4944.	1.30
0.1	1860.	23.80	39244.1	3872.	5025.	1.30
0.1	1890.	23.84	39951.5	3937.	5105.	1.30
0.1	1920.	23.88	40659.9	4001.	5185.	1.30
0.1	1950.	23.92	41369.6	4066.	5265.	1.30
0.1	2040.	24.02	43505.2	4259.	5505.	1.29
0.1	2130.	24.13	45650.4	4453.	5746.	1.29
0.1	2220.	24.23	47804.9	4647.	5986.	1.29
0.1	2310.	24.33	49968.2	4842.	6227.	1.29
0.1	2400.	24.42	52140.0	5036.	6467.	1.28
0.1	2490.	24.51	54320.1	5231.	6707.	1.28
0.1	2580.	24.60	56508.0	5435.	6948.	1.28
0.1	2670.	24.68	58703.6	5630.	7188.	1.28
0.1	2760.	24.76	60906.6	5824.	7429.	1.28
0.1	2850.	24.84	63113.9	6016.	7672.	1.28
0.1	2940.	24.91	65330.8	6212.	7913.	1.27
0.1	3030.	24.99	67554.3	6407.	8153.	1.27
0.1	3120.	25.06	69784.3	6603.	8394.	1.27
0.1	3210.	25.13	72020.7	6798.	8635.	1.27
0.1	3300.	25.19	74263.2	6994.	8875.	1.27
0.1	3390.	25.26	76511.6	7190.	9116.	1.27
0.1	3480.	25.32	78766.0	7386.	9356.	1.27
0.1	3570.	25.38	81025.9	7582.	9597.	1.27
0.1	3660.	25.45	83291.4	7779.	9838.	1.26
0.1	3750.	25.50	85562.2	7975.	10078.	1.26
0.1	3840.	25.56	87838.3	8172.	10319.	1.26
0.1	3930.	25.62	90119.6	8368.	10560.	1.26
0.1	4020.	25.67	92405.8	8565.	10800.	1.26
0.1	4110.	25.73	94697.0	8762.	11041.	1.26
0.1	4200.	25.78	96992.9	8959.	11281.	1.26
0.1	4290.	25.83	99293.7	9156.	11522.	1.26
0.1	4380.	25.88	101598.8	9353.	11763.	1.26
0.1	4470.	25.93	103908.5	9550.	12003.	1.26
0.1	4560.	25.98	106222.6	9748.	12244.	1.26

TABLE A1 (continued)

Π	δ^+	u_e/u_τ	$\int_0^{\delta^+} u^+ dy^+$	Re_θ	Re_{δ^*}	H
0.2	30.	13.99	287.6	57.	132.	2.31
0.2	45.	15.15	499.6	87.	182.	2.10
0.2	60.	15.91	725.6	117.	229.	1.96
0.2	75.	16.48	961.4	147.	274.	1.87
0.2	90.	16.93	1204.7	177.	319.	1.80
0.2	105.	17.31	1454.3	208.	363.	1.74
0.2	120.	17.64	1709.2	239.	407.	1.70
0.2	135.	17.93	1968.6	271.	451.	1.67
0.2	150.	18.18	2232.1	302.	495.	1.64
0.2	165.	18.41	2499.3	334.	539.	1.61
0.2	180.	18.62	2769.8	366.	583.	1.59
0.2	195.	18.82	3043.3	398.	626.	1.57
0.2	210.	19.00	3319.6	430.	670.	1.56
0.2	225.	19.17	3598.6	463.	714.	1.54
0.2	240.	19.32	3880.6	488.	757.	1.55
0.2	255.	19.47	4163.5	528.	801.	1.52
0.2	270.	19.61	4449.3	560.	845.	1.51
0.2	285.	19.74	4738.6	594.	887.	1.49
0.2	300.	19.86	5026.8	626.	932.	1.49
0.2	315.	19.98	5318.3	659.	976.	1.48
0.2	330.	20.09	5611.5	692.	1019.	1.47
0.2	345.	20.20	5906.4	725.	1063.	1.47
0.2	360.	20.30	6202.9	758.	1107.	1.46
0.2	375.	20.40	6500.9	791.	1150.	1.45
0.2	390.	20.50	6800.3	824.	1194.	1.45
0.2	405.	20.59	7101.2	857.	1238.	1.44
0.2	420.	20.68	7403.4	890.	1281.	1.44
0.2	435.	20.76	7706.8	924.	1325.	1.43
0.2	450.	20.85	8012.1	958.	1368.	1.43
0.2	465.	20.92	8318.2	991.	1412.	1.42
0.2	480.	21.00	8625.4	1018.	1455.	1.43
0.2	495.	21.08	8933.8	1059.	1499.	1.42
0.2	510.	21.15	9242.2	1091.	1543.	1.41
0.2	525.	21.22	9552.8	1117.	1587.	1.42
0.2	540.	21.29	9865.5	1152.	1629.	1.42
0.2	555.	21.35	10178.1	1194.	1673.	1.40
0.2	570.	21.42	10491.7	1227.	1717.	1.40
0.2	600.	21.54	11120.0	1293.	1805.	1.40
0.2	630.	21.66	11753.4	1361.	1893.	1.39
0.2	660.	21.77	12390.3	1428.	1980.	1.39
0.2	690.	21.88	13030.5	1496.	2068.	1.38
0.2	720.	21.98	13673.8	1564.	2155.	1.38
0.2	750.	22.08	14320.2	1632.	2242.	1.37
0.2	780.	22.18	14969.6	1700.	2330.	1.37
0.2	810.	22.27	15621.8	1769.	2417.	1.37
0.2	840.	22.36	16276.7	1837.	2504.	1.36
0.2	870.	22.44	16934.2	1905.	2592.	1.36
0.2	900.	22.53	17594.2	1968.	2679.	1.36
0.2	930.	22.61	18256.6	2037.	2766.	1.36
0.2	960.	22.68	18921.5	2105.	2854.	1.36
0.2	990.	22.76	19588.5	2173.	2941.	1.35
0.2	1020.	22.83	20257.8	2242.	3028.	1.35
0.2	1050.	22.90	20929.3	2310.	3116.	1.35
0.2	1080.	22.97	21602.8	2379.	3203.	1.35
0.2	1110.	23.03	22278.3	2447.	3290.	1.34
0.2	1140.	23.10	22955.9	2516.	3378.	1.34
0.2	1170.	23.16	23635.3	2593.	3465.	1.34

TABLE A1 (continued)

Π	δ^+	u_e/u_τ	$\int_0^{\delta^+} u^+ dy^+$	Re_θ	Re_{δ^*}	H
0.2	1200.	23.22	24316.6	2662.	3552.	1.33
0.2	1230.	23.28	24999.7	2732.	3640.	1.33
0.2	1260.	23.34	25682.5	2799.	3729.	1.33
0.2	1290.	23.40	26369.0	2868.	3817.	1.33
0.2	1320.	23.46	27057.2	2937.	3904.	1.33
0.2	1350.	23.51	27747.0	3006.	3992.	1.33
0.2	1380.	23.56	28438.5	3075.	4079.	1.33
0.2	1410.	23.62	29131.6	3145.	4166.	1.32
0.2	1440.	23.67	29826.2	3214.	4254.	1.32
0.2	1470.	23.72	30522.3	3283.	4341.	1.32
0.2	1500.	23.77	31220.0	3353.	4429.	1.32
0.2	1530.	23.81	31919.1	3422.	4516.	1.32
0.2	1560.	23.86	32619.6	3492.	4604.	1.32
0.2	1590.	23.91	33321.5	3561.	4691.	1.32
0.2	1620.	23.95	34024.8	3631.	4779.	1.32
0.2	1650.	24.00	34729.5	3700.	4866.	1.32
0.2	1680.	24.04	35435.4	3766.	4954.	1.32
0.2	1710.	24.08	36142.7	3835.	5041.	1.31
0.2	1740.	24.13	36851.3	3905.	5129.	1.31
0.2	1770.	24.17	37561.2	3974.	5216.	1.31
0.2	1800.	24.21	38272.2	4044.	5303.	1.31
0.2	1830.	24.25	38984.5	4113.	5391.	1.31
0.2	1860.	24.29	39697.9	4183.	5478.	1.31
0.2	1890.	24.33	40412.6	4253.	5566.	1.31
0.2	1920.	24.37	41128.4	4322.	5653.	1.31
0.2	1950.	24.40	41845.4	4392.	5741.	1.31
0.2	2040.	24.51	44002.9	4601.	6003.	1.30
0.2	2130.	24.62	46170.1	4811.	6265.	1.30
0.2	2220.	24.72	48346.5	5021.	6528.	1.30
0.2	2310.	24.81	50531.8	5231.	6790.	1.30
0.2	2400.	24.91	52725.7	5442.	7053.	1.30
0.2	2490.	25.00	54927.7	5652.	7315.	1.29
0.2	2580.	25.08	57137.5	5872.	7577.	1.29
0.2	2670.	25.17	59355.1	6083.	7840.	1.29
0.2	2760.	25.25	61580.0	6292.	8102.	1.29
0.2	2850.	25.33	63809.3	6500.	8367.	1.29
0.2	2940.	25.40	66048.1	6712.	8630.	1.29
0.2	3030.	25.47	68293.6	6923.	8893.	1.28
0.2	3120.	25.55	70545.6	7134.	9155.	1.28
0.2	3210.	25.61	72803.9	7346.	9418.	1.28
0.2	3300.	25.68	75068.4	7558.	9680.	1.28
0.2	3390.	25.75	77338.9	7770.	9943.	1.28
0.2	3480.	25.81	79615.1	7982.	10206.	1.28
0.2	3570.	25.87	81897.0	8194.	10468.	1.28
0.2	3660.	25.93	84184.4	8406.	10731.	1.28
0.2	3750.	25.99	86477.2	8619.	10993.	1.28
0.2	3840.	26.05	88775.3	8831.	11256.	1.27
0.2	3930.	26.11	91078.5	9044.	11518.	1.27
0.2	4020.	26.16	93386.7	9257.	11781.	1.27
0.2	4110.	26.21	95699.8	9469.	12044.	1.27
0.2	4200.	26.27	98017.8	9682.	12306.	1.27
0.2	4290.	26.32	100340.3	9895.	12569.	1.27
0.2	4380.	26.37	102667.5	10109.	12831.	1.27
0.2	4470.	26.42	104999.2	10322.	13094.	1.27
0.2	4560.	26.47	107335.3	10535.	13356.	1.27

TABLE A1 (continued)

Π	δ^+	u_e/u_τ	$\int_0^{\delta^+} u^+ dy^+$	Re_θ	Re_{δ^*}	H
0.3	30.	14.48	294.9	60.	139.	2.33
0.3	45.	15.64	510.6	91.	193.	2.12
0.3	60.	16.40	740.3	123.	244.	1.98
0.3	75.	16.97	979.7	156.	293.	1.88
0.3	90.	17.42	1226.7	188.	341.	1.81
0.3	105.	17.80	1479.9	221.	389.	1.76
0.3	120.	18.13	1738.4	255.	437.	1.71
0.3	135.	18.41	2001.5	289.	484.	1.68
0.3	150.	18.67	2268.7	322.	532.	1.65
0.3	165.	18.90	2539.5	356.	579.	1.62
0.3	180.	19.11	2813.7	391.	627.	1.60
0.3	195.	19.31	3090.9	425.	674.	1.59
0.3	210.	19.49	3370.8	460.	721.	1.57
0.3	225.	19.65	3653.5	494.	769.	1.55
0.3	240.	19.81	3939.2	523.	815.	1.56
0.3	255.	19.96	4225.8	564.	863.	1.53
0.3	270.	20.10	4515.2	599.	911.	1.52
0.3	285.	20.23	4808.1	636.	956.	1.50
0.3	300.	20.35	5100.0	669.	1005.	1.50
0.3	315.	20.47	5395.2	705.	1053.	1.49
0.3	330.	20.58	5692.1	740.	1100.	1.49
0.3	345.	20.69	5990.6	775.	1147.	1.48
0.3	360.	20.79	6290.7	811.	1195.	1.47
0.3	375.	20.89	6592.4	846.	1242.	1.47
0.3	390.	20.99	6895.5	882.	1289.	1.46
0.3	405.	21.08	7200.0	918.	1336.	1.46
0.3	420.	21.17	7505.8	953.	1384.	1.45
0.3	435.	21.25	7813.0	989.	1431.	1.45
0.3	450.	21.33	8121.9	1025.	1478.	1.44
0.3	465.	21.41	8431.6	1061.	1525.	1.44
0.3	480.	21.49	8742.5	1091.	1572.	1.44
0.3	495.	21.56	9054.6	1134.	1620.	1.43
0.3	510.	21.64	9366.7	1169.	1668.	1.43
0.3	525.	21.71	9680.9	1197.	1715.	1.43
0.3	540.	21.77	9997.2	1234.	1761.	1.43
0.3	555.	21.84	10313.5	1278.	1808.	1.41
0.3	570.	21.91	10630.8	1315.	1856.	1.41
0.3	600.	22.03	11266.4	1385.	1952.	1.41
0.3	630.	22.15	11907.1	1458.	2047.	1.40
0.3	660.	22.26	12551.3	1530.	2141.	1.40
0.3	690.	22.37	13198.8	1603.	2236.	1.39
0.3	720.	22.47	13849.5	1676.	2331.	1.39
0.3	750.	22.57	14503.2	1749.	2425.	1.39
0.3	780.	22.67	15160.0	1822.	2520.	1.38
0.3	810.	22.76	15819.4	1895.	2615.	1.38
0.3	840.	22.85	16481.7	1969.	2709.	1.38
0.3	870.	22.93	17146.5	2042.	2804.	1.37
0.3	900.	23.01	17813.8	2110.	2899.	1.37
0.3	930.	23.09	18483.6	2183.	2993.	1.37
0.3	960.	23.17	19155.7	2256.	3088.	1.37
0.3	990.	23.25	19830.1	2330.	3183.	1.37
0.3	1020.	23.32	20506.7	2403.	3277.	1.36
0.3	1050.	23.39	21185.5	2477.	3372.	1.36

TABLE A1 (continued)

Π	δ^+	u_e/u_τ	$\int_0^{\delta^+} u^+ dy^+$	Re_θ	Re_{δ^*}	H
0.3	1080.	23.46	21866.3	2550.	3467.	1.36
0.3	1110.	23.52	22549.2	2624.	3561.	1.36
0.3	1140.	23.59	23234.0	2698.	3656.	1.36
0.3	1170.	23.65	23920.8	2780.	3750.	1.35
0.3	1200.	23.71	24609.4	2854.	3845.	1.35
0.3	1230.	23.77	25299.8	2928.	3940.	1.35
0.3	1260.	23.83	25989.9	3000.	4037.	1.35
0.3	1290.	23.89	26683.7	3074.	4131.	1.34
0.3	1320.	23.94	27379.2	3149.	4226.	1.34
0.3	1350.	24.00	28076.4	3223.	4321.	1.34
0.3	1380.	24.05	28775.2	3297.	4416.	1.34
0.3	1410.	24.10	29475.6	3372.	4511.	1.34
0.3	1440.	24.15	30177.6	3446.	4605.	1.34
0.3	1470.	24.20	30881.0	3520.	4700.	1.34
0.3	1500.	24.25	31586.0	3595.	4795.	1.33
0.3	1530.	24.30	32292.4	3669.	4890.	1.33
0.3	1560.	24.35	33000.3	3744.	4984.	1.33
0.3	1590.	24.40	33709.5	3818.	5079.	1.33
0.3	1620.	24.44	34420.1	3893.	5174.	1.33
0.3	1650.	24.49	35132.1	3968.	5269.	1.33
0.3	1680.	24.53	35845.4	4038.	5364.	1.33
0.3	1710.	24.57	36560.0	4113.	5458.	1.33
0.3	1740.	24.61	37275.9	4187.	5553.	1.33
0.3	1770.	24.66	37993.0	4262.	5648.	1.33
0.3	1800.	24.70	38711.4	4337.	5743.	1.32
0.3	1830.	24.74	39431.0	4411.	5837.	1.32
0.3	1860.	24.78	40151.8	4486.	5932.	1.32
0.3	1890.	24.82	40873.8	4561.	6027.	1.32
0.3	1920.	24.85	41596.9	4636.	6122.	1.32
0.3	1950.	24.89	42321.2	4711.	6217.	1.32
0.3	2040.	25.00	44500.7	4935.	6501.	1.32
0.3	2130.	25.11	46689.8	5160.	6785.	1.31
0.3	2220.	25.21	48888.2	5386.	7070.	1.31
0.3	2310.	25.30	51095.5	5611.	7354.	1.31
0.3	2400.	25.40	53311.3	5837.	7638.	1.31
0.3	2490.	25.49	55535.2	6063.	7923.	1.31
0.3	2580.	25.57	57767.1	6298.	8207.	1.30
0.3	2670.	25.65	60006.6	6522.	8491.	1.30
0.3	2760.	25.74	62253.4	6749.	8776.	1.30
0.3	2850.	25.81	64504.7	6973.	9063.	1.30
0.3	2940.	25.89	66765.5	7200.	9347.	1.30
0.3	3030.	25.96	69032.9	7427.	9632.	1.30
0.3	3120.	26.03	71306.9	7654.	9917.	1.30
0.3	3210.	26.10	73587.2	7881.	10201.	1.29
0.3	3300.	26.17	75873.7	8108.	10486.	1.29
0.3	3390.	26.23	78166.0	8336.	10770.	1.29
0.3	3480.	26.30	80464.2	8563.	11055.	1.29
0.3	3570.	26.36	82768.0	8791.	11339.	1.29
0.3	3660.	26.42	85077.4	9019.	11624.	1.29
0.3	3750.	26.48	87392.3	9247.	11908.	1.29
0.3	3840.	26.54	89712.3	9475.	12193.	1.29
0.3	3930.	26.59	92037.4	9703.	12477.	1.29
0.3	4020.	26.65	94367.6	9932.	12762.	1.28
0.3	4110.	26.70	96702.7	10160.	13046.	1.28
0.3	4200.	26.76	99042.5	10389.	13331.	1.28
0.3	4290.	26.81	101387.1	10618.	13615.	1.28
0.3	4380.	26.86	103736.2	10847.	13900.	1.28
0.3	4470.	26.91	106089.9	11076.	14185.	1.28
0.3	4560.	26.96	108447.8	11305.	14469.	1.28

TABLE A1 (continued)

Π	δ^+	u_e/u_τ	$\int_0^{\delta^+} u^+ dy^+$	Re_θ	Re_{δ^*}	H
0.4	30.	14.96	302.2	62.	147.	2.36
0.4	45.	16.13	521.6	96.	204.	2.13
0.4	60.	16.89	754.9	130.	258.	1.99
0.4	75.	17.45	998.0	164.	311.	1.89
0.4	90.	17.91	1248.6	199.	363.	1.82
0.4	105.	18.29	1505.5	234.	415.	1.77
0.4	120.	18.61	1767.7	270.	466.	1.73
0.4	135.	18.90	2034.5	306.	517.	1.69
0.4	150.	19.16	2305.3	342.	568.	1.66
0.4	165.	19.39	2579.8	378.	619.	1.64
0.4	180.	19.60	2857.6	415.	671.	1.62
0.4	195.	19.79	3138.4	451.	722.	1.60
0.4	210.	19.97	3422.1	488.	773.	1.58
0.4	225.	20.14	3708.4	525.	824.	1.57
0.4	240.	20.30	3997.7	556.	874.	1.57
0.4	255.	20.45	4288.0	600.	926.	1.54
0.4	270.	20.58	4581.1	637.	976.	1.53
0.4	285.	20.71	4877.7	676.	1026.	1.52
0.4	300.	20.84	5173.2	712.	1078.	1.52
0.4	315.	20.96	5472.0	749.	1129.	1.51
0.4	330.	21.07	5772.6	787.	1180.	1.50
0.4	345.	21.18	6074.8	825.	1231.	1.49
0.4	360.	21.28	6378.6	863.	1282.	1.49
0.4	375.	21.38	6683.9	901.	1333.	1.48
0.4	390.	21.47	6990.6	938.	1384.	1.48
0.4	405.	21.57	7298.8	977.	1435.	1.47
0.4	420.	21.65	7608.3	1015.	1486.	1.46
0.4	435.	21.74	7919.1	1053.	1537.	1.46
0.4	450.	21.82	8231.7	1091.	1588.	1.45
0.4	465.	21.90	8545.1	1130.	1639.	1.45
0.4	480.	21.98	8859.7	1162.	1690.	1.45
0.4	495.	22.05	9175.4	1207.	1740.	1.44
0.4	510.	22.12	9491.1	1244.	1792.	1.44
0.4	525.	22.19	9809.0	1275.	1843.	1.45
0.4	540.	22.26	10129.0	1314.	1893.	1.44
0.4	555.	22.33	10448.9	1361.	1944.	1.43
0.4	570.	22.39	10769.9	1400.	1995.	1.43
0.4	600.	22.52	11412.8	1475.	2098.	1.42
0.4	630.	22.64	12060.8	1552.	2200.	1.42
0.4	660.	22.75	12712.3	1630.	2302.	1.41
0.4	690.	22.86	13367.2	1707.	2404.	1.41
0.4	720.	22.96	14025.2	1785.	2506.	1.40
0.4	750.	23.06	14686.2	1863.	2608.	1.40
0.4	780.	23.15	15350.3	1941.	2710.	1.40
0.4	810.	23.25	16017.1	2019.	2812.	1.39
0.4	840.	23.33	16686.6	2097.	2914.	1.39
0.4	870.	23.42	17358.7	2175.	3016.	1.39
0.4	900.	23.50	18033.4	2248.	3118.	1.39
0.4	930.	23.58	18710.5	2326.	3220.	1.38
0.4	960.	23.66	19389.9	2404.	3322.	1.38
0.4	990.	23.73	20071.7	2483.	3424.	1.38
0.4	1020.	23.81	20755.6	2561.	3526.	1.38
0.4	1050.	23.88	21441.7	2639.	3628.	1.37
0.4	1080.	23.94	22129.8	2718.	3730.	1.37
0.4	1110.	24.01	22820.0	2796.	3832.	1.37

TABLE A1 (continued)

Π	δ^+	u_e/u_τ	$\int_0^{\delta^+} u^+ dy^+$	Re_θ	Re_{δ^*}	H
0.4	1140.	24.08	23512.2	2875.	3934.	1.37
0.4	1170.	24.14	24206.3	2962.	4036.	1.36
0.4	1200.	24.20	24902.2	3041.	4138.	1.36
0.4	1230.	24.26	25600.0	3120.	4240.	1.36
0.4	1260.	24.32	26297.4	3197.	4344.	1.36
0.4	1290.	24.38	26998.5	3276.	4446.	1.36
0.4	1320.	24.43	27701.3	3355.	4548.	1.36
0.4	1350.	24.49	28405.9	3435.	4650.	1.35
0.4	1380.	24.54	29112.0	3514.	4752.	1.35
0.4	1410.	24.59	29819.7	3593.	4855.	1.35
0.4	1440.	24.64	30528.9	3672.	4957.	1.35
0.4	1470.	24.69	31239.7	3751.	5059.	1.35
0.4	1500.	24.74	31952.0	3831.	5161.	1.35
0.4	1530.	24.79	32665.7	3910.	5263.	1.35
0.4	1560.	24.84	33380.9	3990.	5365.	1.34
0.4	1590.	24.88	34097.4	4069.	5467.	1.34
0.4	1620.	24.93	34815.4	4149.	5569.	1.34
0.4	1650.	24.97	35534.7	4225.	5671.	1.34
0.4	1680.	25.02	36255.3	4304.	5773.	1.34
0.4	1710.	25.06	36977.2	4384.	5876.	1.34
0.4	1740.	25.10	37700.4	4463.	5978.	1.34
0.4	1770.	25.14	38424.9	4543.	6080.	1.34
0.4	1800.	25.18	39150.6	4623.	6182.	1.34
0.4	1830.	25.22	39877.5	4702.	6284.	1.34
0.4	1860.	25.26	40605.6	4782.	6386.	1.34
0.4	1890.	25.30	41334.9	4862.	6488.	1.33
0.4	1920.	25.34	42065.4	4942.	6590.	1.33
0.4	1950.	25.38	42797.0	5021.	6692.	1.33
0.4	2040.	25.49	44998.4	5261.	6999.	1.33
0.4	2130.	25.59	47209.5	5501.	7305.	1.33
0.4	2220.	25.69	49429.9	5742.	7611.	1.33
0.4	2310.	25.79	51659.1	5982.	7918.	1.32
0.4	2400.	25.88	53896.8	6223.	8224.	1.32
0.4	2490.	25.97	56142.8	6464.	8530.	1.32
0.4	2580.	26.06	58396.6	6714.	8836.	1.32
0.4	2670.	26.14	60658.1	6954.	9143.	1.31
0.4	2760.	26.22	62926.9	7196.	9449.	1.31
0.4	2850.	26.30	65200.1	7435.	9758.	1.31
0.4	2940.	26.38	67482.9	7677.	10065.	1.31
0.4	3030.	26.45	69772.3	7919.	10371.	1.31
0.4	3120.	26.52	72068.2	8161.	10678.	1.31
0.4	3210.	26.59	74370.4	8403.	10984.	1.31
0.4	3300.	26.66	76678.8	8646.	11291.	1.31
0.4	3390.	26.72	78993.2	8889.	11597.	1.30
0.4	3480.	26.79	81313.3	9132.	11904.	1.30
0.4	3570.	26.85	83639.2	9375.	12210.	1.30
0.4	3660.	26.91	85970.4	9618.	12517.	1.30
0.4	3750.	26.97	88307.2	9861.	12823.	1.30
0.4	3840.	27.03	90649.2	10105.	13130.	1.30
0.4	3930.	27.08	92996.3	10348.	13436.	1.30
0.4	4020.	27.14	95348.5	10592.	13743.	1.30
0.4	4110.	27.19	97705.5	10836.	14049.	1.30
0.4	4200.	27.24	100067.3	11080.	14356.	1.30
0.4	4290.	27.30	102433.7	11324.	14662.	1.29
0.4	4380.	27.35	104805.0	11568.	14969.	1.29
0.4	4470.	27.40	107180.5	11812.	15275.	1.29
0.4	4560.	27.44	109560.5	12057.	15582.	1.29

TABLE A1 (continued)

Π	δ^+	u_e/u_τ	$\int_0^{\delta^+} u^+ dy^+$	Re_θ	Re_{δ^*}	H
0.5	30.	15.45	309.6	65.	154.	2.38
0.5	45.	16.62	532.6	100.	215.	2.15
0.5	60.	17.38	769.5	136.	273.	2.00
0.5	75.	17.94	1016.3	173.	329.	1.91
0.5	90.	18.39	1270.6	210.	385.	1.84
0.5	105.	18.77	1531.2	247.	440.	1.78
0.5	120.	19.10	1797.0	285.	495.	1.74
0.5	135.	19.39	2067.4	323.	550.	1.70
0.5	150.	19.65	2341.9	361.	605.	1.68
0.5	165.	19.88	2620.1	399.	660.	1.65
0.5	180.	20.09	2901.5	438.	714.	1.63
0.5	195.	20.28	3186.0	477.	769.	1.61
0.5	210.	20.46	3473.3	516.	824.	1.60
0.5	225.	20.63	3763.3	555.	878.	1.58
0.5	240.	20.79	4056.3	589.	932.	1.58
0.5	255.	20.93	4350.2	634.	988.	1.56
0.5	270.	21.07	4646.9	674.	1042.	1.55
0.5	285.	21.20	4947.2	715.	1095.	1.53
0.5	300.	21.33	5246.4	753.	1152.	1.53
0.5	315.	21.44	5548.9	793.	1206.	1.52
0.5	330.	21.56	5853.1	833.	1261.	1.51
0.5	345.	21.67	6159.0	873.	1316.	1.51
0.5	360.	21.77	6466.4	913.	1370.	1.50
0.5	375.	21.87	6775.4	953.	1425.	1.49
0.5	390.	21.96	7085.8	994.	1479.	1.49
0.5	405.	22.05	7397.6	1034.	1534.	1.48
0.5	420.	22.14	7710.8	1074.	1589.	1.48
0.5	435.	22.23	8025.3	1115.	1643.	1.47
0.5	450.	22.31	8341.5	1156.	1698.	1.47
0.5	465.	22.39	8658.5	1190.	1752.	1.47
0.5	480.	22.47	8976.8	1231.	1807.	1.47
0.5	495.	22.54	9296.1	1278.	1861.	1.46
0.5	510.	22.61	9615.6	1318.	1917.	1.45
0.5	525.	22.68	9937.1	1351.	1971.	1.46
0.5	540.	22.75	10260.8	1393.	2025.	1.45
0.5	555.	22.82	10584.4	1441.	2079.	1.44
0.5	570.	22.88	10908.9	1482.	2134.	1.44
0.5	600.	23.01	11559.2	1563.	2245.	1.44
0.5	630.	23.12	12214.5	1645.	2354.	1.43
0.5	660.	23.24	12873.4	1727.	2463.	1.43
0.5	690.	23.35	13535.5	1809.	2573.	1.42
0.5	720.	23.45	14200.8	1891.	2682.	1.42
0.5	750.	23.55	14869.2	1974.	2791.	1.41
0.5	780.	23.64	15540.6	2056.	2901.	1.41
0.5	810.	23.73	16214.7	2139.	3010.	1.41
0.5	840.	23.82	16891.6	2222.	3119.	1.40
0.5	870.	23.91	17571.0	2305.	3229.	1.40
0.5	900.	23.99	18253.0	2383.	3338.	1.40
0.5	930.	24.07	18937.4	2466.	3447.	1.40
0.5	960.	24.15	19624.2	2549.	3556.	1.40
0.5	990.	24.22	20313.2	2632.	3666.	1.39
0.5	1020.	24.29	21004.5	2715.	3775.	1.39
0.5	1050.	24.36	21697.9	2798.	3884.	1.39
0.5	1080.	24.43	22393.4	2881.	3994.	1.39
0.5	1110.	24.50	23090.9	2965.	4103.	1.38
0.5	1140.	24.56	23790.4	3048.	4212.	1.38
0.5	1170.	24.63	24491.7	3140.	4321.	1.38

ORIGINAL PAGE IS
OF POOR QUALITY

TABLE A1 (continued)

Π	δ^+	u_e/u_τ	$\int_0^{\delta^+} u^+ dy^+$	Re_θ	Re_{δ^*}	H
0.5	1200.	24.69	25195.0	3223.	4431.	1.37
0.5	1230.	24.75	25900.1	3307.	4540.	1.37
0.5	1260.	24.81	26604.8	3389.	4651.	1.37
0.5	1290.	24.86	27313.3	3473.	4761.	1.37
0.5	1320.	24.92	28023.4	3557.	4870.	1.37
0.5	1350.	24.97	28735.2	3641.	4980.	1.37
0.5	1380.	25.03	29448.7	3725.	5089.	1.37
0.5	1410.	25.08	30163.7	3809.	5199.	1.36
0.5	1440.	25.13	30880.3	3893.	5308.	1.36
0.5	1470.	25.18	31598.4	3977.	5417.	1.36
0.5	1500.	25.23	32318.0	4062.	5527.	1.36
0.5	1530.	25.28	33039.1	4146.	5636.	1.36
0.5	1560.	25.33	33761.5	4230.	5746.	1.36
0.5	1590.	25.37	34485.4	4315.	5855.	1.36
0.5	1620.	25.42	35210.7	4399.	5965.	1.36
0.5	1650.	25.46	35937.3	4480.	6074.	1.36
0.5	1680.	25.51	36665.2	4564.	6183.	1.35
0.5	1710.	25.55	37394.5	4649.	6293.	1.35
0.5	1740.	25.59	38125.0	4733.	6402.	1.35
0.5	1770.	25.63	38856.8	4818.	6512.	1.35
0.5	1800.	25.67	39589.8	4902.	6621.	1.35
0.5	1830.	25.71	40324.0	4987.	6730.	1.35
0.5	1860.	25.75	41059.5	5071.	6840.	1.35
0.5	1890.	25.79	41796.1	5156.	6949.	1.35
0.5	1920.	25.83	42533.9	5241.	7059.	1.35
0.5	1950.	25.87	43272.8	5325.	7168.	1.35
0.5	2040.	25.98	45496.2	5580.	7496.	1.34
0.5	2130.	26.08	47729.2	5834.	7825.	1.34
0.5	2220.	26.18	49971.6	6090.	8153.	1.34
0.5	2310.	26.28	52222.8	6345.	8481.	1.34
0.5	2400.	26.37	54482.5	6601.	8809.	1.33
0.5	2490.	26.46	56750.3	6856.	9138.	1.33
0.5	2580.	26.55	59026.1	7121.	9466.	1.33
0.5	2670.	26.63	61309.5	7376.	9794.	1.33
0.5	2760.	26.71	63600.3	7632.	10123.	1.33
0.5	2850.	26.79	65895.5	7886.	10454.	1.33
0.5	2940.	26.86	68200.2	8143.	10782.	1.32
0.5	3030.	26.94	70511.6	8400.	11111.	1.32
0.5	3120.	27.01	72829.5	8657.	11439.	1.32
0.5	3210.	27.08	75153.6	8914.	11768.	1.32
0.5	3300.	27.15	77484.0	9172.	12096.	1.32
0.5	3390.	27.21	79820.3	9429.	12424.	1.32
0.5	3480.	27.27	82162.4	9687.	12753.	1.32
0.5	3570.	27.34	84510.3	9945.	13081.	1.32
0.5	3660.	27.40	86863.5	10203.	13410.	1.31
0.5	3750.	27.46	89222.2	10462.	13738.	1.31
0.5	3840.	27.51	91586.1	10720.	14067.	1.31
0.5	3930.	27.57	93955.3	10979.	14395.	1.31
0.5	4020.	27.63	96329.3	11238.	14724.	1.31
0.5	4110.	27.68	98708.3	11496.	15052.	1.31
0.5	4200.	27.73	101092.1	11756.	15381.	1.31
0.5	4290.	27.78	103480.5	12015.	15709.	1.31
0.5	4380.	27.83	105873.6	12274.	16038.	1.31
0.5	4470.	27.88	108271.2	12533.	16366.	1.31
0.5	4560.	27.93	110673.2	12793.	16694.	1.30

TABLE A1 (continued)

Π	δ^+	u_e/u_τ	$\int_0^{\delta^+} u^+ dy^+$	Re_θ	Re_{δ^*}	H
0.55	30.	15.70	313.2	66.	158.	2.39
0.55	45.	16.86	538.0	102.	221.	2.16
0.55	60.	17.62	776.9	139.	280.	2.01
0.55	75.	18.19	1025.4	177.	338.	1.92
0.55	90.	18.64	1281.6	215.	396.	1.84
0.55	105.	19.02	1544.0	253.	453.	1.79
0.55	120.	19.35	1811.6	292.	510.	1.75
0.55	135.	19.63	2083.9	331.	567.	1.71
0.55	150.	19.89	2360.2	370.	623.	1.68
0.55	165.	20.12	2640.2	410.	680.	1.66
0.55	180.	20.33	2923.5	450.	736.	1.64
0.55	195.	20.53	3209.8	490.	793.	1.62
0.55	210.	20.71	3498.9	530.	849.	1.60
0.55	225.	20.87	3790.7	570.	906.	1.59
0.55	240.	21.03	4085.6	605.	962.	1.59
0.55	255.	21.18	4381.3	651.	1019.	1.56
0.55	270.	21.32	4679.9	692.	1075.	1.55
0.55	285.	21.45	4982.0	734.	1130.	1.54
0.55	300.	21.57	5283.0	774.	1188.	1.54
0.55	315.	21.69	5587.3	815.	1245.	1.53
0.55	330.	21.80	5893.4	856.	1301.	1.52
0.55	345.	21.91	6201.1	897.	1358.	1.51
0.55	360.	22.01	6510.3	938.	1414.	1.51
0.55	375.	22.11	6821.1	979.	1471.	1.50
0.55	390.	22.21	7133.4	1021.	1527.	1.50
0.55	405.	22.30	7447.0	1062.	1584.	1.49
0.55	420.	22.39	7762.0	1104.	1640.	1.49
0.55	435.	22.47	8078.3	1145.	1696.	1.48
0.55	450.	22.55	8396.4	1187.	1752.	1.48
0.55	465.	22.63	8715.3	1223.	1809.	1.48
0.55	480.	22.71	9035.3	1265.	1865.	1.47
0.55	495.	22.78	9356.5	1313.	1922.	1.46
0.55	510.	22.86	9677.8	1354.	1979.	1.46
0.55	525.	22.93	10001.0	1388.	2035.	1.47
0.55	540.	22.99	10326.6	1431.	2091.	1.46
0.55	555.	23.06	10652.1	1481.	2147.	1.45
0.55	570.	23.13	10978.5	1523.	2203.	1.45
0.55	600.	23.25	11632.4	1606.	2318.	1.44
0.55	630.	23.37	12291.4	1690.	2431.	1.44
0.55	660.	23.48	12953.9	1774.	2544.	1.43
0.55	690.	23.59	13619.7	1859.	2657.	1.43
0.55	720.	23.69	14288.7	1943.	2770.	1.43
0.55	750.	23.79	14960.7	2028.	2883.	1.42
0.55	780.	23.89	15635.8	2113.	2996.	1.42
0.55	810.	23.98	16313.6	2198.	3109.	1.41
0.55	840.	24.07	16994.1	2284.	3222.	1.41
0.55	870.	24.15	17677.2	2369.	3335.	1.41
0.55	900.	24.23	18362.8	2449.	3448.	1.41
0.55	930.	24.31	19050.9	2534.	3561.	1.40
0.55	960.	24.39	19741.3	2620.	3674.	1.40
0.55	990.	24.47	20434.0	2705.	3786.	1.40
0.55	1020.	24.54	21128.9	2790.	3899.	1.40
0.55	1050.	24.61	21826.0	2876.	4012.	1.40

TABLE A1 (continued)

Π	δ^+	u_e/u_τ	$\int_0^{\delta^+} u^+ dy^+$	Re_θ	Re_{δ^*}	H
0.55	1080.	24.68	22525.1	2962.	4125.	1.39
0.55	1110.	24.74	23226.3	3047.	4238.	1.39
0.55	1140.	24.81	23929.4	3133.	4351.	1.39
0.55	1170.	24.87	24634.5	3227.	4464.	1.38
0.55	1200.	24.93	25341.4	3313.	4577.	1.38
0.55	1230.	24.99	26050.2	3399.	4690.	1.38
0.55	1260.	25.05	26758.5	3484.	4805.	1.38
0.55	1290.	25.11	27470.6	3570.	4918.	1.38
0.55	1320.	25.16	28184.5	3656.	5031.	1.38
0.55	1350.	25.22	28899.9	3743.	5144.	1.37
0.55	1380.	25.27	29617.0	3829.	5258.	1.37
0.55	1410.	25.32	30335.7	3915.	5371.	1.37
0.55	1440.	25.37	31056.0	4002.	5484.	1.37
0.55	1470.	25.42	31777.7	4088.	5597.	1.37
0.55	1500.	25.47	32501.0	4175.	5710.	1.37
0.55	1530.	25.52	33225.7	4262.	5823.	1.37
0.55	1560.	25.57	33951.8	4348.	5936.	1.37
0.55	1590.	25.62	34679.4	4435.	6049.	1.36
0.55	1620.	25.66	35408.3	4522.	6162.	1.36
0.55	1650.	25.71	36138.6	4605.	6275.	1.36
0.55	1680.	25.75	36870.2	4692.	6388.	1.36
0.55	1710.	25.79	37603.1	4779.	6501.	1.36
0.55	1740.	25.83	38337.3	4866.	6615.	1.36
0.55	1770.	25.88	39072.7	4952.	6728.	1.36
0.55	1800.	25.92	39809.4	5039.	6841.	1.36
0.55	1830.	25.96	40547.3	5126.	6954.	1.36
0.55	1860.	26.00	41286.4	5213.	7067.	1.36
0.55	1890.	26.04	42026.7	5300.	7180.	1.35
0.55	1920.	26.07	42768.1	5388.	7293.	1.35
0.55	1950.	26.11	43510.7	5475.	7406.	1.35
0.55	2040.	26.22	45745.1	5736.	7745.	1.35
0.55	2130.	26.33	47989.1	5998.	8084.	1.35
0.55	2220.	26.43	50242.4	6261.	8424.	1.35
0.55	2310.	26.52	52504.5	6523.	8763.	1.34
0.55	2400.	26.62	54775.3	6786.	9102.	1.34
0.55	2490.	26.71	57054.1	7049.	9441.	1.34
0.55	2580.	26.79	59340.9	7321.	9781.	1.34
0.55	2670.	26.87	61635.3	7583.	10120.	1.33
0.55	2760.	26.96	63937.0	7847.	10459.	1.33
0.55	2850.	27.03	66243.2	8108.	10801.	1.33
0.55	2940.	27.11	68558.8	8372.	11141.	1.33
0.55	3030.	27.18	70881.2	8637.	11480.	1.33
0.55	3120.	27.25	73210.0	8901.	11820.	1.33
0.55	3210.	27.32	75545.3	9166.	12159.	1.33
0.55	3300.	27.39	77886.6	9431.	12499.	1.33
0.55	3390.	27.45	80233.9	9696.	12838.	1.32
0.55	3480.	27.52	82587.0	9961.	13177.	1.32
0.55	3570.	27.58	84945.8	10226.	13517.	1.32
0.55	3660.	27.64	87310.0	10492.	13856.	1.32
0.55	3750.	27.70	89679.7	10757.	14196.	1.32
0.55	3840.	27.76	92054.6	11023.	14535.	1.32
0.55	3930.	27.81	94434.7	11289.	14875.	1.32
0.55	4020.	27.87	96819.7	11555.	15214.	1.32
0.55	4110.	27.92	99209.8	11822.	15554.	1.32
0.55	4200.	27.98	101604.4	12088.	15893.	1.31
0.55	4290.	28.03	104004.0	12355.	16232.	1.31
0.55	4380.	28.08	106408.1	12621.	16572.	1.31
0.55	4470.	28.13	108816.5	12888.	16911.	1.31
0.55	4560.	28.18	111229.5	13155.	17251.	1.31

TABLE A1 (continued)

Π	δ^+	u_e/u_τ	$\int_0^{\delta^+} u^+ dy^+$	Re_θ	Re_{δ^*}	H
0.6	30.	15.94	316.9	67.	161.	2.40
0.6	45.	17.11	543.5	104.	226.	2.17
0.6	60.	17.86	784.2	142.	288.	2.02
0.6	75.	18.43	1034.6	181.	348.	1.92
0.6	90.	18.88	1292.6	220.	407.	1.85
0.6	105.	19.26	1556.8	259.	466.	1.80
0.6	120.	19.59	1826.3	299.	525.	1.75
0.6	135.	19.88	2100.4	339.	583.	1.72
0.6	150.	20.13	2378.5	380.	642.	1.69
0.6	165.	20.37	2660.3	420.	700.	1.67
0.6	180.	20.58	2945.4	461.	758.	1.64
0.6	195.	20.77	3233.6	502.	817.	1.63
0.6	210.	20.95	3524.6	543.	875.	1.61
0.6	225.	21.12	3818.2	585.	933.	1.60
0.6	240.	21.27	4114.9	620.	991.	1.60
0.6	255.	21.42	4412.4	668.	1050.	1.57
0.6	270.	21.56	4712.8	710.	1108.	1.56
0.6	285.	21.69	5016.8	753.	1165.	1.55
0.6	300.	21.81	5319.6	794.	1225.	1.54
0.6	315.	21.93	5625.7	836.	1283.	1.54
0.6	330.	22.05	5933.6	878.	1341.	1.53
0.6	345.	22.15	6243.1	920.	1400.	1.52
0.6	360.	22.26	6554.3	962.	1458.	1.51
0.6	375.	22.36	6866.9	1005.	1516.	1.51
0.6	390.	22.45	7181.0	1047.	1575.	1.50
0.6	405.	22.54	7496.4	1090.	1633.	1.50
0.6	420.	22.63	7813.3	1133.	1691.	1.49
0.6	435.	22.71	8131.4	1175.	1750.	1.49
0.6	450.	22.80	8451.3	1218.	1807.	1.48
0.6	465.	22.88	8772.0	1256.	1866.	1.49
0.6	480.	22.95	9093.9	1298.	1924.	1.48
0.6	495.	23.03	9416.9	1347.	1982.	1.47
0.6	510.	23.10	9740.0	1389.	2041.	1.47
0.6	525.	23.17	10065.1	1425.	2099.	1.47
0.6	540.	23.24	10392.5	1469.	2156.	1.47
0.6	555.	23.31	10719.8	1520.	2215.	1.46
0.6	570.	23.37	11048.0	1563.	2273.	1.45
0.6	600.	23.49	11705.6	1648.	2391.	1.45
0.6	630.	23.61	12368.3	1735.	2508.	1.45
0.6	660.	23.73	13034.4	1821.	2624.	1.44
0.6	690.	23.83	13703.9	1908.	2741.	1.44
0.6	720.	23.94	14376.5	1995.	2858.	1.43
0.6	750.	24.04	15052.2	2082.	2974.	1.43
0.6	780.	24.13	15730.9	2169.	3091.	1.42
0.6	810.	24.22	16412.4	2257.	3208.	1.42
0.6	840.	24.31	17096.5	2344.	3324.	1.42
0.6	870.	24.40	17783.3	2432.	3441.	1.41
0.6	900.	24.48	18472.6	2515.	3557.	1.41
0.6	930.	24.56	19164.3	2602.	3674.	1.41
0.6	960.	24.63	19858.4	2690.	3791.	1.41
0.6	990.	24.71	20554.8	2777.	3907.	1.41
0.6	1020.	24.78	21253.4	2865.	4024.	1.40
0.6	1050.	24.85	21954.1	2953.	4140.	1.40
0.6	1080.	24.92	22656.9	3041.	4257.	1.40
0.6	1110.	24.99	23361.7	3129.	4374.	1.40
0.6	1140.	25.05	24068.5	3217.	4490.	1.40
0.6	1170.	25.11	24777.2	3313.	4607.	1.39
0.6	1200.	25.18	25487.8	3402.	4723.	1.39
0.6	1230.	25.24	26200.2	3490.	4840.	1.39

TABLE A1 (concluded)

Π	δ^+	u_e/u_τ	$\int_0^{\delta^+} u^+ dy^+$	Re_θ	Re_{δ^*}	H
0.6	1260.	25.29	26912.2	3577.	4959.	1.39
0.6	1290.	25.35	27628.0	3666.	5076.	1.38
0.6	1320.	25.41	28345.5	3754.	5192.	1.38
0.6	1350.	25.46	29064.6	3843.	5309.	1.38
0.6	1380.	25.52	29785.4	3932.	5426.	1.38
0.6	1410.	25.57	30507.7	4021.	5543.	1.38
0.6	1440.	25.62	31231.7	4109.	5659.	1.38
0.6	1470.	25.67	31957.1	4198.	5776.	1.38
0.6	1500.	25.72	32684.0	4287.	5893.	1.37
0.6	1530.	25.77	33412.4	4376.	6010.	1.37
0.6	1560.	25.81	34142.2	4465.	6126.	1.37
0.6	1590.	25.86	34873.3	4554.	6243.	1.37
0.6	1620.	25.90	35605.9	4644.	6360.	1.37
0.6	1650.	25.95	36339.9	4729.	6477.	1.37
0.6	1680.	25.99	37075.1	4818.	6593.	1.37
0.6	1710.	26.04	37811.7	4907.	6710.	1.37
0.6	1740.	26.08	38549.6	4997.	6827.	1.37
0.6	1770.	26.12	39288.7	5086.	6944.	1.37
0.6	1800.	26.16	40029.0	5175.	7060.	1.36
0.6	1830.	26.20	40770.6	5265.	7177.	1.36
0.6	1860.	26.24	41513.3	5354.	7294.	1.36
0.6	1890.	26.28	42257.3	5443.	7410.	1.36
0.6	1920.	26.32	43002.4	5533.	7527.	1.36
0.6	1950.	26.36	43748.6	5622.	7644.	1.36
0.6	2040.	26.46	45993.9	5891.	7994.	1.36
0.6	2130.	26.57	48249.0	6160.	8344.	1.35
0.6	2220.	26.67	50513.3	6430.	8695.	1.35
0.6	2310.	26.77	52786.4	6700.	9045.	1.35
0.6	2400.	26.86	55068.1	6970.	9395.	1.35
0.6	2490.	26.95	57357.9	7240.	9745.	1.35
0.6	2580.	27.04	59655.7	7519.	10095.	1.34
0.6	2670.	27.12	61961.0	7788.	10446.	1.34
0.6	2760.	27.20	64273.7	8059.	10796.	1.34
0.6	2850.	27.28	66590.9	8328.	11149.	1.34
0.6	2940.	27.35	68917.5	8599.	11499.	1.34
0.6	3030.	27.43	71250.9	8871.	11850.	1.34
0.6	3120.	27.50	73590.7	9142.	12200.	1.33
0.6	3210.	27.57	75936.9	9414.	12551.	1.33
0.6	3300.	27.63	78289.2	9686.	12901.	1.33
0.6	3390.	27.70	80647.4	9959.	13252.	1.33
0.6	3480.	27.76	83011.6	10231.	13602.	1.33
0.6	3570.	27.82	85381.3	10504.	13952.	1.33
0.6	3660.	27.89	87756.7	10777.	14303.	1.33
0.6	3750.	27.94	90137.3	11050.	14653.	1.33
0.6	3840.	28.00	92523.2	11323.	15004.	1.33
0.6	3930.	28.06	94914.3	11596.	15354.	1.32
0.6	4020.	28.11	97310.2	11870.	15705.	1.32
0.6	4110.	28.17	99711.2	12143.	16055.	1.32
0.6	4200.	28.22	102116.9	12417.	16405.	1.32
0.6	4290.	28.27	104527.4	12691.	16756.	1.32
0.6	4380.	28.32	106942.4	12965.	17106.	1.32
0.6	4470.	28.37	109361.9	13239.	17457.	1.32
0.6	4560.	28.42	111785.9	13514.	17807.	1.32

TABLE A2

INTEGRAL PROPERTIES OF THE MUSKER-COLES-GRANVILLE PROFILE

Π	δ^+	u_e/u_τ	$\int_0^{\delta^+} u^+ dy^+$	Re_θ	Re_{δ^*}	H
0.0	30.	13.01	279.1	48.	111.	2.34
0.0	45.	14.18	486.8	71.	151.	2.14
0.0	60.	14.94	708.5	93.	188.	2.01
0.0	75.	15.50	940.0	116.	223.	1.91
0.0	90.	15.95	1179.1	139.	257.	1.84
0.0	105.	16.33	1424.4	163.	291.	1.79
0.0	120.	16.66	1675.0	187.	324.	1.74
0.0	135.	16.95	1930.2	210.	358.	1.70
0.0	150.	17.21	2189.4	234.	391.	1.67
0.0	165.	17.44	2452.3	259.	425.	1.64
0.0	180.	17.65	2718.5	283.	458.	1.62
0.0	195.	17.84	2987.8	308.	492.	1.60
0.0	210.	18.02	3259.8	332.	525.	1.58
0.0	225.	18.19	3534.5	357.	558.	1.56
0.0	240.	18.35	3812.3	375.	591.	1.58
0.0	255.	18.49	4090.9	407.	625.	1.54
0.0	270.	18.63	4372.4	432.	658.	1.52
0.0	285.	18.76	4657.5	458.	690.	1.51
0.0	300.	18.89	4941.4	482.	725.	1.50
0.0	315.	19.00	5228.6	507.	758.	1.49
0.0	330.	19.12	5517.6	532.	791.	1.49
0.0	345.	19.23	5808.2	558.	824.	1.48
0.0	360.	19.33	6100.4	583.	858.	1.47
0.0	375.	19.43	6394.1	608.	891.	1.46
0.0	390.	19.52	6689.3	634.	924.	1.46
0.0	405.	19.61	6985.9	659.	958.	1.45
0.0	420.	19.70	7283.8	685.	991.	1.45
0.0	435.	19.79	7583.0	711.	1024.	1.44
0.0	450.	19.87	7884.0	737.	1057.	1.43
0.0	465.	19.95	8185.8	763.	1090.	1.43
0.0	480.	20.03	8488.8	781.	1123.	1.44
0.0	495.	20.10	8792.9	814.	1157.	1.42
0.0	510.	20.17	9097.1	839.	1191.	1.42
0.0	525.	20.24	9403.3	857.	1224.	1.43
0.0	540.	20.31	9711.8	884.	1256.	1.42
0.0	555.	20.38	10020.1	918.	1289.	1.40
0.0	570.	20.44	10329.4	944.	1322.	1.40
0.0	600.	20.57	10949.2	994.	1391.	1.40
0.0	630.	20.68	11574.0	1046.	1457.	1.39
0.0	660.	20.80	12202.4	1098.	1524.	1.39
0.0	690.	20.91	12834.0	1150.	1591.	1.38
0.0	720.	21.01	13468.8	1203.	1657.	1.38
0.0	750.	21.11	14106.7	1255.	1724.	1.37
0.0	780.	21.20	14747.6	1307.	1790.	1.37
0.0	810.	21.29	15391.2	1360.	1857.	1.37
0.0	840.	21.38	16037.6	1412.	1924.	1.36
0.0	870.	21.47	16686.5	1465.	1990.	1.36
0.0	900.	21.55	17338.0	1518.	2057.	1.36
0.0	930.	21.63	17991.9	1565.	2123.	1.36
0.0	960.	21.71	18648.2	1617.	2190.	1.35
0.0	990.	21.78	19306.7	1669.	2257.	1.35
0.0	1020.	21.85	19967.5	1722.	2323.	1.35
0.0	1050.	21.92	20630.4	1775.	2390.	1.35

TABLE A2 (continued)

Π	δ^+	u_e/u_τ	$\int_0^{\delta^+} u^+ dy^+$	Re_θ	Re_{δ^*}	H
0.0	1080.	21.99	21295.4	1827.	2456.	1.34
0.0	1110.	22.06	21962.4	1880.	2523.	1.34
0.0	1140.	22.12	22631.4	1942.	2590.	1.33
0.0	1170.	22.19	23302.3	1995.	2656.	1.33
0.0	1200.	22.25	23975.0	2048.	2723.	1.33
0.0	1230.	22.31	24649.6	2101.	2789.	1.33
0.0	1260.	22.37	25323.8	2152.	2858.	1.33
0.0	1290.	22.42	26001.8	2206.	2925.	1.33
0.0	1320.	22.48	26681.4	2259.	2991.	1.32
0.0	1350.	22.53	27362.7	2312.	3058.	1.32
0.0	1380.	22.59	28045.7	2365.	3125.	1.32
0.0	1410.	22.64	28730.2	2418.	3192.	1.32
0.0	1440.	22.69	29416.3	2472.	3258.	1.32
0.0	1470.	22.74	30103.9	2525.	3325.	1.32
0.0	1500.	22.79	30793.0	2579.	3392.	1.32
0.0	1530.	22.84	31483.5	2632.	3459.	1.31
0.0	1560.	22.89	32175.5	2686.	3525.	1.31
0.0	1590.	22.93	32868.9	2739.	3592.	1.31
0.0	1620.	22.98	33563.7	2793.	3659.	1.31
0.0	1650.	23.02	34259.8	2846.	3725.	1.31
0.0	1680.	23.07	34957.2	2895.	3792.	1.31
0.0	1710.	23.11	35656.0	2949.	3859.	1.31
0.0	1740.	23.15	36356.0	3002.	3926.	1.31
0.0	1770.	23.19	37057.3	3056.	3992.	1.31
0.0	1800.	23.23	37759.8	3109.	4059.	1.31
0.0	1830.	23.27	38463.6	3163.	4126.	1.30
0.0	1860.	23.31	39168.5	3216.	4193.	1.30
0.0	1890.	23.35	39874.6	3270.	4259.	1.30
0.0	1920.	23.39	40581.9	3324.	4326.	1.30
0.0	1950.	23.43	41290.3	3377.	4393.	1.30
0.0	2040.	23.54	43422.2	3538.	4593.	1.30
0.0	2130.	23.64	45563.8	3700.	4793.	1.30
0.0	2220.	23.74	47714.6	3861.	4993.	1.29
0.0	2310.	23.84	49874.3	4023.	5193.	1.29
0.0	2400.	23.93	52042.4	4185.	5393.	1.29
0.0	2490.	24.02	54218.8	4347.	5594.	1.29
0.0	2580.	24.11	56403.1	4518.	5794.	1.28
0.0	2670.	24.19	58595.0	4681.	5994.	1.28
0.0	2760.	24.27	60794.3	4841.	6194.	1.28
0.0	2850.	24.35	62998.1	5001.	6397.	1.28
0.0	2940.	24.42	65211.2	5164.	6598.	1.28
0.0	3030.	24.50	67431.1	5326.	6798.	1.28
0.0	3120.	24.57	69657.5	5489.	6998.	1.27
0.0	3210.	24.64	71890.1	5652.	7199.	1.27
0.0	3300.	24.71	74129.0	5815.	7399.	1.27
0.0	3390.	24.77	76373.8	5978.	7599.	1.27
0.0	3480.	24.83	78624.4	6141.	7800.	1.27
0.0	3570.	24.90	80880.7	6304.	8000.	1.27
0.0	3660.	24.96	83142.5	6468.	8200.	1.27
0.0	3750.	25.02	85409.7	6631.	8401.	1.27
0.0	3840.	25.07	87682.2	6795.	8601.	1.27
0.0	3930.	25.13	89959.7	6959.	8802.	1.26
0.0	4020.	25.19	92242.4	7122.	9002.	1.26
0.0	4110.	25.24	94529.8	7286.	9202.	1.26
0.0	4200.	25.29	96822.1	7450.	9403.	1.26
0.0	4290.	25.34	99119.0	7614.	9603.	1.26
0.0	4380.	25.39	101420.6	7778.	9803.	1.26
0.0	4470.	25.44	103726.7	7942.	10004.	1.26
0.0	4560.	25.49	106037.2	8107.	10204.	1.26

TABLE A2 (continued)

Π	δ^+	u_e/u_τ	$\int_0^{\delta^+} u^+ dy^+$	Re_θ	Re_{δ^*}	H
0.1	30.	13.50	286.4	50.	119.	2.35
0.1	45.	14.67	497.8	75.	162.	2.15
0.1	60.	15.42	723.2	101.	202.	2.01
0.1	75.	15.99	958.3	126.	241.	1.91
0.1	90.	16.44	1201.1	151.	279.	1.84
0.1	105.	16.82	1450.0	177.	316.	1.78
0.1	120.	17.15	1704.3	203.	354.	1.74
0.1	135.	17.44	1963.1	230.	391.	1.70
0.1	150.	17.69	2226.0	256.	428.	1.67
0.1	165.	17.93	2492.6	283.	465.	1.64
0.1	180.	18.14	2762.4	310.	502.	1.62
0.1	195.	18.33	3035.4	337.	539.	1.60
0.1	210.	18.51	3311.1	364.	576.	1.58
0.1	225.	18.68	3589.4	391.	613.	1.57
0.1	240.	18.83	3870.9	412.	649.	1.58
0.1	255.	18.98	4153.2	446.	687.	1.54
0.1	270.	19.12	4438.3	474.	724.	1.53
0.1	285.	19.25	4727.0	503.	759.	1.51
0.1	300.	19.37	5014.6	529.	798.	1.51
0.1	315.	19.49	5305.5	557.	835.	1.50
0.1	330.	19.61	5598.1	585.	872.	1.49
0.1	345.	19.71	5892.4	613.	909.	1.48
0.1	360.	19.82	6188.3	640.	946.	1.48
0.1	375.	19.92	6485.6	668.	983.	1.47
0.1	390.	20.01	6784.5	697.	1020.	1.46
0.1	405.	20.10	7084.7	725.	1056.	1.46
0.1	420.	20.19	7386.3	753.	1093.	1.45
0.1	435.	20.27	7689.1	781.	1130.	1.45
0.1	450.	20.36	7993.8	810.	1167.	1.44
0.1	465.	20.44	8299.3	838.	1204.	1.44
0.1	480.	20.51	8605.9	860.	1241.	1.44
0.1	495.	20.59	8913.7	895.	1277.	1.43
0.1	510.	20.66	9221.5	923.	1315.	1.43
0.1	525.	20.73	9531.4	943.	1352.	1.43
0.1	540.	20.80	9843.5	972.	1388.	1.43
0.1	555.	20.87	10155.5	1009.	1425.	1.41
0.1	570.	20.93	10468.5	1038.	1462.	1.41
0.1	600.	21.05	11095.6	1093.	1537.	1.41
0.1	630.	21.17	11727.8	1151.	1611.	1.40
0.1	660.	21.29	12363.4	1208.	1685.	1.39
0.1	690.	21.39	13002.4	1265.	1759.	1.39
0.1	720.	21.50	13644.5	1323.	1833.	1.39
0.1	750.	21.60	14289.7	1380.	1907.	1.38
0.1	780.	21.69	14937.9	1438.	1981.	1.38
0.1	810.	21.78	15588.9	1496.	2055.	1.37
0.1	840.	21.87	16242.5	1554.	2129.	1.37
0.1	870.	21.96	16898.8	1612.	2203.	1.37
0.1	900.	22.04	17557.6	1664.	2276.	1.37
0.1	930.	22.12	18218.8	1722.	2350.	1.37
0.1	960.	22.19	18882.4	1780.	2424.	1.36
0.1	990.	22.27	19548.3	1837.	2498.	1.36
0.1	1020.	22.34	20216.3	1895.	2572.	1.36
0.1	1050.	22.41	20886.6	1953.	2646.	1.35
0.1	1080.	22.48	21558.9	2011.	2720.	1.35
0.1	1110.	22.55	22233.2	2070.	2794.	1.35

TABLE A2 (continued)

Π	δ^+	u_e/u_τ	$\int_0^{\delta^+} u^+ dy^+$	Re_θ	Re_{δ^*}	H
0.1	1140.	22.61	22909.5	2128.	2868.	1.35
0.1	1170.	22.67	23587.7	2195.	2942.	1.34
0.1	1200.	22.74	24267.8	2253.	3015.	1.34
0.1	1230.	22.80	24949.7	2312.	3089.	1.34
0.1	1260.	22.85	25631.2	2368.	3165.	1.34
0.1	1290.	22.91	26316.5	2427.	3240.	1.33
0.1	1320.	22.97	27003.5	2485.	3314.	1.33
0.1	1350.	23.02	27692.1	2544.	3388.	1.33
0.1	1380.	23.08	28382.4	2603.	3462.	1.33
0.1	1410.	23.13	29074.3	2661.	3536.	1.33
0.1	1440.	23.18	29767.7	2720.	3610.	1.33
0.1	1470.	23.23	30462.6	2779.	3684.	1.33
0.1	1500.	23.28	31159.0	2838.	3758.	1.32
0.1	1530.	23.33	31856.9	2896.	3832.	1.32
0.1	1560.	23.37	32556.2	2955.	3906.	1.32
0.1	1590.	23.42	33256.8	3014.	3980.	1.32
0.1	1620.	23.46	33958.9	3073.	4054.	1.32
0.1	1650.	23.51	34662.4	3132.	4128.	1.32
0.1	1680.	23.55	35367.1	3187.	4202.	1.32
0.1	1710.	23.60	36073.2	3246.	4276.	1.32
0.1	1740.	23.64	36780.6	3305.	4350.	1.32
0.1	1770.	23.68	37489.2	3363.	4424.	1.32
0.1	1800.	23.72	38199.0	3422.	4498.	1.31
0.1	1830.	23.76	38910.1	3481.	4572.	1.31
0.1	1860.	23.80	39622.3	3540.	4646.	1.31
0.1	1890.	23.84	40335.8	3599.	4720.	1.31
0.1	1920.	23.88	41050.3	3658.	4794.	1.31
0.1	1950.	23.92	41766.1	3717.	4868.	1.31
0.1	2040.	24.02	43919.9	3895.	5091.	1.31
0.1	2130.	24.13	46083.5	4072.	5313.	1.30
0.1	2220.	24.23	48256.2	4250.	5535.	1.30
0.1	2310.	24.33	50437.9	4428.	5757.	1.30
0.1	2400.	24.42	52628.0	4607.	5979.	1.30
0.1	2490.	24.51	54826.4	4785.	6201.	1.30
0.1	2580.	24.60	57032.7	4973.	6423.	1.29
0.1	2670.	24.68	59246.5	5152.	6645.	1.29
0.1	2760.	24.76	61467.7	5328.	6868.	1.29
0.1	2850.	24.84	63693.4	5505.	7093.	1.29
0.1	2940.	24.91	65928.5	5684.	7315.	1.29
0.1	3030.	24.99	68170.4	5863.	7537.	1.29
0.1	3120.	25.06	70418.7	6042.	7760.	1.28
0.1	3210.	25.13	72673.4	6221.	7982.	1.28
0.1	3300.	25.19	74934.2	6401.	8204.	1.28
0.1	3390.	25.26	77201.0	6581.	8427.	1.28
0.1	3480.	25.32	79473.6	6760.	8649.	1.28
0.1	3570.	25.38	81751.8	6940.	8871.	1.28
0.1	3660.	25.45	84035.6	7120.	9093.	1.28
0.1	3750.	25.50	86324.7	7300.	9316.	1.28
0.1	3840.	25.56	88619.2	7480.	9538.	1.28
0.1	3930.	25.62	90918.7	7660.	9760.	1.27
0.1	4020.	25.67	93223.3	7841.	9983.	1.27
0.1	4110.	25.73	95532.7	8021.	10205.	1.27
0.1	4200.	25.78	97847.0	8202.	10427.	1.27
0.1	4290.	25.83	100165.8	8382.	10650.	1.27
0.1	4380.	25.88	102489.4	8563.	10872.	1.27
0.1	4470.	25.93	104817.4	8744.	11094.	1.27
0.1	4560.	25.98	107149.8	8925.	11317.	1.27

TABLE A2 (continued)

Π	δ^+	u_e/u_τ	$\int_0^{\delta^+} u^+ dy^+$	Re_θ	Re_{δ^*}	H
0.2	30.	13.99	293.7	53.	126.	2.37
0.2	45.	15.15	508.8	80.	173.	2.16
0.2	60.	15.91	737.8	108.	217.	2.02
0.2	75.	16.48	976.6	135.	259.	1.92
0.2	90.	16.93	1223.0	163.	301.	1.85
0.2	105.	17.31	1475.7	191.	342.	1.79
0.2	120.	17.64	1733.6	220.	383.	1.74
0.2	135.	17.93	1996.0	248.	424.	1.71
0.2	150.	18.18	2262.6	277.	465.	1.67
0.2	165.	18.41	2532.8	307.	505.	1.65
0.2	180.	18.62	2806.4	336.	546.	1.63
0.2	195.	18.82	3082.9	365.	587.	1.61
0.2	210.	19.00	3362.3	395.	627.	1.59
0.2	225.	19.17	3644.3	425.	668.	1.57
0.2	240.	19.32	3929.4	448.	708.	1.58
0.2	255.	19.47	4215.4	485.	749.	1.55
0.2	270.	19.61	4504.2	515.	790.	1.54
0.2	285.	19.74	4796.6	546.	829.	1.52
0.2	300.	19.86	5087.8	575.	871.	1.52
0.2	315.	19.98	5382.3	605.	912.	1.51
0.2	330.	20.09	5678.6	635.	952.	1.50
0.2	345.	20.20	5976.6	666.	993.	1.49
0.2	360.	20.30	6276.1	696.	1033.	1.48
0.2	375.	20.40	6577.1	727.	1074.	1.48
0.2	390.	20.50	6879.6	757.	1115.	1.47
0.2	405.	20.59	7183.5	788.	1155.	1.47
0.2	420.	20.68	7488.8	819.	1196.	1.46
0.2	435.	20.76	7795.3	849.	1237.	1.46
0.2	450.	20.85	8103.6	881.	1277.	1.45
0.2	465.	20.92	8412.7	912.	1317.	1.44
0.2	480.	21.00	8723.0	936.	1358.	1.45
0.2	495.	21.08	9034.5	974.	1398.	1.44
0.2	510.	21.15	9345.9	1004.	1440.	1.43
0.2	525.	21.22	9659.5	1027.	1480.	1.44
0.2	540.	21.29	9975.3	1059.	1520.	1.44
0.2	555.	21.35	10290.9	1098.	1560.	1.42
0.2	570.	21.42	10607.6	1129.	1601.	1.42
0.2	600.	21.54	11242.0	1190.	1683.	1.41
0.2	630.	21.66	11881.5	1252.	1765.	1.41
0.2	660.	21.77	12524.5	1314.	1846.	1.40
0.2	690.	21.88	13170.8	1377.	1927.	1.40
0.2	720.	21.98	13820.2	1440.	2009.	1.40
0.2	750.	22.08	14472.7	1502.	2090.	1.39
0.2	780.	22.18	15128.2	1565.	2171.	1.39
0.2	810.	22.27	15786.5	1628.	2252.	1.38
0.2	840.	22.36	16447.5	1691.	2334.	1.38
0.2	870.	22.44	17111.1	1754.	2415.	1.38
0.2	900.	22.53	17777.2	1812.	2496.	1.38
0.2	930.	22.61	18445.7	1875.	2577.	1.37
0.2	960.	22.68	19116.6	1938.	2659.	1.37
0.2	990.	22.76	19789.8	2001.	2740.	1.37
0.2	1020.	22.83	20465.2	2064.	2821.	1.37
0.2	1050.	22.90	21142.8	2127.	2902.	1.36
0.2	1080.	22.97	21822.4	2190.	2983.	1.36
0.2	1110.	23.03	22504.0	2254.	3065.	1.36
0.2	1140.	23.10	23187.7	2317.	3146.	1.36
0.2	1170.	23.16	23873.2	2389.	3227.	1.35

TABLE A2 (continued)

Π	δ^+	u_e/u_τ	$\int_0^{\delta^+} u^+ dy^+$	Re_θ	Re_{δ^*}	H
0.2	1200.	23.22	24560.6	2453.	3308.	1.35
0.2	1230.	23.28	25249.8	2517.	3390.	1.35
0.2	1260.	23.34	25938.7	2578.	3473.	1.35
0.2	1290.	23.40	26631.3	2642.	3554.	1.35
0.2	1320.	23.46	27325.6	2706.	3636.	1.34
0.2	1350.	23.51	28021.5	2770.	3717.	1.34
0.2	1380.	23.56	28719.1	2834.	3798.	1.34
0.2	1410.	23.62	29418.3	2898.	3880.	1.34
0.2	1440.	23.67	30119.0	2962.	3961.	1.34
0.2	1470.	23.72	30821.2	3026.	4043.	1.34
0.2	1500.	23.77	31525.0	3090.	4124.	1.33
0.2	1530.	23.81	32230.2	3154.	4205.	1.33
0.2	1560.	23.86	32936.8	3218.	4287.	1.33
0.2	1590.	23.91	33644.8	3282.	4368.	1.33
0.2	1620.	23.95	34354.2	3346.	4449.	1.33
0.2	1650.	24.00	35065.0	3411.	4531.	1.33
0.2	1680.	24.04	35777.1	3471.	4612.	1.33
0.2	1710.	24.08	36490.5	3535.	4693.	1.33
0.2	1740.	24.13	37205.1	3599.	4775.	1.33
0.2	1770.	24.17	37921.1	3663.	4856.	1.33
0.2	1800.	24.21	38638.2	3727.	4937.	1.32
0.2	1830.	24.25	39356.6	3792.	5019.	1.32
0.2	1860.	24.29	40076.2	3856.	5100.	1.32
0.2	1890.	24.33	40796.9	3920.	5182.	1.32
0.2	1920.	24.37	41518.8	3984.	5263.	1.32
0.2	1950.	24.40	42241.9	4049.	5344.	1.32
0.2	2040.	24.51	44417.7	4242.	5588.	1.32
0.2	2130.	24.62	46603.2	4436.	5832.	1.31
0.2	2220.	24.72	48798.0	4630.	6076.	1.31
0.2	2310.	24.81	51001.5	4823.	6321.	1.31
0.2	2400.	24.91	53213.6	5018.	6565.	1.31
0.2	2490.	25.00	55434.0	5212.	6809.	1.31
0.2	2580.	25.08	57662.2	5416.	7053.	1.30
0.2	2670.	25.17	59898.0	5611.	7297.	1.30
0.2	2760.	25.25	62141.2	5804.	7541.	1.30
0.2	2850.	25.33	64388.8	5996.	7788.	1.30
0.2	2940.	25.40	66645.9	6191.	8032.	1.30
0.2	3030.	25.47	68909.7	6386.	8277.	1.30
0.2	3120.	25.55	71180.0	6582.	8521.	1.29
0.2	3210.	25.61	73456.6	6777.	8765.	1.29
0.2	3300.	25.68	75739.4	6973.	9009.	1.29
0.2	3390.	25.75	78028.2	7168.	9254.	1.29
0.2	3480.	25.81	80322.6	7364.	9498.	1.29
0.2	3570.	25.87	82622.9	7560.	9742.	1.29
0.2	3660.	25.93	84928.6	7756.	9987.	1.29
0.2	3750.	25.99	87239.7	7952.	10231.	1.29
0.2	3840.	26.05	89556.1	8149.	10475.	1.29
0.2	3930.	26.11	91877.6	8345.	10719.	1.28
0.2	4020.	26.16	94204.1	8542.	10964.	1.28
0.2	4110.	26.21	96535.5	8738.	11208.	1.28
0.2	4200.	26.27	98871.7	8935.	11452.	1.28
0.2	4290.	26.32	101212.6	9132.	11696.	1.28
0.2	4380.	26.37	103558.1	9329.	11941.	1.28
0.2	4470.	26.42	105908.0	9526.	12185.	1.28
0.2	4560.	26.47	108262.5	9723.	12429.	1.28

TABLE A2 (continued)

Π	δ^+	u_e/u_τ	$\int_0^{\delta^+} u^+ dy^+$	Re_θ	Re_{δ^*}	H
0.3	30.	14.48	301.0	56.	133.	2.39
0.3	45.	15.64	519.7	85.	184.	2.17
0.3	60.	16.40	752.5	114.	231.	2.02
0.3	75.	16.97	994.9	144.	277.	1.93
0.3	90.	17.42	1245.0	174.	323.	1.85
0.3	105.	17.80	1501.3	205.	368.	1.80
0.3	120.	18.13	1762.8	236.	412.	1.75
0.3	135.	18.41	2029.0	267.	457.	1.71
0.3	150.	18.67	2299.2	298.	501.	1.68
0.3	165.	18.90	2573.1	329.	546.	1.66
0.3	180.	19.11	2850.3	361.	590.	1.63
0.3	195.	19.31	3130.5	393.	634.	1.61
0.3	210.	19.49	3413.5	425.	679.	1.60
0.3	225.	19.65	3699.2	457.	723.	1.58
0.3	240.	19.81	3988.0	483.	766.	1.59
0.3	255.	19.96	4277.6	522.	811.	1.56
0.3	270.	20.10	4570.1	554.	856.	1.54
0.3	285.	20.23	4866.1	588.	898.	1.53
0.3	300.	20.35	5161.0	619.	944.	1.52
0.3	315.	20.47	5459.2	652.	989.	1.52
0.3	330.	20.58	5759.2	685.	1033.	1.51
0.3	345.	20.69	6060.8	718.	1077.	1.50
0.3	360.	20.79	6363.9	750.	1121.	1.49
0.3	375.	20.89	6668.6	783.	1166.	1.49
0.3	390.	20.99	6974.8	816.	1210.	1.48
0.3	405.	21.08	7282.3	850.	1254.	1.48
0.3	420.	21.17	7591.2	883.	1298.	1.47
0.3	435.	21.25	7901.4	916.	1343.	1.47
0.3	450.	21.33	8213.4	950.	1386.	1.46
0.3	465.	21.41	8526.2	983.	1431.	1.46
0.3	480.	21.49	8840.1	1010.	1475.	1.46
0.3	495.	21.56	9155.2	1050.	1519.	1.45
0.3	510.	21.64	9470.4	1082.	1564.	1.45
0.3	525.	21.71	9787.6	1108.	1608.	1.45
0.3	540.	21.77	10107.0	1143.	1651.	1.45
0.3	555.	21.84	10426.4	1184.	1696.	1.43
0.3	570.	21.91	10746.7	1218.	1740.	1.43
0.3	600.	22.03	11388.4	1283.	1830.	1.43
0.3	630.	22.15	12035.2	1351.	1918.	1.42
0.3	660.	22.26	12685.5	1418.	2007.	1.42
0.3	690.	22.37	13339.1	1486.	2096.	1.41
0.3	720.	22.47	13995.9	1553.	2184.	1.41
0.3	750.	22.57	14655.7	1621.	2273.	1.40
0.3	780.	22.67	15318.6	1689.	2361.	1.40
0.3	810.	22.76	15984.2	1757.	2450.	1.39
0.3	840.	22.85	16652.4	1825.	2539.	1.39
0.3	870.	22.93	17323.4	1893.	2627.	1.39
0.3	900.	23.01	17996.8	1956.	2716.	1.39
0.3	930.	23.09	18672.7	2024.	2804.	1.39
0.3	960.	23.17	19350.9	2092.	2893.	1.38
0.3	990.	23.25	20031.4	2160.	2981.	1.38
0.3	1020.	23.32	20714.1	2228.	3070.	1.38
0.3	1050.	23.39	21399.0	2296.	3158.	1.38

TABLE A2 (continued)

Π	δ^+	u_e/u_τ	$\int_0^{\delta^+} u^+ dy^+$	Re_θ	Re_{δ^*}	H
0.3	1080.	23.46	22085.9	2365.	3247.	1.37
0.3	1110.	23.52	22774.9	2433.	3335.	1.37
0.3	1140.	23.59	23465.8	2502.	3424.	1.37
0.3	1170.	23.65	24158.7	2579.	3513.	1.36
0.3	1200.	23.71	24853.4	2648.	3601.	1.36
0.3	1230.	23.77	25549.9	2716.	3690.	1.36
0.3	1260.	23.83	26246.1	2783.	3780.	1.36
0.3	1290.	23.89	26946.0	2852.	3869.	1.36
0.3	1320.	23.94	27647.7	2921.	3958.	1.35
0.3	1350.	24.00	28351.0	2990.	4046.	1.35
0.3	1380.	24.05	29055.8	3059.	4135.	1.35
0.3	1410.	24.10	29762.3	3128.	4224.	1.35
0.3	1440.	24.15	30470.3	3197.	4313.	1.35
0.3	1470.	24.20	31179.9	3266.	4401.	1.35
0.3	1500.	24.25	31891.0	3335.	4490.	1.35
0.3	1530.	24.30	32603.5	3405.	4579.	1.34
0.3	1560.	24.35	33317.4	3474.	4667.	1.34
0.3	1590.	24.40	34032.8	3543.	4756.	1.34
0.3	1620.	24.44	34749.5	3613.	4845.	1.34
0.3	1650.	24.49	35467.6	3678.	4933.	1.34
0.3	1680.	24.53	36187.0	3747.	5022.	1.34
0.3	1710.	24.57	36907.7	3817.	5111.	1.34
0.3	1740.	24.61	37629.7	3886.	5199.	1.34
0.3	1770.	24.66	38352.9	3955.	5288.	1.34
0.3	1800.	24.70	39077.4	4025.	5377.	1.34
0.3	1830.	24.74	39803.1	4094.	5465.	1.33
0.3	1860.	24.78	40530.0	4163.	5554.	1.33
0.3	1890.	24.82	41258.1	4233.	5643.	1.33
0.3	1920.	24.85	41987.3	4302.	5731.	1.33
0.3	1950.	24.89	42717.6	4372.	5820.	1.33
0.3	2040.	25.00	44915.5	4581.	6086.	1.33
0.3	2130.	25.11	47122.9	4790.	6352.	1.33
0.3	2220.	25.21	49339.6	4999.	6618.	1.32
0.3	2310.	25.30	51565.2	5209.	6884.	1.32
0.3	2400.	25.40	53799.2	5419.	7150.	1.32
0.3	2490.	25.49	56041.5	5629.	7416.	1.32
0.3	2580.	25.57	58291.7	5848.	7682.	1.31
0.3	2670.	25.65	60549.4	6057.	7948.	1.31
0.3	2760.	25.74	62814.6	6267.	8215.	1.31
0.3	2850.	25.81	65084.2	6475.	8483.	1.31
0.3	2940.	25.89	67363.2	6686.	8750.	1.31
0.3	3030.	25.96	69649.0	6897.	9016.	1.31
0.3	3120.	26.03	71941.3	7108.	9282.	1.31
0.3	3210.	26.10	74239.9	7319.	9548.	1.30
0.3	3300.	26.17	76544.6	7531.	9815.	1.30
0.3	3390.	26.23	78855.3	7742.	10081.	1.30
0.3	3480.	26.30	81171.8	7954.	10347.	1.30
0.3	3570.	26.36	83494.0	8166.	10613.	1.30
0.3	3660.	26.42	85821.7	8377.	10880.	1.30
0.3	3750.	26.48	88154.6	8589.	11146.	1.30
0.3	3840.	26.54	90493.0	8802.	11412.	1.30
0.3	3930.	26.59	92836.4	9014.	11678.	1.30
0.3	4020.	26.65	95185.0	9226.	11945.	1.29
0.3	4110.	26.70	97538.4	9439.	12211.	1.29
0.3	4200.	26.76	99896.5	9651.	12477.	1.29
0.3	4290.	26.81	102259.4	9864.	12743.	1.29
0.3	4380.	26.86	104626.9	10077.	13009.	1.29
0.3	4470.	26.91	106998.7	10290.	13276.	1.29
0.3	4560.	26.96	109375.2	10503.	13542.	1.29

TABLE A2 (continued)

Π	δ^+	u_e/u_τ	$\int_o^{\delta^+} u^+ dy^+$	Re_θ	Re_{δ^*}	H
0.4	30.	14.96	308.3	58.	141.	2.40
0.4	45.	16.13	530.7	89.	195.	2.18
0.4	60.	16.89	767.1	121.	246.	2.03
0.4	75.	17.45	1013.2	153.	296.	1.94
0.4	90.	17.91	1266.9	185.	345.	1.86
0.4	105.	18.29	1526.9	218.	393.	1.80
0.4	120.	18.61	1792.1	251.	442.	1.76
0.4	135.	18.90	2061.9	284.	490.	1.72
0.4	150.	19.16	2335.8	318.	538.	1.69
0.4	165.	19.39	2613.4	352.	586.	1.67
0.4	180.	19.60	2894.2	386.	634.	1.64
0.4	195.	19.79	3178.1	420.	682.	1.62
0.4	210.	19.97	3464.8	454.	730.	1.61
0.4	225.	20.14	3754.1	489.	778.	1.59
0.4	240.	20.30	4046.5	517.	825.	1.60
0.4	255.	20.45	4339.8	558.	874.	1.57
0.4	270.	20.58	4636.0	593.	922.	1.55
0.4	285.	20.71	4935.6	629.	968.	1.54
0.4	300.	20.84	5234.2	663.	1017.	1.54
0.4	315.	20.96	5536.1	698.	1065.	1.53
0.4	330.	21.07	5839.7	733.	1113.	1.52
0.4	345.	21.18	6144.9	768.	1161.	1.51
0.4	360.	21.28	6451.8	803.	1209.	1.51
0.4	375.	21.38	6760.1	839.	1257.	1.50
0.4	390.	21.47	7070.0	874.	1305.	1.49
0.4	405.	21.57	7381.2	909.	1353.	1.49
0.4	420.	21.65	7693.7	945.	1401.	1.48
0.4	435.	21.74	8007.6	981.	1449.	1.48
0.4	450.	21.82	8323.2	1017.	1496.	1.47
0.4	465.	21.90	8639.6	1046.	1544.	1.48
0.4	480.	21.98	8957.3	1082.	1592.	1.47
0.4	495.	22.05	9276.0	1124.	1640.	1.46
0.4	510.	22.12	9594.8	1159.	1689.	1.46
0.4	525.	22.19	9915.7	1188.	1736.	1.46
0.4	540.	22.26	10238.8	1224.	1783.	1.46
0.4	555.	22.33	10561.8	1268.	1831.	1.44
0.4	570.	22.39	10885.8	1304.	1879.	1.44
0.4	600.	22.52	11534.8	1375.	1976.	1.44
0.4	630.	22.64	12188.9	1447.	2072.	1.43
0.4	660.	22.75	12846.5	1519.	2168.	1.43
0.4	690.	22.86	13507.5	1592.	2264.	1.42
0.4	720.	22.96	14171.6	1664.	2360.	1.42
0.4	750.	23.06	14838.7	1737.	2456.	1.41
0.4	780.	23.15	15508.9	1809.	2552.	1.41
0.4	810.	23.25	16181.8	1882.	2648.	1.41
0.4	840.	23.33	16857.4	1955.	2744.	1.40
0.4	870.	23.42	17535.6	2028.	2839.	1.40
0.4	900.	23.50	18216.4	2096.	2935.	1.40
0.4	930.	23.58	18899.6	2169.	3031.	1.40
0.4	960.	23.66	19585.1	2242.	3127.	1.39
0.4	990.	23.73	20273.0	2315.	3223.	1.39
0.4	1020.	23.81	20963.0	2388.	3319.	1.39
0.4	1050.	23.88	21655.2	2462.	3415.	1.39
0.4	1080.	23.94	22349.4	2535.	3510.	1.38
0.4	1110.	24.01	23045.7	2608.	3606.	1.38

TABLE A2 (continued)

Π	δ^+	u_e/u_τ	$\int_0^{\delta^+} u^+ dy^+$	Re_θ	Re_{δ^*}	H
0.4	1140.	24.08	23744.0	2682.	3702.	1.38
0.4	1170.	24.14	24444.2	2763.	3798.	1.37
0.4	1200.	24.20	25146.2	2837.	3894.	1.37
0.4	1230.	24.26	25850.1	2911.	3990.	1.37
0.4	1260.	24.32	26553.5	2983.	4088.	1.37
0.4	1290.	24.38	27260.8	3057.	4184.	1.37
0.4	1320.	24.43	27969.7	3131.	4280.	1.37
0.4	1350.	24.49	28680.3	3205.	4376.	1.37
0.4	1380.	24.54	29392.6	3279.	4472.	1.36
0.4	1410.	24.59	30106.4	3353.	4568.	1.36
0.4	1440.	24.64	30821.7	3427.	4664.	1.36
0.4	1470.	24.69	31538.6	3501.	4760.	1.36
0.4	1500.	24.74	32257.0	3575.	4856.	1.36
0.4	1530.	24.79	32976.8	3649.	4952.	1.36
0.4	1560.	24.84	33698.1	3724.	5048.	1.36
0.4	1590.	24.88	34420.7	3798.	5144.	1.35
0.4	1620.	24.93	35144.8	3873.	5240.	1.35
0.4	1650.	24.97	35870.2	3943.	5336.	1.35
0.4	1680.	25.02	36596.9	4017.	5432.	1.35
0.4	1710.	25.06	37324.9	4092.	5528.	1.35
0.4	1740.	25.10	38054.2	4166.	5624.	1.35
0.4	1770.	25.14	38784.8	4240.	5720.	1.35
0.4	1800.	25.18	39516.6	4315.	5816.	1.35
0.4	1830.	25.22	40249.6	4389.	5912.	1.35
0.4	1860.	25.26	40983.8	4464.	6008.	1.35
0.4	1890.	25.30	41719.3	4538.	6104.	1.34
0.4	1920.	25.34	42455.8	4613.	6200.	1.34
0.4	1950.	25.38	43193.5	4688.	6296.	1.34
0.4	2040.	25.49	45413.2	4912.	6584.	1.34
0.4	2130.	25.59	47642.6	5136.	6872.	1.34
0.4	2220.	25.69	49881.3	5361.	7160.	1.34
0.4	2310.	25.79	52128.8	5585.	7448.	1.33
0.4	2400.	25.88	54384.8	5811.	7736.	1.33
0.4	2490.	25.97	56649.0	6036.	8024.	1.33
0.4	2580.	26.06	58921.2	6270.	8312.	1.33
0.4	2670.	26.14	61200.9	6494.	8600.	1.32
0.4	2760.	26.22	63488.1	6720.	8888.	1.32
0.4	2850.	26.30	65779.6	6943.	9179.	1.32
0.4	2940.	26.38	68080.7	7170.	9467.	1.32
0.4	3030.	26.45	70388.4	7396.	9755.	1.32
0.4	3120.	26.52	72702.6	7622.	10043.	1.32
0.4	3210.	26.59	75023.1	7849.	10332.	1.32
0.4	3300.	26.66	77349.8	8076.	10620.	1.32
0.4	3390.	26.72	79682.4	8303.	10908.	1.31
0.4	3480.	26.79	82020.9	8530.	11196.	1.31
0.4	3570.	26.85	84365.1	8757.	11484.	1.31
0.4	3660.	26.91	86714.8	8984.	11773.	1.31
0.4	3750.	26.97	89069.7	9212.	12061.	1.31
0.4	3840.	27.03	91430.0	9440.	12349.	1.31
0.4	3930.	27.08	93795.4	9667.	12637.	1.31
0.4	4020.	27.14	96165.9	9895.	12925.	1.31
0.4	4110.	27.19	98541.2	10123.	13214.	1.31
0.4	4200.	27.24	100921.3	10351.	13502.	1.30
0.4	4290.	27.30	103306.1	10580.	13790.	1.30
0.4	4380.	27.35	105695.6	10808.	14078.	1.30
0.4	4470.	27.40	108089.4	11036.	14366.	1.30
0.4	4560.	27.44	110487.7	11265.	14655.	1.30

TABLE A2 (continued)

Π	δ^+	u_e/u_τ	$\int_0^{\delta^+} u^+ dy^+$	Re_θ	Re_{δ^*}	H
0.5	30.	15.45	315.7	61.	148.	2.42
0.5	45.	16.62	541.7	94.	206.	2.19
0.5	60.	17.38	781.7	127.	261.	2.05
0.5	75.	17.94	1031.5	161.	314.	1.95
0.5	90.	18.39	1288.9	196.	367.	1.87
0.5	105.	18.77	1552.5	231.	419.	1.82
0.5	120.	19.10	1821.4	266.	471.	1.77
0.5	135.	19.39	2094.9	302.	523.	1.73
0.5	150.	19.65	2372.4	337.	574.	1.70
0.5	165.	19.88	2653.6	373.	626.	1.68
0.5	180.	20.09	2938.1	410.	678.	1.65
0.5	195.	20.28	3225.7	446.	729.	1.64
0.5	210.	20.46	3516.0	483.	781.	1.62
0.5	225.	20.63	3809.0	519.	833.	1.60
0.5	240.	20.79	4105.1	550.	884.	1.61
0.5	255.	20.93	4402.0	593.	936.	1.58
0.5	270.	21.07	4701.8	630.	987.	1.57
0.5	285.	21.20	5005.2	669.	1038.	1.55
0.5	300.	21.33	5307.4	705.	1091.	1.55
0.5	315.	21.44	5612.9	742.	1142.	1.54
0.5	330.	21.56	5920.2	780.	1194.	1.53
0.5	345.	21.67	6229.1	817.	1245.	1.52
0.5	360.	21.77	6539.6	855.	1297.	1.52
0.5	375.	21.87	6851.6	892.	1349.	1.51
0.5	390.	21.96	7165.1	930.	1400.	1.51
0.5	405.	22.05	7480.0	968.	1452.	1.50
0.5	420.	22.14	7796.2	1006.	1503.	1.49
0.5	435.	22.23	8113.7	1044.	1555.	1.49
0.5	450.	22.31	8433.0	1082.	1606.	1.48
0.5	465.	22.39	8753.1	1114.	1658.	1.49
0.5	480.	22.47	9074.4	1152.	1709.	1.48
0.5	495.	22.54	9396.8	1197.	1761.	1.47
0.5	510.	22.61	9719.3	1234.	1813.	1.47
0.5	525.	22.68	10043.7	1265.	1865.	1.47
0.5	540.	22.75	10370.6	1304.	1915.	1.47
0.5	555.	22.82	10697.2	1350.	1966.	1.46
0.5	570.	22.88	11024.8	1389.	2018.	1.45
0.5	600.	23.01	11681.2	1464.	2123.	1.45
0.5	630.	23.12	12342.7	1541.	2226.	1.44
0.5	660.	23.24	13007.6	1618.	2329.	1.44
0.5	690.	23.35	13675.8	1695.	2432.	1.44
0.5	720.	23.45	14347.3	1772.	2536.	1.43
0.5	750.	23.55	15021.7	1849.	2639.	1.43
0.5	780.	23.64	15699.2	1927.	2742.	1.42
0.5	810.	23.73	16379.4	2005.	2845.	1.42
0.5	840.	23.82	17062.4	2083.	2948.	1.42
0.5	870.	23.91	17747.9	2160.	3052.	1.41
0.5	900.	23.99	18436.0	2233.	3155.	1.41
0.5	930.	24.07	19126.5	2311.	3258.	1.41
0.5	960.	24.15	19819.4	2389.	3361.	1.41
0.5	990.	24.22	20514.5	2467.	3464.	1.40
0.5	1020.	24.29	21211.9	2545.	3568.	1.40
0.5	1050.	24.36	21911.4	2623.	3671.	1.40
0.5	1080.	24.43	22613.0	2701.	3774.	1.40
0.5	1110.	24.50	23316.6	2779.	3877.	1.40
0.5	1140.	24.56	24022.1	2858.	3980.	1.39
0.5	1170.	24.63	24729.7	2944.	4083.	1.39

TABLE A2 (continued)

Π	δ^+	u_e/u_τ	$\int_0^{\delta^+} u^+ dy^+$	Re_θ	Re_{δ^*}	H
0.5	1200.	24.69	25439.0	3023.	4187.	1.39
0.5	1230.	24.75	26150.2	3101.	4290.	1.38
0.5	1260.	24.81	26861.0	3178.	4395.	1.38
0.5	1290.	24.86	27575.5	3257.	4499.	1.38
0.5	1320.	24.92	28291.8	3336.	4602.	1.38
0.5	1350.	24.97	29009.7	3415.	4705.	1.38
0.5	1380.	25.03	29729.3	3493.	4809.	1.38
0.5	1410.	25.08	30450.4	3572.	4912.	1.37
0.5	1440.	25.13	31173.1	3651.	5015.	1.37
0.5	1470.	25.18	31897.3	3730.	5119.	1.37
0.5	1500.	25.23	32623.0	3809.	5222.	1.37
0.5	1530.	25.28	33350.1	3889.	5325.	1.37
0.5	1560.	25.33	34078.7	3968.	5429.	1.37
0.5	1590.	25.37	34808.7	4047.	5532.	1.37
0.5	1620.	25.42	35540.1	4126.	5635.	1.37
0.5	1650.	25.46	36272.8	4202.	5738.	1.37
0.5	1680.	25.51	37006.8	4281.	5842.	1.36
0.5	1710.	25.55	37742.2	4360.	5945.	1.36
0.5	1740.	25.59	38478.8	4440.	6048.	1.36
0.5	1770.	25.63	39216.7	4519.	6152.	1.36
0.5	1800.	25.67	39955.8	4598.	6255.	1.36
0.5	1830.	25.71	40696.1	4678.	6358.	1.36
0.5	1860.	25.75	41437.7	4757.	6462.	1.36
0.5	1890.	25.79	42180.4	4837.	6565.	1.36
0.5	1920.	25.83	42924.3	4916.	6668.	1.36
0.5	1950.	25.87	43669.3	4996.	6772.	1.36
0.5	2040.	25.98	45911.0	5235.	7082.	1.35
0.5	2130.	26.08	48162.3	5474.	7392.	1.35
0.5	2220.	26.18	50423.0	5713.	7701.	1.35
0.5	2310.	26.28	52692.4	5953.	8011.	1.35
0.5	2400.	26.37	54970.5	6193.	8321.	1.34
0.5	2490.	26.46	57256.7	6434.	8631.	1.34
0.5	2580.	26.55	59550.7	6682.	8941.	1.34
0.5	2670.	26.63	61852.4	6922.	9251.	1.34
0.5	2760.	26.71	64161.5	7163.	9561.	1.33
0.5	2850.	26.79	66475.0	7401.	9874.	1.33
0.5	2940.	26.86	68797.9	7642.	10184.	1.33
0.5	3030.	26.94	71127.6	7884.	10495.	1.33
0.5	3120.	27.01	73463.8	8125.	10805.	1.33
0.5	3210.	27.08	75806.4	8367.	11115.	1.33
0.5	3300.	27.15	78155.0	8609.	11425.	1.33
0.5	3390.	27.21	80509.7	8851.	11735.	1.33
0.5	3480.	27.27	82870.0	9093.	12045.	1.32
0.5	3570.	27.34	85236.1	9335.	12356.	1.32
0.5	3660.	27.40	87607.7	9578.	12666.	1.32
0.5	3750.	27.46	89984.8	9821.	12976.	1.32
0.5	3840.	27.51	92367.0	10063.	13286.	1.32
0.5	3930.	27.57	94754.4	10306.	13596.	1.32
0.5	4020.	27.63	97146.8	10550.	13906.	1.32
0.5	4110.	27.68	99544.0	10793.	14216.	1.32
0.5	4200.	27.73	101946.2	11036.	14527.	1.32
0.5	4290.	27.78	104352.9	11280.	14837.	1.32
0.5	4380.	27.83	106764.2	11523.	15147.	1.31
0.5	4470.	27.88	109180.2	11767.	15457.	1.31
0.5	4560.	27.93	111600.4	12011.	15767.	1.31

TABLE A2 (continued)

Π	δ^+	u_e/u_τ	$\int_0^{\delta^+} u^+ dy^+$	Re_θ	Re_{δ^*}	H
0.55	30.	15.70	319.3	62.	152.	2.43
0.55	45.	16.86	547.2	96.	212.	2.20
0.55	60.	17.62	789.1	131.	268.	2.05
0.55	75.	18.19	1040.7	166.	323.	1.95
0.55	90.	18.64	1299.9	201.	378.	1.88
0.55	105.	19.02	1565.3	237.	432.	1.82
0.55	120.	19.35	1836.0	273.	485.	1.78
0.55	135.	19.63	2111.3	310.	539.	1.74
0.55	150.	19.89	2390.7	347.	593.	1.71
0.55	165.	20.12	2673.7	384.	646.	1.68
0.55	180.	20.33	2960.1	421.	700.	1.66
0.55	195.	20.53	3249.5	459.	753.	1.64
0.55	210.	20.71	3541.6	497.	807.	1.62
0.55	225.	20.87	3836.5	535.	860.	1.61
0.55	240.	21.03	4134.4	567.	913.	1.61
0.55	255.	21.18	4433.2	611.	967.	1.58
0.55	270.	21.32	4734.8	649.	1020.	1.57
0.55	285.	21.45	5039.9	689.	1072.	1.56
0.55	300.	21.57	5344.0	725.	1127.	1.55
0.55	315.	21.69	5651.4	764.	1181.	1.55
0.55	330.	21.80	5960.5	803.	1234.	1.54
0.55	345.	21.91	6271.2	841.	1287.	1.53
0.55	360.	22.01	6583.5	880.	1341.	1.52
0.55	375.	22.11	6897.4	919.	1394.	1.52
0.55	390.	22.21	7212.7	958.	1448.	1.51
0.55	405.	22.30	7529.4	997.	1501.	1.51
0.55	420.	22.39	7847.4	1036.	1555.	1.50
0.55	435.	22.47	8166.8	1075.	1608.	1.50
0.55	450.	22.55	8487.9	1114.	1661.	1.49
0.55	465.	22.63	8809.8	1148.	1714.	1.49
0.55	480.	22.71	9132.9	1187.	1768.	1.49
0.55	495.	22.78	9457.2	1232.	1821.	1.48
0.55	510.	22.86	9781.5	1271.	1875.	1.48
0.55	525.	22.93	10107.8	1303.	1929.	1.48
0.55	540.	22.99	10436.4	1343.	1981.	1.47
0.55	555.	23.06	10764.9	1390.	2034.	1.46
0.55	570.	23.13	11094.4	1430.	2087.	1.46
0.55	600.	23.25	11754.4	1507.	2196.	1.46
0.55	630.	23.37	12419.5	1587.	2303.	1.45
0.55	660.	23.48	13088.1	1666.	2410.	1.45
0.55	690.	23.59	13760.0	1746.	2517.	1.44
0.55	720.	23.69	14435.1	1825.	2623.	1.44
0.55	750.	23.79	15113.2	1905.	2730.	1.43
0.55	780.	23.89	15794.4	1985.	2837.	1.43
0.55	810.	23.98	16478.3	2065.	2944.	1.43
0.55	840.	24.07	17164.9	2145.	3051.	1.42
0.55	870.	24.15	17854.1	2225.	3158.	1.42
0.55	900.	24.23	18545.8	2301.	3265.	1.42
0.55	930.	24.31	19240.0	2381.	3372.	1.42
0.55	960.	24.39	19936.5	2461.	3478.	1.41
0.55	990.	24.47	20635.3	2541.	3585.	1.41
0.55	1020.	24.54	21336.3	2621.	3692.	1.41
0.55	1050.	24.61	22039.5	2702.	3799.	1.41

TABLE A2 (continued)

Π	δ^+	u_e/u_τ	$\int_0^{\delta^+} u^+ dy^+$	Re_θ	Re_{δ^*}	H
0.55	1080.	24.68	22744.7	2782.	3906.	1.40
0.55	1110.	24.74	23452.0	2863.	4013.	1.40
0.55	1140.	24.81	24161.2	2944.	4119.	1.40
0.55	1170.	24.87	24872.4	3032.	4226.	1.39
0.55	1200.	24.93	25585.4	3114.	4333.	1.39
0.55	1230.	24.99	26300.2	3195.	4440.	1.39
0.55	1260.	25.05	27014.7	3274.	4549.	1.39
0.55	1290.	25.11	27732.9	3355.	4656.	1.39
0.55	1320.	25.16	28452.8	3436.	4763.	1.39
0.55	1350.	25.22	29174.5	3518.	4870.	1.38
0.55	1380.	25.27	29897.7	3599.	4977.	1.38
0.55	1410.	25.32	30622.4	3680.	5084.	1.38
0.55	1440.	25.37	31348.8	3762.	5191.	1.38
0.55	1470.	25.42	32076.6	3843.	5298.	1.38
0.55	1500.	25.47	32806.0	3924.	5405.	1.38
0.55	1530.	25.52	33536.8	4006.	5512.	1.38
0.55	1560.	25.57	34269.0	4088.	5619.	1.37
0.55	1590.	25.62	35002.7	4169.	5726.	1.37
0.55	1620.	25.66	35737.7	4251.	5833.	1.37
0.55	1650.	25.71	36474.1	4329.	5940.	1.37
0.55	1680.	25.75	37211.8	4411.	6047.	1.37
0.55	1710.	25.79	37950.8	4492.	6154.	1.37
0.55	1740.	25.83	38691.1	4574.	6261.	1.37
0.55	1770.	25.88	39432.6	4656.	6368.	1.37
0.55	1800.	25.92	40175.4	4738.	6475.	1.37
0.55	1830.	25.96	40919.4	4819.	6582.	1.37
0.55	1860.	26.00	41664.6	4901.	6689.	1.36
0.55	1890.	26.04	42411.0	4983.	6796.	1.36
0.55	1920.	26.07	43158.5	5065.	6903.	1.36
0.55	1950.	26.11	43907.2	5147.	7010.	1.36
0.55	2040.	26.22	46159.9	5393.	7330.	1.36
0.55	2130.	26.33	48422.2	5640.	7651.	1.36
0.55	2220.	26.43	50693.8	5887.	7972.	1.35
0.55	2310.	26.52	52974.3	6134.	8293.	1.35
0.55	2400.	26.62	55263.3	6382.	8614.	1.35
0.55	2490.	26.71	57560.4	6629.	8935.	1.35
0.55	2580.	26.79	59865.5	6884.	9256.	1.34
0.55	2670.	26.87	62178.2	7132.	9577.	1.34
0.55	2760.	26.96	64498.2	7380.	9898.	1.34
0.55	2850.	27.03	66822.8	7626.	10222.	1.34
0.55	2940.	27.11	69156.6	7875.	10543.	1.34
0.55	3030.	27.18	71497.3	8123.	10864.	1.34
0.55	3120.	27.25	73844.5	8373.	11185.	1.34
0.55	3210.	27.32	76198.0	8622.	11506.	1.33
0.55	3300.	27.39	78557.6	8871.	11828.	1.33
0.55	3390.	27.45	80923.1	9120.	12149.	1.33
0.55	3480.	27.52	83294.6	9370.	12470.	1.33
0.55	3570.	27.58	85671.7	9620.	12791.	1.33
0.55	3660.	27.64	88054.2	9870.	13112.	1.33
0.55	3750.	27.70	90442.2	10120.	13433.	1.33
0.55	3840.	27.76	92835.5	10370.	13754.	1.33
0.55	3930.	27.81	95233.8	10621.	14076.	1.33
0.55	4020.	27.87	97637.2	10871.	14397.	1.32
0.55	4110.	27.92	100045.5	11122.	14718.	1.32
0.55	4200.	27.98	102458.5	11373.	15039.	1.32
0.55	4290.	28.03	104876.3	11624.	15360.	1.32
0.55	4380.	28.08	107298.6	11875.	15681.	1.32
0.55	4470.	28.13	109725.5	12126.	16002.	1.32
0.55	4560.	28.18	112156.7	12378.	16324.	1.32

TABLE A2 (continued)

Π	δ^+	u_e/u_τ	$\int_0^{\delta^+} u^+ dy^+$	Re_θ	Re_{δ^*}	H
0.6	30.	15.94	323.0	64.	155.	2.44
0.6	45.	17.11	552.7	98.	217.	2.21
0.6	60.	17.86	796.4	134.	275.	2.06
0.6	75.	18.43	1049.8	170.	332.	1.96
0.6	90.	18.88	1310.9	206.	389.	1.88
0.6	105.	19.26	1578.1	243.	444.	1.83
0.6	120.	19.59	1850.7	281.	500.	1.78
0.6	135.	19.88	2127.8	318.	556.	1.75
0.6	150.	20.13	2409.0	356.	611.	1.71
0.6	165.	20.37	2693.9	395.	666.	1.69
0.6	180.	20.58	2982.0	433.	722.	1.67
0.6	195.	20.77	3273.3	472.	777.	1.65
0.6	210.	20.95	3567.3	510.	832.	1.63
0.6	225.	21.12	3863.9	549.	888.	1.62
0.6	240.	21.27	4163.7	583.	942.	1.62
0.6	255.	21.42	4464.3	628.	998.	1.59
0.6	270.	21.56	4767.7	667.	1053.	1.58
0.6	285.	21.69	5074.7	708.	1107.	1.56
0.6	300.	21.81	5380.6	746.	1164.	1.56
0.6	315.	21.93	5689.8	785.	1219.	1.55
0.6	330.	22.05	6000.7	825.	1274.	1.54
0.6	345.	22.15	6313.3	865.	1330.	1.54
0.6	360.	22.26	6627.5	905.	1385.	1.53
0.6	375.	22.36	6943.1	945.	1440.	1.52
0.6	390.	22.45	7260.3	985.	1495.	1.52
0.6	405.	22.54	7578.8	1025.	1551.	1.51
0.6	420.	22.63	7898.7	1065.	1606.	1.51
0.6	435.	22.71	8219.8	1105.	1661.	1.50
0.6	450.	22.80	8542.8	1146.	1716.	1.50
0.6	465.	22.88	8866.6	1181.	1771.	1.50
0.6	480.	22.95	9191.5	1221.	1826.	1.50
0.6	495.	23.03	9517.6	1267.	1881.	1.48
0.6	510.	23.10	9843.7	1307.	1937.	1.48
0.6	525.	23.17	10171.8	1340.	1993.	1.49
0.6	540.	23.24	10502.3	1382.	2047.	1.48
0.6	555.	23.31	10832.6	1430.	2102.	1.47
0.6	570.	23.37	11163.9	1471.	2157.	1.47
0.6	600.	23.49	11827.6	1551.	2269.	1.46
0.6	630.	23.61	12496.4	1632.	2380.	1.46
0.6	660.	23.73	13168.6	1714.	2490.	1.45
0.6	690.	23.83	13844.2	1796.	2601.	1.45
0.6	720.	23.94	14522.9	1878.	2711.	1.44
0.6	750.	24.04	15204.7	1960.	2822.	1.44
0.6	780.	24.13	15889.5	2042.	2932.	1.44
0.6	810.	24.22	16577.1	2124.	3043.	1.43
0.6	840.	24.31	17267.3	2207.	3153.	1.43
0.6	870.	24.40	17960.2	2289.	3264.	1.43
0.6	900.	24.48	18655.6	2367.	3374.	1.43
0.6	930.	24.56	19353.4	2449.	3485.	1.42
0.6	960.	24.63	20053.6	2532.	3595.	1.42
0.6	990.	24.71	20756.1	2615.	3706.	1.42
0.6	1020.	24.78	21460.8	2697.	3816.	1.41
0.6	1050.	24.85	22167.6	2780.	3927.	1.41
0.6	1080.	24.92	22876.5	2863.	4037.	1.41
0.6	1110.	24.99	23587.4	2946.	4148.	1.41
0.6	1140.	25.05	24300.3	3029.	4258.	1.41
0.6	1170.	25.11	25015.1	3120.	4369.	1.40
0.6	1200.	25.18	25731.8	3204.	4479.	1.40
0.6	1230.	25.24	26450.3	3287.	4590.	1.40

TABLE A2 (continued)

Π	δ^+	u_e/u_τ	$\int_0^{\delta^+} u^+ dy^+$	Re_θ	Re_{δ^*}	H
0.6	1260.	25.29	27168.4	3369.	4703.	1.40
0.6	1290.	25.35	27890.3	3452.	4813.	1.39
0.6	1320.	25.41	28613.9	3536.	4924.	1.39
0.6	1350.	25.46	29339.1	3619.	5035.	1.39
0.6	1380.	25.52	30066.0	3703.	5145.	1.39
0.6	1410.	25.57	30794.4	3787.	5256.	1.39
0.6	1440.	25.62	31524.5	3871.	5367.	1.39
0.6	1470.	25.67	32256.0	3955.	5477.	1.39
0.6	1500.	25.72	32989.0	4038.	5588.	1.38
0.6	1530.	25.77	33723.5	4122.	5699.	1.38
0.6	1560.	25.81	34459.4	4206.	5809.	1.38
0.6	1590.	25.86	35196.7	4290.	5920.	1.38
0.6	1620.	25.90	35935.3	4374.	6030.	1.38
0.6	1650.	25.95	36675.4	4455.	6141.	1.38
0.6	1680.	25.99	37416.7	4539.	6252.	1.38
0.6	1710.	26.04	38159.4	4623.	6362.	1.38
0.6	1740.	26.08	38903.4	4707.	6473.	1.38
0.6	1770.	26.12	39648.6	4791.	6584.	1.37
0.6	1800.	26.16	40395.0	4875.	6694.	1.37
0.6	1830.	26.20	41142.7	4960.	6805.	1.37
0.6	1860.	26.24	41891.5	5044.	6916.	1.37
0.6	1890.	26.28	42641.6	5128.	7026.	1.37
0.6	1920.	26.32	43392.7	5213.	7137.	1.37
0.6	1950.	26.36	44145.1	5297.	7247.	1.37
0.6	2040.	26.46	46408.8	5551.	7579.	1.37
0.6	2130.	26.57	48682.1	5804.	7911.	1.36
0.6	2220.	26.67	50964.6	6058.	8243.	1.36
0.6	2310.	26.77	53256.1	6313.	8575.	1.36
0.6	2400.	26.86	55556.0	6568.	8907.	1.36
0.6	2490.	26.95	57864.2	6823.	9239.	1.35
0.6	2580.	27.04	60180.2	7084.	9571.	1.35
0.6	2670.	27.12	62503.9	7340.	9903.	1.35
0.6	2760.	27.20	64835.0	7596.	10235.	1.35
0.6	2850.	27.28	67170.4	7849.	10570.	1.35
0.6	2940.	27.35	69515.3	8105.	10902.	1.35
0.6	3030.	27.43	71867.0	8361.	11234.	1.34
0.6	3120.	27.50	74225.1	8617.	11566.	1.34
0.6	3210.	27.57	76589.6	8874.	11898.	1.34
0.6	3300.	27.63	78960.2	9130.	12230.	1.34
0.6	3390.	27.70	81336.8	9387.	12562.	1.34
0.6	3480.	27.76	83719.2	9644.	12894.	1.34
0.6	3570.	27.82	86107.2	9901.	13227.	1.34
0.6	3660.	27.89	88500.7	10159.	13559.	1.33
0.6	3750.	27.94	90899.8	10416.	13891.	1.33
0.6	3840.	28.00	93304.0	10674.	14223.	1.33
0.6	3930.	28.06	95713.3	10932.	14555.	1.33
0.6	4020.	28.11	98127.6	11190.	14887.	1.33
0.6	4110.	28.17	100546.9	11448.	15219.	1.33
0.6	4200.	28.22	102970.9	11706.	15551.	1.33
0.6	4290.	28.27	105399.7	11965.	15883.	1.33
0.6	4380.	28.32	107833.1	12223.	16216.	1.33
0.6	4470.	28.37	110270.8	12482.	16548.	1.33
0.6	4560.	28.42	112713.0	12741.	16880.	1.32

TABLE A2 (continued)

Π	δ^+	u_e/u_τ	$\int_0^{\delta^+} u^+ dy^+$	Re_θ	Re_{δ^*}	H
-0.167	30.	12.20	266.9	43.	99.	2.32
-0.167	45.	13.36	468.5	62.	133.	2.14
-0.167	60.	14.12	684.1	81.	163.	2.02
-0.167	75.	14.69	909.5	100.	192.	1.93
-0.167	90.	15.14	1142.5	119.	220.	1.86
-0.167	105.	15.52	1381.7	138.	248.	1.80
-0.167	120.	15.85	1626.2	157.	276.	1.75
-0.167	135.	16.14	1875.3	177.	303.	1.72
-0.167	150.	16.39	2128.4	196.	330.	1.68
-0.167	165.	16.62	2385.2	216.	358.	1.65
-0.167	180.	16.84	2645.3	236.	385.	1.63
-0.167	195.	17.03	2908.5	256.	412.	1.61
-0.167	210.	17.21	3174.4	277.	440.	1.59
-0.167	225.	17.38	3443.0	297.	467.	1.57
-0.167	240.	17.53	3714.7	310.	493.	1.59
-0.167	255.	17.68	3987.2	338.	521.	1.54
-0.167	270.	17.82	4262.6	359.	548.	1.53
-0.167	285.	17.95	4541.6	381.	574.	1.51
-0.167	300.	18.07	4819.4	400.	603.	1.51
-0.167	315.	18.19	5100.5	421.	630.	1.50
-0.167	330.	18.30	5383.4	441.	657.	1.49
-0.167	345.	18.41	5667.9	462.	684.	1.48
-0.167	360.	18.52	5954.0	483.	711.	1.47
-0.167	375.	18.61	6241.6	504.	739.	1.47
-0.167	390.	18.71	6530.7	525.	766.	1.46
-0.167	405.	18.80	6821.2	546.	793.	1.45
-0.167	420.	18.89	7113.0	567.	820.	1.45
-0.167	435.	18.97	7406.1	588.	847.	1.44
-0.167	450.	19.06	7701.0	610.	874.	1.43
-0.167	465.	19.14	7996.7	631.	901.	1.43
-0.167	480.	19.21	8293.6	645.	928.	1.44
-0.167	495.	19.29	8591.6	674.	955.	1.42
-0.167	510.	19.36	8889.8	694.	983.	1.42
-0.167	525.	19.43	9189.8	707.	1011.	1.43
-0.167	540.	19.50	9492.2	729.	1037.	1.42
-0.167	555.	19.56	9794.4	760.	1064.	1.40
-0.167	570.	19.63	10097.6	781.	1091.	1.40
-0.167	600.	19.75	10705.2	822.	1147.	1.39
-0.167	630.	19.87	11317.8	865.	1201.	1.39
-0.167	660.	19.98	11934.0	908.	1256.	1.38
-0.167	690.	20.09	12553.4	951.	1310.	1.38
-0.167	720.	20.20	13176.1	994.	1364.	1.37
-0.167	750.	20.29	13801.7	1038.	1419.	1.37
-0.167	780.	20.39	14430.2	1081.	1473.	1.36
-0.167	810.	20.48	15061.8	1124.	1528.	1.36
-0.167	840.	20.57	15696.0	1168.	1582.	1.35
-0.167	870.	20.65	16332.7	1211.	1636.	1.35
-0.167	900.	20.74	16972.0	1255.	1691.	1.35
-0.167	930.	20.82	17613.7	1292.	1745.	1.35
-0.167	960.	20.89	18257.8	1335.	1800.	1.35
-0.167	990.	20.97	18904.1	1379.	1854.	1.34
-0.167	1020.	21.04	19552.7	1422.	1908.	1.34
-0.167	1050.	21.11	20203.4	1465.	1963.	1.34

TABLE A2 (concluded)

Π	δ^+	u_e/u_τ	$\int_0^{\delta^+} u^+ dy^+$	Re_θ	Re_{δ^*}	H
-0.167	1080.	21.18	20856.2	1509.	2017.	1.34
-0.167	1110.	21.25	21511.0	1552.	2072.	1.33
-0.167	1140.	21.31	22167.7	1605.	2126.	1.32
-0.167	1170.	21.37	22826.4	1649.	2180.	1.32
-0.167	1200.	21.43	23487.0	1693.	2235.	1.32
-0.167	1230.	21.49	24149.4	1737.	2289.	1.32
-0.167	1260.	21.55	24811.4	1779.	2346.	1.32
-0.167	1290.	21.61	25477.2	1823.	2400.	1.32
-0.167	1320.	21.67	26144.6	1867.	2455.	1.31
-0.167	1350.	21.72	26813.8	1911.	2509.	1.31
-0.167	1380.	21.77	27484.5	1955.	2564.	1.31
-0.167	1410.	21.83	28156.8	1999.	2618.	1.31
-0.167	1440.	21.88	28830.7	2043.	2673.	1.31
-0.167	1470.	21.93	29506.1	2087.	2727.	1.31
-0.167	1500.	21.98	30183.0	2131.	2782.	1.31
-0.167	1530.	22.02	30861.3	2175.	2836.	1.30
-0.167	1560.	22.07	31541.1	2219.	2891.	1.30
-0.167	1590.	22.12	32222.3	2263.	2945.	1.30
-0.167	1620.	22.16	32904.9	2308.	3000.	1.30
-0.167	1650.	22.21	33588.8	2352.	3054.	1.30
-0.167	1680.	22.25	34274.0	2392.	3109.	1.30
-0.167	1710.	22.29	34960.6	2436.	3164.	1.30
-0.167	1740.	22.34	35648.4	2480.	3218.	1.30
-0.167	1770.	22.38	36337.5	2524.	3273.	1.30
-0.167	1800.	22.42	37027.8	2568.	3327.	1.30
-0.167	1830.	22.46	37719.3	2612.	3382.	1.29
-0.167	1860.	22.50	38412.1	2657.	3436.	1.29
-0.167	1890.	22.54	39106.0	2701.	3491.	1.29
-0.167	1920.	22.58	39801.1	2745.	3545.	1.29
-0.167	1950.	22.61	40497.3	2790.	3600.	1.29
-0.167	2040.	22.72	42592.6	2923.	3763.	1.29
-0.167	2130.	22.83	44697.6	3056.	3927.	1.29
-0.167	2220.	22.93	46811.8	3189.	4090.	1.28
-0.167	2310.	23.03	48934.8	3323.	4254.	1.28
-0.167	2400.	23.12	51066.4	3456.	4417.	1.28
-0.167	2490.	23.21	53206.2	3599.	4581.	1.27
-0.167	2580.	23.29	55353.9	3734.	4745.	1.27
-0.167	2670.	23.38	57509.3	3868.	4908.	1.27
-0.167	2760.	23.46	59671.9	4003.	5072.	1.27
-0.167	2850.	23.54	61839.0	4132.	5238.	1.27
-0.167	2940.	23.61	64015.6	4266.	5402.	1.27
-0.167	3030.	23.68	66198.8	4400.	5566.	1.26
-0.167	3120.	23.76	68388.6	4535.	5729.	1.26
-0.167	3210.	23.82	70584.7	4669.	5893.	1.26
-0.167	3300.	23.89	72787.1	4804.	6057.	1.26
-0.167	3390.	23.96	74995.2	4938.	6221.	1.26
-0.167	3480.	24.02	77209.3	5073.	6384.	1.26
-0.167	3570.	24.08	79428.9	5208.	6548.	1.26
-0.167	3660.	24.14	81654.2	5343.	6712.	1.26
-0.167	3750.	24.20	83884.8	5478.	6876.	1.26
-0.167	3840.	24.26	86120.6	5613.	7040.	1.25
-0.167	3930.	24.32	88361.5	5748.	7203.	1.25
-0.167	4020.	24.37	90607.6	5884.	7367.	1.25
-0.167	4110.	24.43	92858.5	6019.	7531.	1.25
-0.167	4200.	24.48	95114.1	6154.	7695.	1.25
-0.167	4290.	24.53	97374.5	6290.	7858.	1.25
-0.167	4380.	24.58	99639.4	6425.	8022.	1.25
-0.167	4470.	24.63	101909.0	6561.	8186.	1.25
-0.167	4560.	24.68	104182.9	6696.	8350.	1.25

TABLE A3

PROPERTIES OF THE COLES-GRANVILLE WAKE FUNCTION

Π	$\left(\frac{\Delta u}{u_\tau}\right)_{max}$	$\left(\frac{y}{\delta}\right)_{max}$	$\left(\frac{\Delta u}{u_\tau}\right)_{\frac{y}{\delta}=1}$	$u_e^+ - (u^+)_{\left(\frac{y}{\delta}\right)_{max}}$
-1/6	0	0	-0.813	-
-0.15	0.002	0.167	-0.732	3.557
-0.1	0.064	0.444	-0.488	1.426
0	0.361	0.667	0	0.628
0.1	0.755	0.762	0.488	0.396
0.2	1.188	0.815	0.976	0.283
0.3	1.639	0.849	1.463	0.225
0.4	2.101	0.872	1.951	0.185
0.5	2.570	0.889	2.439	0.157
0.6	3.043	0.902	2.927	0.136
0.7	3.519	0.912	3.415	0.120

$$\left(\frac{\Delta u}{u_\tau}\right)_{max} = \frac{4}{27K}\,\frac{(6\pi+1)^3}{(4\pi+1)^2} \quad \text{at} \quad \left(\frac{y}{\delta}\right)_{max} = \frac{2}{3}\,\frac{(6\pi+1)}{(4\pi+1)}$$

$$\left(\frac{\Delta u}{u_\tau}\right)_{\frac{y}{\delta}=1} = \frac{2\pi}{K}$$

ORIGINAL PAGE IS
OF POOR QUALITY

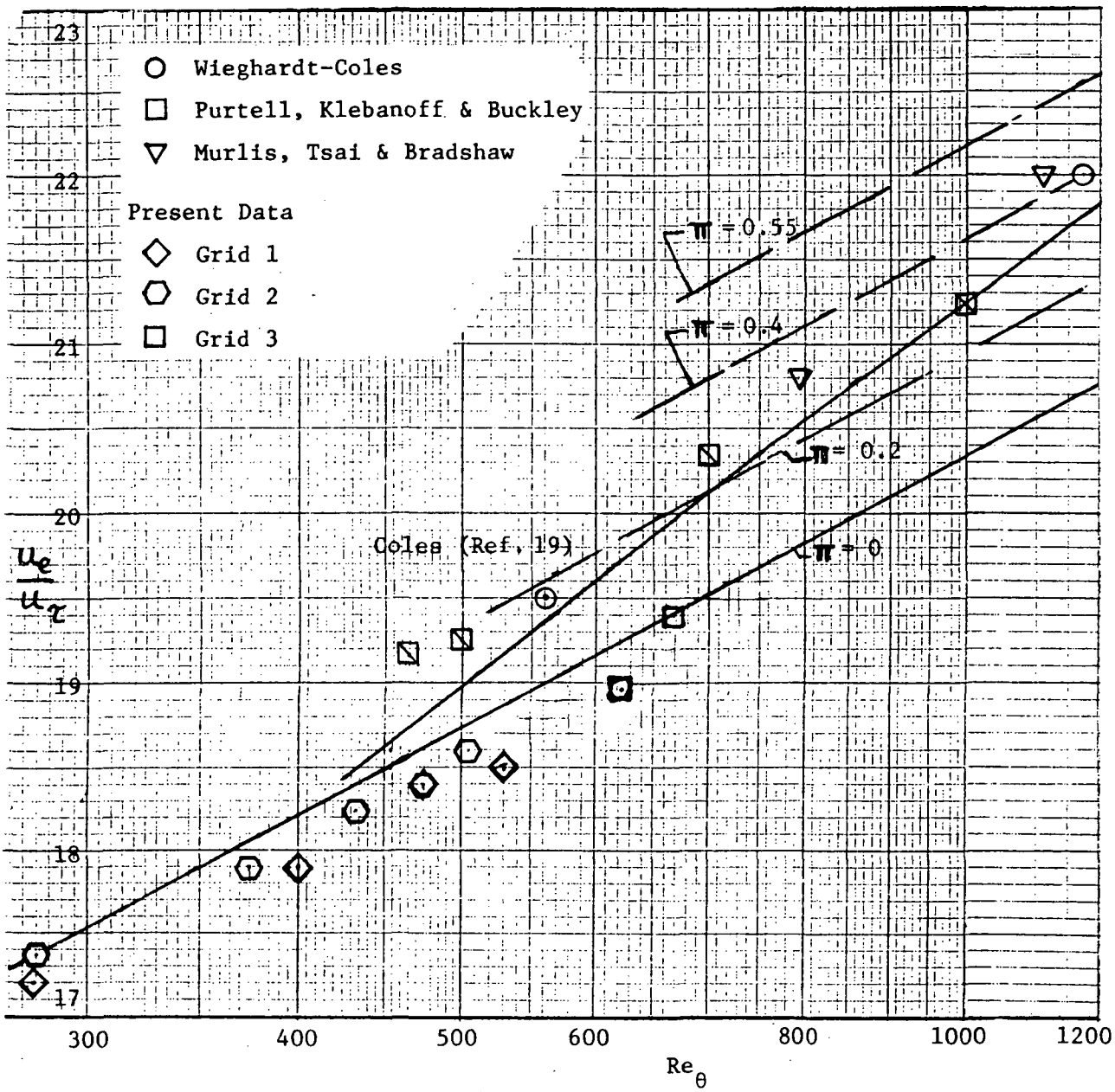

Fig. A-1. Comparison of skin friction data at low Reynolds numbers with calculations based on the Musker-Coles profile representation.

ORIGINAL PAGE IS
OF POOR QUALITY

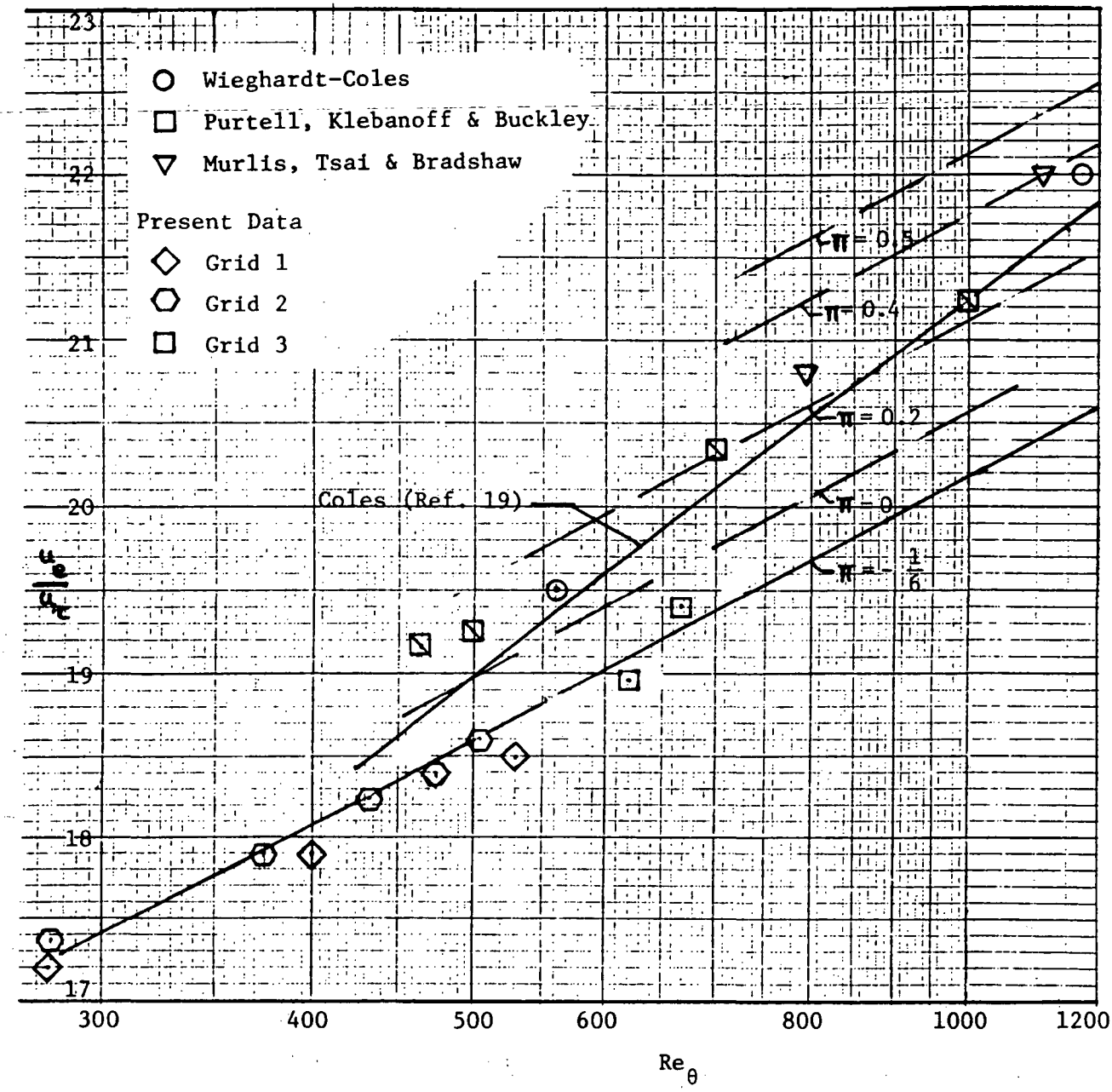

Fig. A-2. Comparison of skin friction data at low Reynolds numbers with calculations based on the Musker-Coles-Granville profile representation.

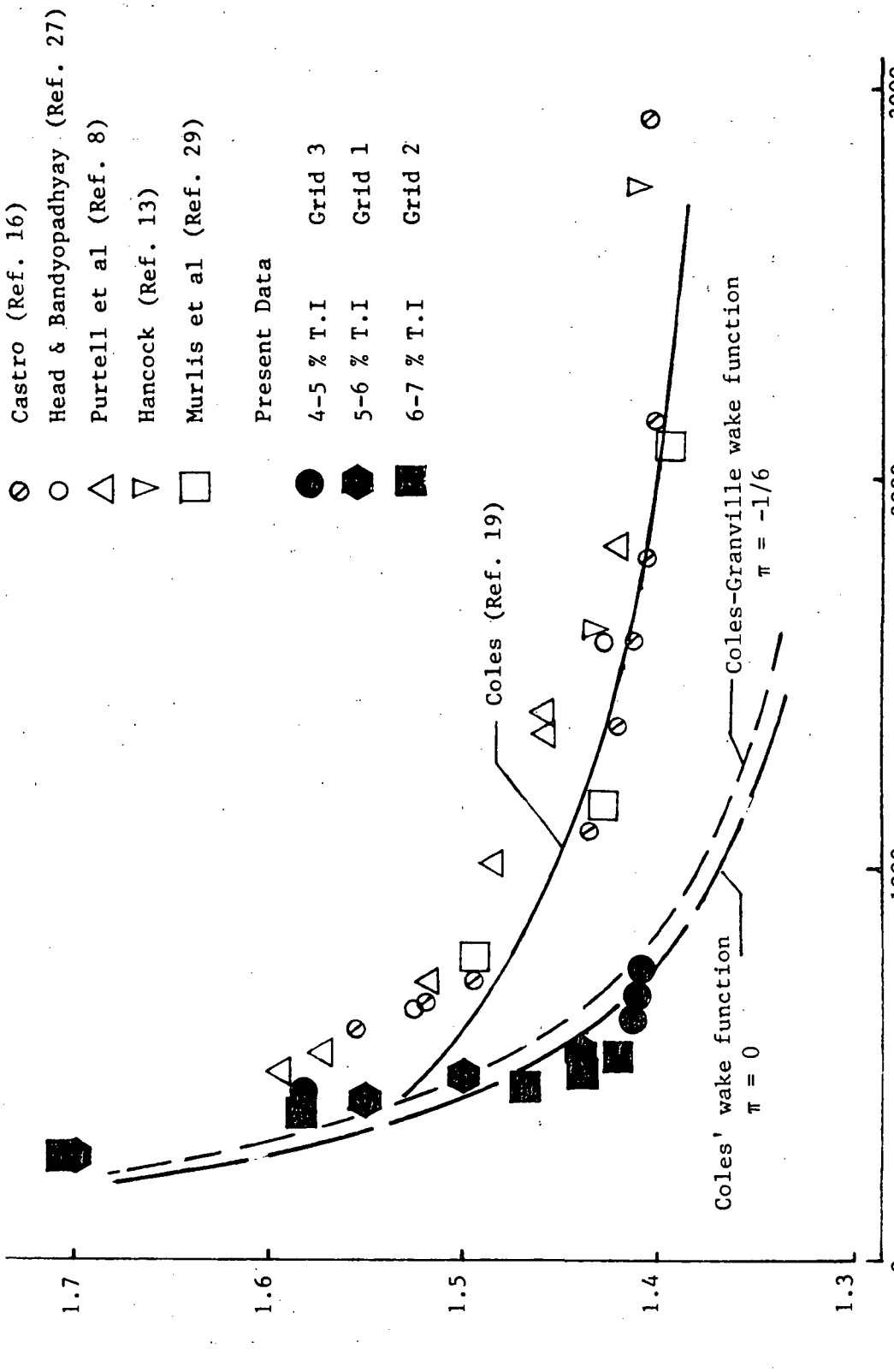

Fig. A-3. Comparison of shape factor data at low Reynolds numbers with calculations based on different zero-wake-strength profile representations.

1. Report No.	2. Government Accession No.	3. Recipient's Catalog No.
NASA CR-175031		

4. Title and Subtitle	5. Report Date
Low Reynolds Number Boundary Layers in a Disturbed Environment	January 1986
	6. Performing Organization Code

7. Author(s)	8. Performing Organization Report No.
Dong-Kee Paik and Eli Reshotko	None
	10. Work Unit No.

9. Performing Organization Name and Address	11. Contract or Grant No.
Case Western Reserve University Dept. of Mechanical and Aerospace Engineering Cleveland, Ohio	NAG 3-230
	13. Type of Report and Period Covered
12. Sponsoring Agency Name and Address	Contractor Report
National Aeronautics and Space Administration Washington, D.C. 20546	14. Sponsoring Agency Code
	505-36-22

15. Supplementary Notes

Final report. Project Managers, Raymond E. Gaugler and G. James Van Fossen, Internal Fluid Mechanics Division, NASA Lewis Research Center, Cleveland, Ohio 44135. This report was a dissertation submitted by Dong-Kee Paik in partial fulfillment of the requirements for the degree Doctor of Philosophy in Mechanical and Aerospace Engineering to Case Western Reserve University, Cleveland, Ohio in August 1985.

16. Abstract

Studies of flat plate boundary layer development were made in a low speed wind tunnel at turbulence levels from 2% to 7%. Only transitional and turbulent flows were observed in the range $280 < Re_\theta < 700$. The mean turbulent velocity profiles display law-of-the-wall behavior but have negligible wake component. The u' disturbance profiles compare well with those of other experiments, the peak value of u'/u_τ being about 2.5. The effect of free-stream turbulence level on turbulent skin friction can be nicely correlated with those of other investigations on a plot of u_e/u_τ versus Re_θ. A discussion on the u' spectra for the transitional boundary-layers is presented.

17. Key Words (Suggested by Author(s))	18. Distribution Statement
Boundary layer	Unclassified - unlimited STAR Category 34

19. Security Classif. (of this report)	20. Security Classif. (of this page)	21. No. of pages	22. Price*
Unclassified	Unclassified	96	A05

*For sale by the National Technical Information Service, Springfield, Virginia 22161

C-2

National Aeronautics and
Space Administration

Lewis Research Center
Cleveland, Ohio 44135

SECOND CLASS MAIL

ADDRESS CORRECTION REQUESTED

Official Business
Penalty for Private Use $300

Postage and Fees Paid
National Aeronautics and
Space Administration
NASA-451

NASA